Proceedings of the 16th International Students Conference "Modern Analytical Chemistry"

Prague, 17—18 September 2020

Edited by Karel Nesměrák

FACULTY OF SCIENCE
Charles University

Prague 2020

Proceedings of the
16th International Students Conference
"Modern Analytical Chemistry"

Proceedings of the 16th International Students Conference "Modern Analytical Chemistry"

Prague, 17—18 September 2020

Edited by Karel Nesměrák

FACULTY OF SCIENCE
Charles University

Prague 2020

The electronic version of the Proceedings is available at the conference webpage:
http://www.natur.cuni.cz/isc-mac/

Preface

Despite the fact that the year 2020 is marked by COVID-19, more than 40 young analytical chemists gathered in Prague for the 16th annual international conference "Modern Analytical Chemistry". They meet to present the results of their research, to master their presentation and language skills, and to exchange and discuss ideas and experiences of analytical chemistry.

This volume of conference proceedings brings you a total of 25 papers from this conference. As in previous years, the contributions presented are assorted by the sequence of their delivery, supplemented by indexes at the end of the proceedings allowing easy navigation through the pages. You will see, that topics of contributions cover all the aspects of modern analytical chemistry from theoretical problems, through development of new analytical methods and improvement of analytical techniques, to the applications involving the solution of medicinal, technical, or environmental problems. Let us hope that, like procee-dings of previous years of our conference, this one will also be an interesting, beneficial, and enjoyable reading.

It seems to us that the authors of the contributions are a guarantee of that a new generation of analytical chemists will protect bright and thrilling future of our science.

We are very grateful to the Division of Analytical Chemistry of EuChemS for its long-lasting auspices of our conference. Also, we are thankful to our sponsors, not only for their kind sponsorship making the conference possible, but also for all their cooperation and support in many of our other activities.

Enjoy reading these proceedings,

doc. RNDr. Karel Nesměrák, Ph.D.
　　　　　editor

Sponsors

The organizers of 16th International Students Conference "Modern Analytical Chemistry" gratefully acknowledge the generous sponsorship of following companies:

ZENTIVA	**QUINTA ANALYTICA**
www.zentiva.cz	www.quinta.cz
ECOM HPLC FROM PRAGUE	**fisher**scientific by Thermo Fisher Scientific
www.ecomsro.com	www.thermofisher.cz
lach:ner	**SHIMADZU** Excellence in Science
www.lach-ner.com	www.shimadzu.eu.com
2 THETA Analytical standards and equipment	**Waters** THE SCIENCE OF WHAT'S POSSIBLE.®
www.2theta.cz	www.waters.com

Contents

Determination of 2-methoxyphenol in model solutions by spectrophotometry

Valeriya Alikova[a, *], Anna Chernova[a], Vladimir Shormanov[b], Elena Korotkova[a]

[a] *Department of Chemical Engineering, Engineering School of National Resources, National Research Tomsk Polytechnic University, Lenin avenue 30, 634 050 Tomsk, Russia*
✉ *alikovalera@mail.ru*
[b] *Department of Pharmaceutical, Toxicological and Analytical Chemistry, Kursk State Medical University, st. Karla Marks 3, 305 000 Kursk, Russia*

Keywords
quantitation
2-methoxyphenol
UV/VIS spectrophotometry

Abstract
A spectrophotometric approach for determination of 2-methoxyphenol in model solutions has been developed. The absorption spectra of 2-methoxyphenol were determined in the wavelength range from 200 to 400 nm in solutions of 95% ethanol, acetonitrile, 0.1 M sodium hydroxide and ethyl acetate with a concentration of the analyte of $0.05\,mg\,dm^{-3}$. For the quantitative determination of 2-methoxyphenol, a series of solutions was prepared with various concentrations from $0.001\,mg\,dm^{-3}$ to $0.05\,mg\,dm^{-3}$ in 95% ethanol, acetonitrile, 0.1 M sodium hydroxide. The optical density of 2-methoxyphenol in solvents was measured at a wavelength of 276 nm and 289 nm. The developed method was tested using the method analysis of spiked samples.

1. Introduction

2-Methoxyphenol (guaiacol) is used in medicine as an expectorant. The structural formula is shown in Fig. 1. It is widely used in the pharmaceutical industry [1] for the synthesis of antituberculosis, expectorant drugs (Kasnol, Sudafed, Ascoril, Prothiazine Expectorant, Guaiphenesinum).

Moreover, 2-methoxyphenol is often used as an aromatic substance [2], in the food industry. In particular, it was widely used in the production of smoked fish and meat products using smokeless smoking technology using flavourings.

On the other hand, 2-methoxyphenol has the symbol GHS07 and has a hazard code Xn, T, Xi [2] according to the GHS system. It is very toxic by inhalation, it can irritate the mucous membrane of the respiratory tract and the conjunctiva of the
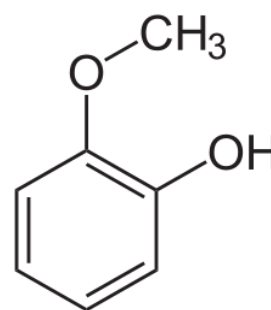
Fig. 1 Structural formula of 2-methoxyphenol.

eyeball, in high concentrations when it penetrates the skin can lead to neurosis when administered orally can stimulate the esophagus and stomach, resulting in heart failure, collapse, and death. Nowadays, there are published data on cases of a systemic allergic reaction [3] caused by 2-methoxyphenol derivatives, and there is a fatal case known [4] for oral administration of guaifenesin (3-(2-methoxy-phenoxy)propane-1,2-diol), one of the components of commonly available cough medications.

The determination of 2-methoxyphenol in environmental objects, as well as in the food industry, is carried out using gas chromatography methods with solid-phase microextraction [5]. In order to control 2-methoxyphenol in natural, drinking, and treated wastewater, gas chromatography is used, followed by optical detection of the eluate [6]. The main disadvantages of this method of analysis are the low selectivity and duration of determination (about 3 hours). Also, according to Russian State Standart GOST 33312-2015, the method of gas chromatography is used for the qualitative and quantitative determination of 2-metoxyphenolin juice products.

Commonly, for the analysis of toxic substances in various biological samples (blood, plasma, urine, saliva, sweat, hair) by gas chromatography, it is necessary to carry out multistage sample preparation, which complicates and slows down the course of the study [7]. At the same time, it is important that during the preparation of samples in the analyzed compounds their structure is not violated, as this will lead to the difficulty of their identification.

Spectrophotometry in the ultraviolet region has lower sensitivity compared to the above methods, however, this method does not require such complicated preparation of the analyzed samples, it is a relatively affordable, simple and inexpensive analysis method. In addition, its sensitivity can be significantly improved by applying an appropriate separation procedure and preconcentration before detection [8]. Method UV spectrophotometry is used to assess the quality of both medicinal substances and preparations made from them in terms of authenticity, good quality and quantitative content. In addition, it is a relatively affordable, simple and low-cost analysis method.

An analysis of the literature data showed that today there are fast and sensitive spectrophotometric methods for the determination of pyrocatechol derivatives in medicines [9], vanillin in food products [10] and other phenols in wastewater and wine products [11, 12]. However, as far as we know, information on the determination of 2-methoxyphenol from the absorption spectra in the ultraviolet region is absent.

The aim of this study is to develop methods for the qualitative and quantitative of 2-methoxyphenol in model solutions using UV spectrophotometry.
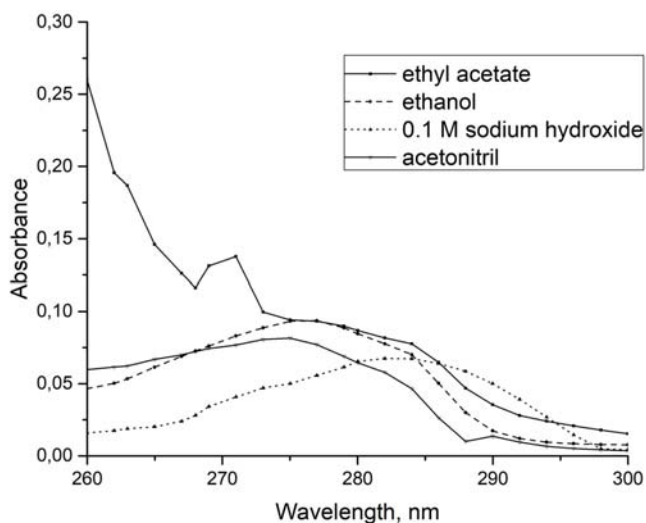
Fig. 1 The spectra of 2-methoxyphenol of concentration 0.05 mg dm^{-3} in the medium of solvents (an absorbing layer thickness of 10 mm).

2. Experimental

2.1 Reagents and chemicals

A sample of 2-methoxyphenol from Fluka with a basic substance content of ≥ 98% was taken as the object of study. As solvents, we used acetonitrile (ChP), 95% ethanol, ethyl acetate and 0.1 M sodium hydroxide solution. All other chemicals used were of analytical reagent grade.

2.2 Instrumentation

The optical density was measured in cuvettee with an absorbing layer thickness of 10 mm using a Cary 60 spectrophotometer (Agilent, USA). All measurements were carried out at room temperature.

3. Results and discussion

The change in the behavior of the absorption spectrum was investigated in the wavelength range of 200–400 nm. Figure 2 is showed that, with an increase in the polarity of the solvent, the absorption maximum shifts toward the visible part of the spectrum. The wavelength of absorption maxima of 2-methoxyphenol is presented in Table 1.

A study of the photometric behavior of 2-metoxyphenolin various solvents showed that acetonitrile, 95% ethanol and 0.1 M sodium hydroxide are the most suitable solvents for the qualitative determination of the test substance.

Table 1

Values of optical density and wavelengths in appropriate solvents with 2-methoxyphenol

Solvent	λ / nm	ε / g dm^{-3} cm^{-1}
Acetonitrile	276	0.0828
95% ethanol	276	0.0853
Ethyl acetate	277	0.0831
0.1 M sodium hydroxide	289	0.0744

Table 2

Results of the determination of 2-methoxyphenol (average of three measurements) in model solutions by the method analysis of spiked samples, the concentration of introduced 2-methoxyphenol was 5.00×10^{-3} g (S – standard deviation, RSD – relative standard deviation; Δx – absolute error; δ – relative error).

Solvent	Regression equation	Found 2-metoxy-phenol / g	S	RSD / %	Δx	δ / %
Acetonitrile	$y = 18.294\,C + 0.1130$ $R^2 = 0.9985$	4.99×10^{-3}	5.0×10^{-6}	0.28	2×10^{-5}	0.44
95% ethanol	$y = 35.131\,C + 0.0269$ $R^2 = 0.9956$	5.03×10^{-3}	0.3×10^{-6}	0.21	7×10^{-5}	1.37
0.1 M sodium hydroxide	$y = 31.196\,C + 0.1101$ $R^2 = 0.9997$	4.95×10^{-3}	0.1×10^{-6}	0.18	1×10^{-5}	0.28

For the quantitative determination of 2-methoxyphenol, a series of solutions with a concentration rage from 0.001 mg dm^{-3} to 0.05 mg dm^{-3}, were prepared in acetonitrile and 95% ethanol. The optical density of 2-methoxyphenol in solvents was measured by wavelength of 276 nm. The dependence of the intensity of the optical density on the concentration of 2-methoxyphenol in 0.1 M sodium hydroxide was plotted in the concentration range from 0.005 mg dm^{-3} to 0.03 mg dm^{-3}. The measurement were carried out by wavelength of 276 nm. The obtained regression equations are presented in Table 2. Data analysis obtained was performed using least-squares method. The developed method was tested using the method analysis of spiked samples. The results are presented in Table 2.

4. Conclusions

Studies have shown the possibility of using spectrophotometric analysis for the qualitative and quantitative determination of 2-methoxyphenol. The absorption maxima of were determined in solutions of ethanol and acetonitrile (276 nm), in a solution of ethyl acetate (277 nm) and 0.1 M sodium hydroxide (289 nm). The constructed calibration curves of the pure substance of 2-methoxyphenol has shown a good regression coefficient (R>0.99) and can be used for quantitative determination of 2-metoxyphenolin biological objects. In the future, it is planned to apply this technique to determine 2-metoxyphenolin in cadaveric material.

References

[1]   Мельникова И.М., Мизерницкий Ю.Л.: Комбинированные отхаркивающие препараты растительного происхождения в педиатрической практике. *Медицинский совет* **2** (2018), 93–97.

[2]   http://www.thegoodscentscompany.com/data/rw1032272.html (accessed 27st February, 2020)

[3]   Ray M., Faltay B.. Haller N.A.: Case report: anaphylactic reaction to guaifenesin. *Hosp. Pract.* **37** (2009), 60–63.

[4]   Okic M., Johnson T., Crifasi J.A., Long C., Mitchell E.K.: Swift onset of central nervous system depression and asystole following an overdose of guaifenesin. *J. Anal. Toxicol.* **37** (2013), 318–319.

[5]   Волков С.М., ЧерновецА.Н.: Определение концентрации фенолов в газовых выбросах промышленных предприятий методом газовой хроматографии с твердофазной микроэкстракцией. *Сорбционные и хроматографические процессы* **10** (2010), 723–728.

[6]   Шачнева Е.Ю., Онькова Д.В., Серекова С.М.: Способы определения фенолов в объектах окружающей среды. *Астраханский вестник экологического образования* **4** (2013), 138–142.

[7]   Гладилович В.Д., Подольская Е.П.: Возможности применения метода ГХ-МС (Обзор). *Научное приборостроение* **4** (2010), 36–49.

[8]   Pena-Pereira F., Lavilla I., Bendicho C.: Headspace single-drop microextraction coupled to microvolume UV–Vis spectrophotometry for iodine determination. *Anal. Chim. Acta* **631** (2009), 223–228.

[9]   Nagaraja P., Murthy K.C.S., Rangappa K.S., Gowda N.M.M.: Spectrophotometric methods for the determination of certain catecholamine derivatives in pharmaceutical preparations. *Talanta* **46** (1998), 39–44.

[10]   Altunay N.: Development of vortex-assisted ionic liquid-dispersive microextraction methodology for vanillin monitoring in food products using ultraviolet-visible spectro-photometry. *LWT* **93** (2018), 9–15.

[11]   Lupetti K.O., Rocha F.R.P., Fatibello-Filho O.: An improved flow system for phenols determination exploiting multicommutation and long pathlength spectrophotometry. *Talanta* 62 (2004), 463–467.

[12]   Figueiredo-González M., Cancho-Grande B., Simal-Gándara J.: Garnacha tintorera-based sweet wines: chromatic properties and global phenolic composition by means of UV–Vis spectrophotometry. *Food Chem.* **140** (2013), 217–224.

The effects of linearly assembled capillaries with various inner diameters on capillary electrophoresis

Daniel Böhm*, Frank-Michael Matysik

Institute of Analytical Chemistry, Chemo- and Biosensors, Faculty of Chemistry and Pharmacy, University of Regensburg, Universitätsstraße 31, 93053 Regensburg, Germany
✉ *daniel.boehm@chemie.uni-regensburg.de*

Keywords
assembled capillaries
capillary electrophoresis
capillary flow injection
    analysis
dual detection concept
non-aqueous system

Abstract
Due to the increasing need of powerful analytical methods, a new dual detection concept for capillary electrophoresis (CE) with parallel amperometric detection and mass spectrometry shall be developed. For this concept, the CE flow has to be divided into two streams utilizing a flow splitter. In this work, the effects of combined capillaries with various inner diameters were studied. For preliminary investigations the capillaries were connected in a serial configuration without dead volume. Using capillary flow injection analysis hyphenated to contactless conductivity detection, it could be shown that the coupling of identical capillaries leads to a slight decrease of the flow rates. With CE hyphenated to UV detection, it could be shown that the coupling of capillaries with different inner diameter has a much stronger effect on the electroosmotic flow, than the combination with the same inner diameter. Furthermore, no significant change in peak shape was observed.

1. Introduction

The number of samples, the sample complexity and also the number of substances which need to be analysed simultaneously is increasing steadily. Therefore, powerful separation and detection methods are required. One way to achieve this is the coupling of a separation system with more than one detector [1, 2].

In recent years, capillary electrophoresis (CE) was established as a potent separation system due to its high separation efficiency and the low sample consumption [3]. To generate more information, numerous dual detection concepts for CE were developed which are summarised elsewhere [1, 2]. A combination of amperometric detection and mass spectrometry (MS) is an interesting dual detection concept for CE, because both detectors supply complementary information. For electroactive species amperometric detection is a robust and one of the most sensitive detection method [4]. Thus, it is well suited for the
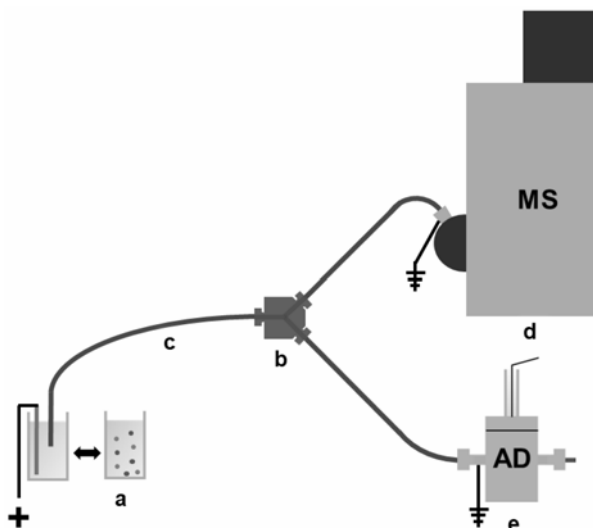
Fig. 1 Schematic illustration of the new dual detection concept with parallel amperometric detection and mass spectrometric detection for CE. After injection from (a) the sample vial the components are separated by CE, next (b) the flow splitter divides (c) the capillary into two parts and leads the CE flow towards (d) the mass spectrometer and (e) the amperometric detector.

quantification of substances, whereas MS is well suited for the identification of unknown substances [3]. In most dual detection concepts the detectors are arranged in a serial configuration which is not possible in case of amperometric detection-mass spectrometry [1]. The instrumental implementation is more complicated with both detectors being destructive. Furthermore, they must be decoupled from the high voltage field of the CE. Therefore, the CE flow must be divided into two streams with a flow splitter. A simplified sketch of the possible new dual detection concept is shown in Fig. 1.

For the development of the new dual detection concept, three capillaries with potentially different inner diameters must be coupled. For this reason, the dead volume-free coupling of capillaries with different inner diameters was investigated in a first step. To keep the setup simple, we focused on the linear coupling of capillaries and the resulting effects. Non-fragmented capillaries were compared with fragmented capillaries of the same or different inner diameters. Effects on the flow rate were investigated with capillary flow injection analysis (CFIA) hyphenated to contactless conductivity detection (C^4D). Effects, like changes in the migration behaviour or peak shapes occurring in CE were investigated with CE hyphenated to UV detection (CE-UV).

2. Experimental

2.1 Reagents and chemicals

The following chemicals were used, all of analytical grade: ferrocenemethanol, decamethylferrocene (ABCR, Germany), acetonitrile, ammonium acetate, 0.1 M sodium hydroxide solution, ultra-pure water provided by a Milli Q Advantage A10 system (Merck, Germany), acetic acid (Roth, Germany).

2.2 Instrumentation

2.2.1 Capillaries

For both experiments (CFIA-C^{4}D and CE-UV) capillaries with inner diameters of 25, 50, and 75 µm, an outer diameter of 360 µm and a total length of 70 cm were used. They were purchased from Polymicro Technologies (USA). Measurements were carried out with fragmented and non-fragmented capillaries. For the measurements with the fragmented capillaries, the original capillaries were cut into two pieces yielding a total of 9 capillary combinations with lengths of 70 cm (20 cm first capillary piece and 50 cm second capillary piece). These combinations are summarized in Tab. 1 (section 3.1). At both ends of the capillaries about 0.2 cm of the polyimide coating was removed. Both sides of the capillary pieces were polished to receive planar capillary tips. For the linear assembling of the capillary pieces, Micro Tight Sleeves F 185X and a capillary connector Union Assembly Micro Tight P 720 from IDEX Health & Science (USA) were used. Prior to the first CE measurements, the capillaries were conditioned by flushing them for 10 min with 0.1 M sodium hydroxide solution, 5 min with ultra-pure water and 30 min with separation buffer.

2.2.2 Capillary flow injection analysis hyphenated to contactless conductivity detection setup

The flow rates for the fragmented and non-fragmented capillaries were determined with a CFIA-C^{4}D setup schematically depicted in Fig. 2 A. The flow in the capillary was gravitation driven by a height difference between the inlet and outlet carrier solution vial. The concept of CFIA with gravitation driven flow was first described by Matysik et al. [5]. A laboratory constructed autosampler of a CE device was used for the hydrodynamic injection. The sample solution consisted of 10 mM decamethylferrocene in carrier solution (10 mM CH_3COONH_4 and 1 M CH_3COOH in acetonitrile). A high resolution C^{4}D was placed after 40 cm for detection. The detector described elsewhere [6] was constructed in the do Lago group (Brazil). A double determination at two different heights was done for the determination of the flow rates.
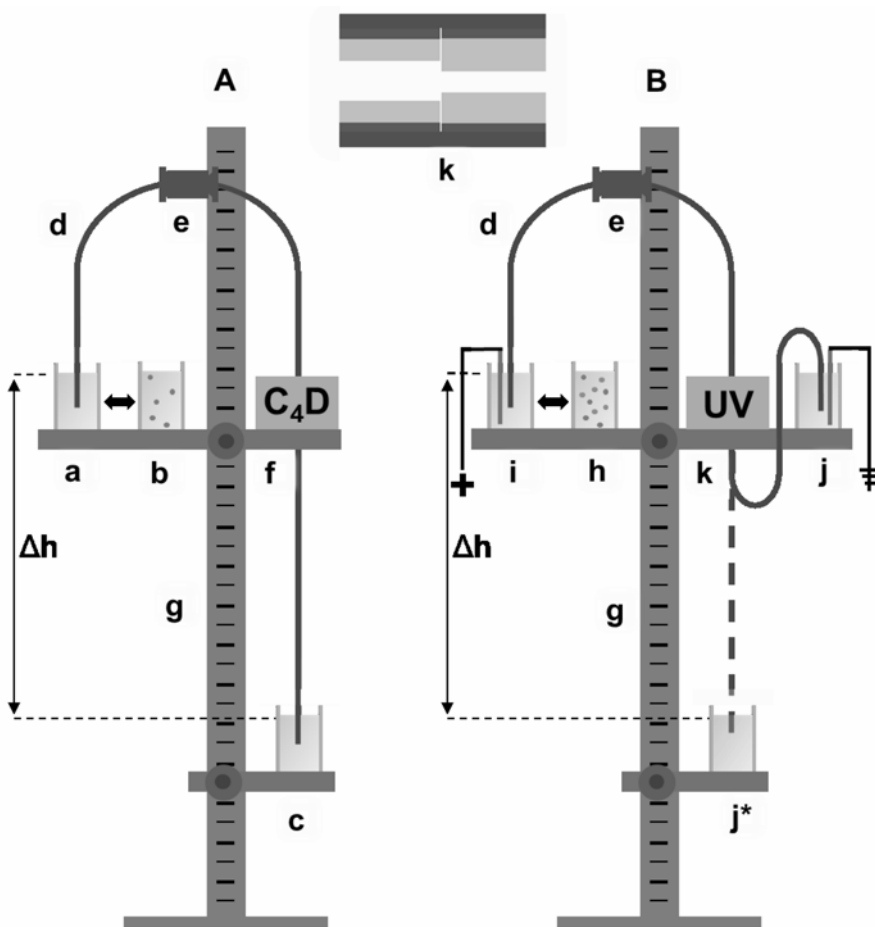
Fig. 2 Scheme of (A) the capillary flow injection analysis (CFIA) hyphenated to contactless conductivity detection (C^4D) setup, and (B) the capillary electrophoresis hyphenated to UV detection (CE-UV) setup. Components of the CFIA-C^4D setup: (a) sample, (b) inlet and (c) outlet carrier solution vial, (d) fused silica capillary, (e) linear capillary connector, (f) C^4D, and (g) stand. Components of the CE-UV setup: (h) sample, (i) inlet and (j) outlet buffer vial, and (k) UV detector; the rest of the components were identical to the CFIA-C^4D setup. The outlet buffer vial was lowered for the hydrodynamic injection (j*). The enlarged view (k) depicts the coupling of two capillaries with different inner diameters in the connection side without dead volume.

2.2.3 Capillary electrophoresis-UV detection setup

Fig. 2 B shows a sketch of the CE-UV setup. It consisted of a lab-built CE device, which was connected to a high voltage power supply from ISEG (Germany). The separations were carried out with a non-fragmented 50 μm capillary and with capillary combinations implementing a 50 μm downstream capillary segment (25+50, 50+50 and 75+50 μm). A Lambda 1010 UV-VIS detector from Bischoff (Germany) was used for detection at 210 nm. The detector was placed after 40 cm.

A sample solution containing 1 mM ferrocenemethanol and decamethylferrocene in separation buffer (10 mM CH_3COONH_4 and 1 M CH_3COOH in acetonitrile) was utilized. The injection was performed hydrodynamically by lowering the outlet buffer vial by 20 cm. A uniform sample plug was injected to compare band broadening effects. The injection segment had a length of 0.35 cm (0.5% of the total capillary length) and the respective injection time was determined based on the flow rates of the corresponding capillary combination. For the electrophoretic separation, a separation voltage of 25 kV was applied and the inlet and the outlet buffer vials were placed at the same height, so that there was no gravity flow which affected the migration behaviour.

3. Results and discussion

3.1 Capillary flow injection analysis hyphenated to contactless conductivity detection experiments

As shown in Tab. 1 the flow rates for a height difference of 20 cm were calculated based on the CFIA-C⁴D measurements. It was observable that the flow rates are slightly lower for fragmented capillaries than for non-fragmented capillaries of the same dimension. This indicates that a flow resistance arises when two capillaries are combined. Furthermore, it was observed that the flow rate decreases for upstream capillaries with lower inner diameters and vice versa. The flow rate for the combination 25+75 µm could not be determined due to the formation of air bubbles at the connection side.

Table 1

Flow rates and the corresponding standard deviations (*SD*, 4 measurements) of different capillary combinations for a height difference between inlet and outlet vial of 20 cm by means of capillary flow injection analysis hyphenated to contactless conductivity detection.

capillary combination /µm	flow rate/ nL s⁻¹	± SD flow rate / nL s⁻¹
25	0.0577	0.0005
25+25	0.057	0.001
50+25	0.0775	0.0007
75+25	–	–
25+50	0.137	0.005
50	0.865	0.002
50+50	0.80	0.05
75+50	1.05	0.06
25+75	0.187	0.002
50+75	1.941	0.003
75	4.56	0.02
75+75	4.2	0.1
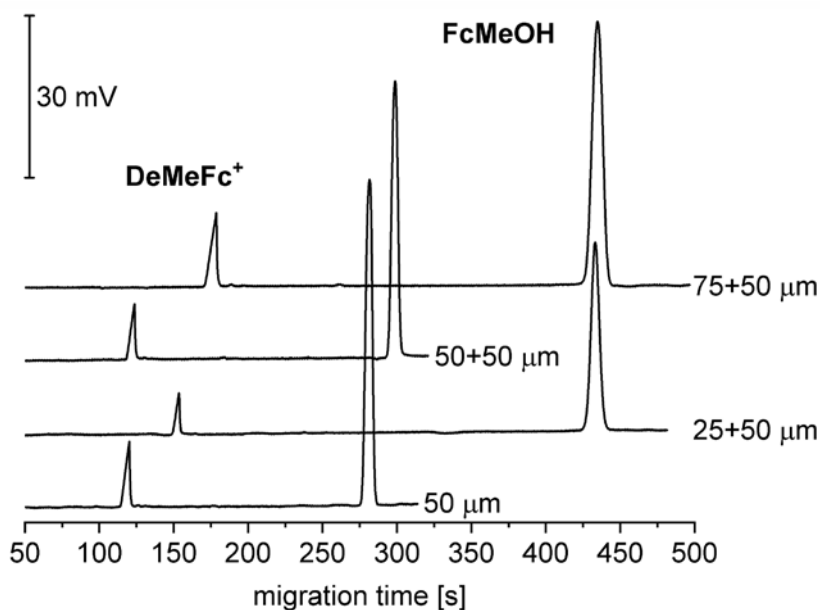
Fig. 3 Electropherograms of the model mixture ferrocenemethanol (FcMeOH) and decamethyl-ferrocene (DeMeFc) measured with a non-fragmented capillary (50 µm) and fragmented capillaries (25+50, 50+50 and 75+50 µm). Experimental parameters: 1 mM FcMeOH and DeMeFc in separation buffer (10 mM CH_3COONH_4 and 1 M CH_3COOH in acetonitrile), injection segment 0.35 cm, separation voltage 25 kV, capillary length 70 cm (40 cm to the detector, fragmented capillaries 20 cm first part and 50 cm second part), UV detection at 210 nm.

3.2 Capillary electrophoresis-UV detection experiments

The electropherograms for the non-fragmented 50 µm capillary and the capillary combinations with downstream 50 µm capillary are presented in Fig. 3. The two ferrocene derivates decamethylferrocene and ferrocenemethanol were used as model analytes. Decamethylferrocene was only detected as cationic species as it is easily oxidized by dissolved oxygen in solution.

For the combination 50+50 µm slightly higher migration times for the cationic (decamethylferrocene) and neutral species (ferrocenemethanol) were observable compared to the non-fragmented 50 µm capillary. This indicated a flow resistance at the connection, which was also observed for the CFIA-C⁴D experiments in section 3.1. In contrast to the combination with the same inner diameter, a strong shift in the migration times for the neural species was visible for the combinations with different inner diameters. This showed that the coupling had an effect on the electroosmotic flow.

Looking at the peak shape, it was found that all peaks showed nearly Gaussian shape for all combinations. Furthermore, there was no tailing visible. The ferrocenemethanol peaks for the combination 25+50 µm and 75+50 µm were

slightly broader than the peaks for the non-fragmented 50 µm capillary or for the 50+50 µm combination. But this probably results from longitudinal diffusion effects due to the longer residence times.

4. Conclusions

From the CFIA measurements it can be concluded that there was a mechanical disturbance of the flow due to the coupling. Furthermore, it could be shown that CE measurements with linear coupled capillaries of various inner diameter were possible. Unlike to the capillary combination with the same inner diameter a strong shift of the electroosmotic flow towards higher migration times was found for capillary combinations with different inner diameters. In this work the capillaries were coupled with almost no dead volume, which resulted in no significant changes of the peak shape or peak tailing. Contrary to expectations, the coupling of capillaries with various inner diameters had no significant impact on the peak width.

The knowledge gained from the linear coupling of capillaries is a good basis for the development of the new dual detection concept. In a next step three capillaries should be coupled with each other.

References

[1]   Opekar F., Štulík K.: Some important combinations of detection techniques for electrophoresis in capillaries and on chips with emphasis on electrochemical principles. *Electrophoresis* **32** (2011), 795–810.

[2]   Beutner A., Herl T., Matysik F.-M.: Selectivity enhancement in capillary electrophoresis by means of two-dimensional separation or dual detection concepts. *Anal. Chim. Acta* **1057** (2018), 18–35.

[3]   Beutner A., Cunha R.R., Richter E.M., Matysik F.-M.: Combining C^{4}D and MS as a dual detection approach for capillary electrophoresis. *Electrophoresis* **37** (2016), 931–935.

[4]   Matysik F.-M.: End-column electrochemical detection for capillary electrophoresis. *Electroanalysis* **12** (2000), 1349–1355.

[5]   Matysik F.-M., Werner G.: Trace metal determination in tears by anodic stripping voltammetry in a capillary flow injection system. *Analyst* **118** (1993), 1523–1526.

[6]   Francisco K.J.M., do Lago C.L.: A compact and high-resolution version of a capacitively coupled contactless conductivity detector. *Electrophoresis* **30** (2009), 3458–3464.

Voltammetric determination of vitamins

Radosław Porada*, Bogusław Baś

Department of Analytical Chemistry, Faculty of Materials Science and Ceramics, AGH University of Science and Technology, Mickiewicza 30, 30-059 Kraków, Poland ✉ rporada@agh.edu.pl

Keywords
mercury electrode
vitamins
voltammetry

Abstract
Vitamins belong to the group of chemical compounds essential for the proper functioning of the body. Since both their deficiency and excess may result in serious health problems, the amount of vitamins supplemented in the diet, as well as vitamin content in their sources, have to be strictly controlled. In this work, the possibility of simultaneous determination of vitamins by means of differential pulse adsorptive stripping voltammetry is discussed. The research has shown that the determination of singular vitamin at the micromolar level is relatively fast and straightforward, and the most important hindrance is related to the analyte adsorption at the electrode surface. In the case of vitamins with different redox potentials, they can be analyzed simultaneously, without the need to reach for the advanced methods for signal processing.

1. Introduction

The term "vitamins" describes the heterogeneous group of chemical compounds, which are important for the proper functioning of the human body [1, 2]. By definition, vitamins are not synthesized by the human body, or the synthesized amount is not sufficient to cover the demand. That is why they have to be supplemented from the external sources, like food products or pharmaceuticals [1–3]. Based on their solubility, vitamins are divided into water-soluble (B-group and vitamin C) and fat-soluble vitamins (A, D, E, and K) [3]. Vitamin C (ascorbic acid) is the most important antioxidant and participates in the activation of enzymes [4]. Vitamin B1 (thiamine) facilitates wound healing and is crucial for the human nervous system [1, 5]. Vitamin B2 (riboflavin) participates in the enzymatic reactions and the biotransformation of glucose and amino acids [6]. Vitamin B3 (niacin) is the main constituent of the NAD^+ and NADH coenzymes, which are responsible for the transfer of electrons and hydrogen ions in the cellular respiration [1–3]. Vitamin B6 possesses six related structures (vitamers) that easily interconvert. The most important one is pyridoxine which helps to prevent tongue inflammation and microcytic anemia [2]. For the production of well-functioning red blood cells and the avoidance of megaloblastic anemia and fetus defects, vitamin B9 (folic acid) has to be supplemented in the proper amount [1, 2].

Vitamin K3 (menadione) does not occur naturally, but it serves as a precursor for the synthesis of other K-group vitamins and can be used to treat hypoprothrombinemia. Vitamin K3 is partially soluble in water [1, 7].

All of the vitamins are electrochemically active [3], therefore, the electrochemical methods can be applied for the determination of vitamin content in food products, pharmaceuticals, and body fluids. Voltammetric techniques are characterized by high sensitivity and selectivity, and they do not require time-consuming sample preparation. Moreover, the electrochemical instrumentation is relatively inexpensive and can be applied in the on-site conditions for the online analyses, e.g., in quality control. Most of the papers report the construction, development, and characterization of a novel, modified working electrodes for quantitative analyses of a singular vitamin in the variety of matrices. Unfortunately, only a limited number of papers describe the simultaneous determination of multiple vitamins in a single run [2, 3].

The preliminary research devoted to the simultaneous determination of B-group, C, and K3 vitamins with the use of the controlled growth mercury drop working electrode in aqueous solutions is presented in this work. Particular attention has been paid to the redox potentials of the studied compounds, the shape of the calibration curves, and adsorption phenomena. As an attempt to overcome the latter, the neutral surfactant Triton X-100 has been introduced into the studied system.

2. Experimental

2.1 Reagents and chemicals

The applied reagents were of analytical grade and used as supplied. Phosphate and McIlvaine buffers were obtained by mixing the appropriate amount of $0.2\,mol\,L^{-1}$ Na_2HPO_4 with $0.2\,mol\,L^{-1}$ NaH_2PO_4 and $0.1\,mol\,L^{-1}$ citric acid, respectively (all reagents purchased from Avantor Performance Materials Poland). The standard solutions of vitamin B1, B2, B3, B9, and C were prepared by dissolving the corresponding amount of the standard (all Sigma-Aldrich) in distilled water. In the case of B2 and B9, the addition of $0.2\,mol\,L^{-1}$ NaOH was inevitable to obtain a clear solution. Vitamin K3 standard (Sigma-Aldrich) was dissolved in the mixture of methanol and $1\,mol\,L^{-1}$ phosphate buffer (pH = 8.2) (*v:v* = 2:5). Laboratory grade Triton X-100 (Sigma-Aldrich) was used in the study of the adsorption processes.

2.2 Instrumentation

All the electrochemical measurements were conducted in the three-electrode system, composed of the Pt auxiliary electrode, double-junction silver/silver chloride reference electrode, and controlled-growth mercury drop electrode

acting as the working electrode. The used measurement equipment involved the M164 electrode stand and M161 multipurpose electrochemical analyzer (both mtm-anko, Kraków). To control the buffer pH-value, the SevenCompact S210 laboratory pH-meter (Mettler Toledo, Switzerland) was employed.

2.3 Voltammetric measurements

Throughout the course of the study, differential pulse adsorptive stripping voltammetry has been used for recording the current-potential curves. Both cathodic and anodic scans were recorded in a potential range adjusted for the studied vitamins. The influence of various measurement conditions on the registered signals has been investigated. Finally, the possibility of the simultaneous determination of multiple vitamins in one scan has been verified.

3. Results and discussion

Figure 1 depicts the redox potentials of the studied vitamins in the aqueous solutions for the mercury electrode. The only exception is vitamin B6, whose redox potential is higher than the potential of mercury oxidation (ca. +0.2 V). Therefore, the given value refers to the glassy carbon electrode. The redox potential value of studied vitamins is not a singular value, but it falls within a certain range. This can be ascribed to the dependence of redox potential on the solution pH value, which results from the participation of protons in the redox reactions of vitamins. Moreover, the potentials for individual vitamins are relatively well separated, indicating that the simultaneous determination of several vitamins in the one run may be possible. The only encountered problems
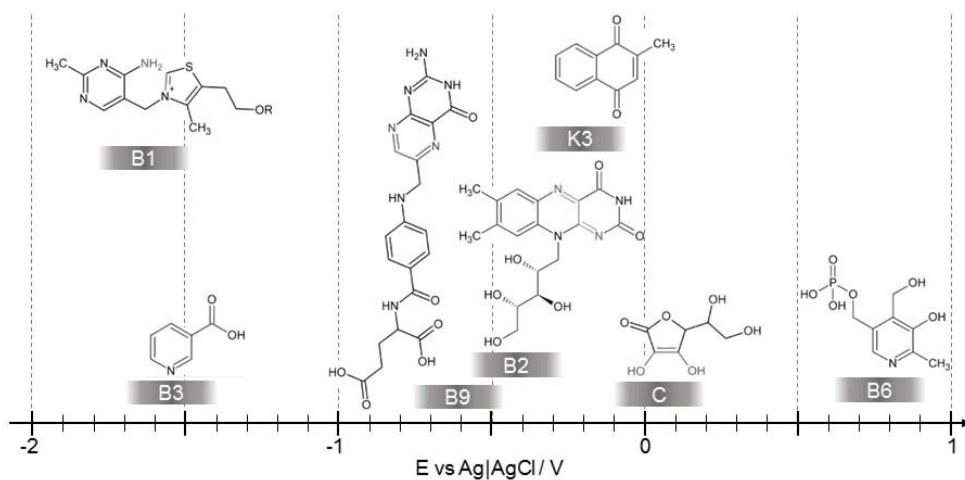
Fig. 1 Redox potentials of chosen vitamins.
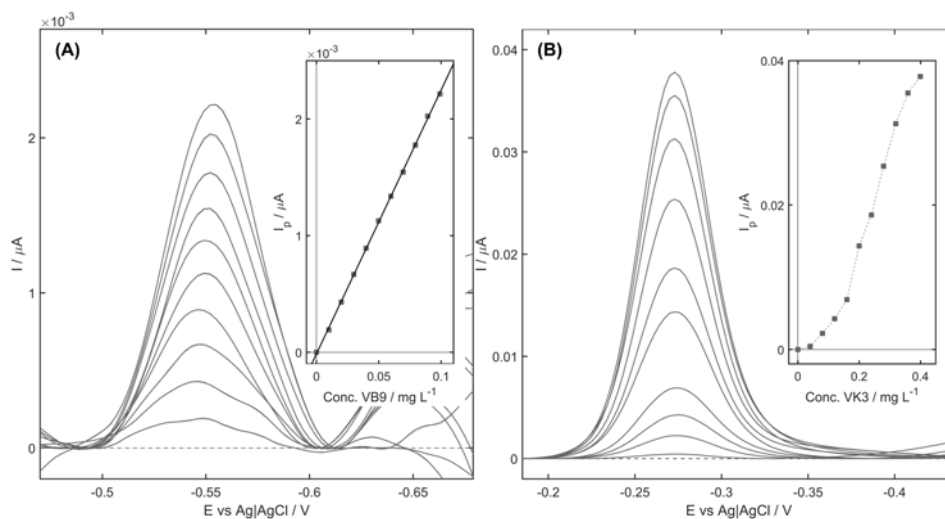
Fig. 2 Differential pulse adsorptive stripping voltammograms of (A) vitamin B9, and (B) vitamin K3 reduction recorded in the concentration range from blank to 0.1 and from blank to 0.4 mg L^{-1}, respectively. Inset: corresponding calibration curves. Supporting electrolyte: (A) McIlvaine buffer (pH = 5.2), (B) 0.4 mol L^{-1} phosphate buffer (pH = 8.2).

regard the vitamins B1, B3, and B12, whose redox potentials oscillate between –1.5 and –1.7 V, and the K-group vitamins (K1, K2, K3), in which only the common structural motif – the quinone ring – is electrochemically active, resulting in the value of the redox potential of ca. –0.2 V [8].

A typical calibration curve is depicted in Fig. 2A based on the differential pulse voltammograms of the vitamin B9 reduction in the concentration range from blank to 0.1 mg L^{-1}, recorded in the McIlvaine buffer of pH = 5.2 using the controlled growth mercury drop electrode working electrode. The relationship between the peak current and the concentration of VB9 is linear in the whole tested range ($r = 0.9999$). Based on the parameters of the regression curve, the limit of detection and limit of quantitation were estimated to 4.2 and 14.2 nmol L^{-1}, respectively. Similar dependencies and figures of merit can be obtained for other vitamins.

Quite different behavior was observed in the case of the vitamin K3, for which the increase in current was not strictly proportional to the increase in the concentration, and the calibration plot resembles an S-shape curve (Fig. 2B). The latter indicates that vitamin K3 adsorbs at the surface of the working electrode. However, as no pre- or post-peak were observed, we are dealing here with the weak adsorption [9]. Adsorption also plays a significant role in the case of vitamin B2, for which both the pre- and post-peaks were observed, indicating its strong affinity to the mercury electrodes.

To overcome this issue, attempts with Triton X-100 were performed. Triton X-100 is a neutral surfactant that easily adsorbs at the surface of the mercury
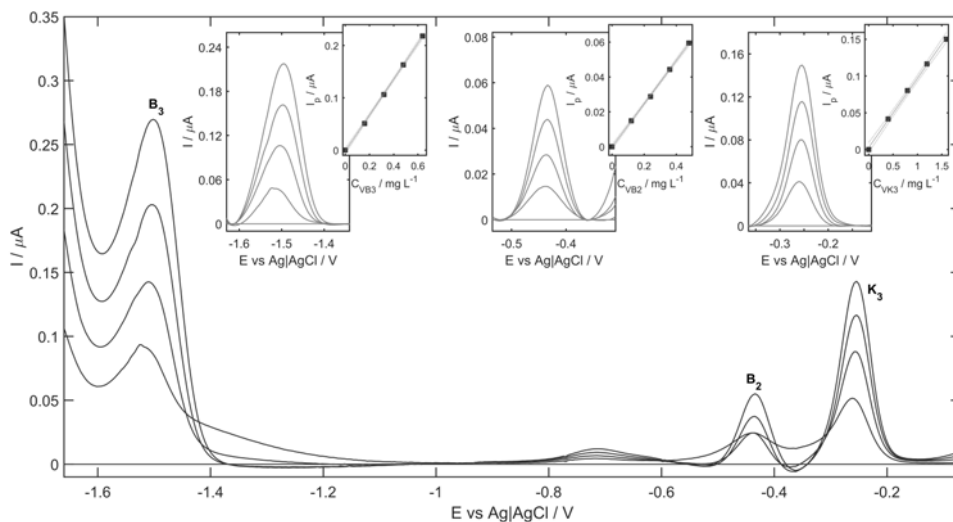
Fig. 3 Cathodic voltammograms for the simulatanous determination of vitamin B2, B3, and K3. Depicted in the insets are the voltammograms after background subtraction with the corresponding callibration plots. Supporting electrolye: 0.4 mol L^{-1} phosphate buffer (pH = 8.2) with 40 ppm Triton X-100. Accumulation conditions: E_{acc} = −0.05 V, t_{acc} = 20 s.

electrode, partially blocking its surface. Doing so, it prevents the undesired adsorption of other molecules and thus allows to obtain a linear relationship between the peak current and the vitamin concentration (Fig. 3). Unfortunately, due to the blocking of the electrode surface, the slopes of the calibration lines are smaller in comparison to the ones obtained in the absence of any surfactants. This means that the sensitivity, defined as the increase in current caused by a unit increase in concentration, and the resolution, understood as the possibility to distinguish small variation in concentration, are correspondingly decreased.

Figure 3 also presents the possibility to determine multiple vitamins in a single run. Chosen vitamins have well-separated potentials, and they do not interfere with each other, therefore, no advanced, multivariate calibration strategies are needed. The problems in the simultaneous analysis include various sensitivities with respect to the studied analytes and differences in the influence of the measurement conditions on the recorded signals. Due to that, the experimental conditions will never ensure the highest possible signal values for all analyzed compounds.

4. Conclusions

Differential pulse voltammetry in conjunction with the controlled growth mercury drop electrode is a perfect tool for quantitative analyses of vitamins. The adsorption of vitamin B2 and K3 can be prevented by the addition of the neutral surfactant Triton X-100, which selectively blocks the working electrode surface.

The proposed methodology allows for the simultaneous determination of micromolar amounts of vitamin B2, B3, and K3. Such a procedure will help to reduce the time and costs of analyses of multivitamin formulations and food products.

Acknowledgments

References

[1]   Combs G.F. Jr.: *The Vitamins: Fundamental Aspects in Nutrition and Health.* 3rd ed. Ithaca, Elsevier Academic Press 2008.
[2]   Lovander M.D., Lyon J.D., Parr D.L., Wang J., Parke B., Leddy J.: Review: Electrochemical properties of 13 vitamins: A critical review and assessment. *J. Electrochm. Soc.* **165** (2018), G18–G49.
[3]   Brunetti B.: Recent advances in electroanalysis of vitamins. *Electroanalysis* **28** (2016), 1930–1942.
[4]   Brubacher G., Müller-Mulot W., Southgate D.A.T.: *Methods for Determination of Vitamins in Food.* New York, Elsevier 1985.
[5]   Szpikowska-Sroka B.: A simple and sensitive analytical method for the determination of thiamine in pharmaceutical preparations. *J. Anal. Chem.* **68** (2013), 218–222.
[6]   Petteys B.J., Frank E.L.: Rapid determination of vitamin B_2 (riboflavin) in plasma by HPLC. *Clin. Chim. Acta* **412** (2011), 38–43.
[7]   Zhang Z., Xu J., Wen Y., Zhang J., Ding W.: The electro-syntesized imprinted PEDOT film as a simple voltammetric sensor for highly sensitive and selective detection of vitamin K_3 in poultry drug samples. *Synth. Met.* **230** (2017), 79–88.
[8]   Jedlińska K., Strus M., Baś B.: A new electrochemical sensor with the Refreshable Silver Liquid Amalgam Film multi-Electrode for sensitive voltammetric determination of vitamin K2 (menaquinone). *Electrochim. Acta* **265** (2018), 355–363.
[9]   Southampton Electrochemistry Group: *Instrumental Methods in Electrochemistry*. Chichester, Horwood 1985.

Dopamine detection at antifouling conical-tip carbon electrodes

Simona Baluchová[a, *], Jan Klouda[a], Jiří Barek[a], Karolina Schwarzová-Pecková[a], Danny K. Y. Wong[b]

[a] *UNESCO Laboratory of Environmental Electrochemistry, Department of Analytical Chemistry, Faculty of Science, Charles University, Hlavova 8, 128 00 Prague, Czech Republic,*
✉ *simona.baluchova@natur.cuni.cz*
[b] *Department of Molecular Sciences, Macquarie University, Sydney, NSW 2109, Australia*

Keywords

antifouling electrodes
diphenylsilane reduction
method
hydrogenated conical-tip
carbon electrodes
voltammetric dopamine
detection

Abstract

A significant achievement in this work is the development of antifouling conical-tip carbon electrodes ($\sim$2.7 µm tip diameter and $\sim$165 µm axial length) suitable for detection of the neurotransmitter dopamine *in-vivo*. These electrodes were hydrogenated using a diphenylsilane reduction method to yield a hydrophobic surface to deter adsorption of amphiphilic biomolecules. Initially, hydrogenated carbon electrodes were electrochemically characterised using several redox markers. The degree of antifouling was then assessed by the voltammetric signal change of dopamine at these electrodes before and after being incubated in a fouling solution containing bovine serum albumin, cytochrome C (both are proteins) and caproic acid (a lipid). In our work, we have obtained only a 6.9% (standard deviation 3.5%, $N = 40$) decrease in dopamine signals at the hydrogenated carbon electrodes. These results strongly support the diphenylsilane reduction strategy for the development of antifouling biosensors for dopamine detection in biological matrices.

1. Introduction

Carbon electrodes are commonly applied to sensitive electrochemical detection of neurotransmitters, e.g. dopamine, (nor)epinephrine and serotonin, *in-vivo* and *in-vitro* [1, 2]. Nevertheless, adsorption of high-molecular weight biomolecules in the matrix on a sensing electrode, which then hinders the electron transfer reaction of neurotransmitters, will result in biofouling of electrodes. This remains a challenging problem as biofouling will compromise electrochemical measurements. Thus, several strategies for addressing biofouling have previously been reported [3, 4].

This work reports on an effective approach for minimising biofouling based on the hypothesis that a hydrophobic electrode surface will repel against adsorption of amphiphilic biomolecules. Briefly, structurally small conical-tip electrodes

(denoted as CTEs) are fabricated by thermally pyrolysing acetylene gas in a nitrogen atmosphere to deposit carbon at the tip and on the shank of pulled quartz capillaries [5]. Spectroscopic studies confirmed that the electrode surface consists of sp^2-like graphitic carbon and sp^3-hybridised diamond-like carbon [6]. In addition, there is also a range of carbon-oxygen functionalities including carbonyl, quinone, carboxyl, phenols, alcohols and ether groups on the electrode surface [6], which can interact with spectator biomolecules through dipole-dipole or ion-dipole interaction, leading to their irreversible adsorption on the electrode surface [7]. However, by subjecting these carbon electrodes to silane reduction, C–O bonds are converted to C–H bonds and phenolic groups are transformed to siloxane dendrimers [6] to yield a more hydrophobic carbon surface that is expected to be similarly less susceptible to biofouling compared to boron-doped diamond electrodes [7, 8].

In this work, we will present a methodology involving diphenylsilane reduction to fabricate physically small, hydrogenated conical-tip carbon electrodes (denoted as HCTEs) with anti-fouling capability. Both CTEs and HCTEs were electrochemically characterised using several redox probes to elucidate their surface properties, before evaluating their resistance to biofouling during dopamine detection *in-vitro*.

2. Experimental

2.1 Reagents and chemicals

Analytical grade reagents (Sigma-Aldrich, Australia) including 4-methylcatechol, hexaammineruthenium(III) chloride, potassium hexacyanoferrate(III), dopamine hydrochloride, sodium phosphate dibasic, citric acid, perchloric acid, potassium chloride, sodium hydroxide, anhydrous dichloromethane, diphenylsilane, tris-(pentafluorophenyl)borane, and graphite powder were used as-received. Ultra-high purity gases acetylene and nitrogen were obtained from BOC Gases (Australia). All aqueous solutions were prepared with deionised water (Millipore Mili plus Q system, USA) with a resistivity of 18.2 MΩ cm.

2.2 Instrumentation

Chronoamperometric and voltammetric experiments were carried out using a low-current picostat eDAQ operated by an EChem version 2.1.2 software via an E-corder interface (eDAQ Pty Ltd., Australia). A three-electrode set-up involving either a CTE or HCTE as a working electrode, a Ag│AgCl (3 mol L^{-1} KCl) reference electrode (Bioanalytical Systems, USA) and a platinum wire counter electrode (Cypress Systems, USA) was used. Cyclic voltammetry at a scan rate of 100 mV s^{-1} and differential pulse voltammetry (pulse height +25 mV, pulse width 50 ms, sampling time 20 ms, and scan rate 20 mV s^{-1}) were used in this work. All

electroanalytical experiments were performed in an aluminium Faraday cage at an ambient temperature (23±1 °C).

2.3 Preparation of hydrogenated conical-tip carbon electrodes

As reported previously [5], structurally small CTEs were fabricated by thermally pyrolysing C_2H_2 (a pressure of 50 kPa) in a pulled quartz capillary (Sutter Instrument, USA) housed in a N_2 atmosphere (counter flow of 60 mL min^{-1}). Prior to hydrogenation, the catalyst tris(pentafluorophenyl) borane (10.0 mg) was dissolved in anhydrous CH_2Cl_2 (5.0 mL) by stirring for 5 min, before the hydrogenating agent, diphenylsilane (25 μL), was added. CTEs were then placed in the reagent mixture for 2 h. The prepared HCTEs were dried overnight before use.

2.4 Biofouling experiments

A laboratory synthetic fouling solution consisting of 4% (*w/v*) bovine serum albumin, 0.01% (*w/v*) cytochrome C (both are proteins), and 1.0% (*v/v*) caproic acid (a lipid) was prepared by homogenising them in a pH = 7.4 citrate-phosphate buffer (0.1 mol L^{-1}). All fouling compounds were acquired from Sigma Aldrich, Australia.

3. Results and discussion

3.1 Electrochemical characterisation

In this work, all CTEs were characterised by cyclic voltammetry of 1.0 mmol L^{-1} [Ru(NH$_3$)$_6$]$^{3+}$ in 1.0 mol L^{-1} KCl. As displayed in Fig. 1(A), only CTEs that show a sigmoidal-shaped voltammogram with a small charging current were employed in further experiments. Using chronoamperometry [5], a mean tip diameter of 2.7 μm (standard deviation (*SD*) 2.8 μm; $N = 142$), a mean axial length of 165 μm (*SD* = 114 μm; $N = 142$) were estimated for these CTEs.

To compare surface characteristics of both CTEs and HCTEs, cyclic voltammetry of (1) 1.0 mmol L^{-1} [Ru(NH$_3$)$_6$]$^{3+/2+}$ in 1.0 mol L^{-1} KCl, (2) 1.0 mmol L^{-1} [Fe(CN)$_6$]$^{3-/4-}$ in 1.0 mol L^{-1} KCl and (3) 1.0 mmol L^{-1} 4-methylcatechol in 0.1 mol L^{-1} HClO$_4$ was conducted at the same electrodes before and after hydrogenation. The results obtained are shown in Fig. 1(A-C). We observed a ∼20% (*SD* = 5%; $N = 10$) decrease in the limiting current of all three redox markers after diphenylsilane reduction, most likely attributable to the hindrance to their electron transfer reactions by the phenylsiloxane group formed on HCTEs. Moreover, as an inner-sphere redox probe, both [Fe(CN)$_6$]$^{3-/4-}$ and 4-methylcatechol reactions are sensitive to the presence of oxygen functionalities on a carbon surface [7]. Accordingly, the conversion of these functionalities to C–H bonds by diphenylsilane reduction was expected to yield more sluggish electron
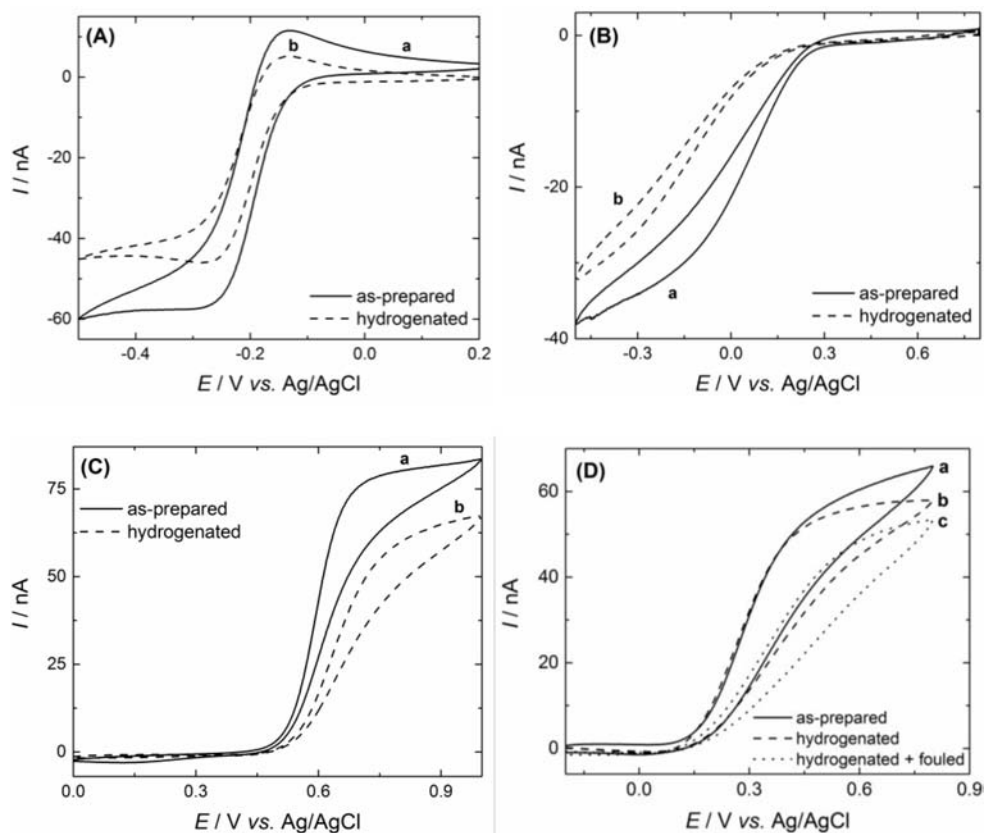
Fig. 1 Cyclic voltammetry of (A) 1.0 mmol L^{-1} $[Ru(NH_3)_6]^{3+}$ in 1.0 mol L^{-1} KCl, (B) 1.0 mmol L^{-1} $[Fe(CN)_3]^{3-/4-}$ in 1.0 mol L^{-1} KCl and (C) 1.0 mmol L^{-1} 4-methylcatechol in 0.1 mol L^{-1} $HClO_4$ at (a) a CTE and (b) a HCTE. (D) 1.0 mmol L^{-1} dopamine in a pH = 7.4 citrate-phosphate buffer recorded at (a) a CTE and a HCTE (b) before and (c) after biofouling. Scan rate 100 mV s^{-1}.

transfer kinetics at HCTEs, as supported by a negative potential shift (from +75 mV to −10 mV) in the cyclic voltammogram of $[Fe(CN)_6]^{3-/4-}$ and a positive potential shift (from +580 mV to +675 mV) in the corresponding cyclic voltammogram of 4-methylcatechol. In addition, the conversion of sp^2-carbon to sp^3-diamond-like carbon [6] is also expected to reduce the conductivity of the carbon electrode surface.

3.2 Dopamine detection during biofouling experiments

The electrochemical behaviour of 1 mmol L^{-1} dopamine in a pH = 7.4 citrate-phosphate buffer (0.1 mol L^{-1}) at CTEs and HCTEs was studied by cyclic voltammetry. The results obtained are shown in Fig. 1(D). A comparable 12% decrease (SD = 6%; N = 10) in the dopamine oxidation limiting current to that of 4-methylcatechol was observed. A positive potential shift from +285 mV to +305 mV in the voltammograms is also accounted for as described above.
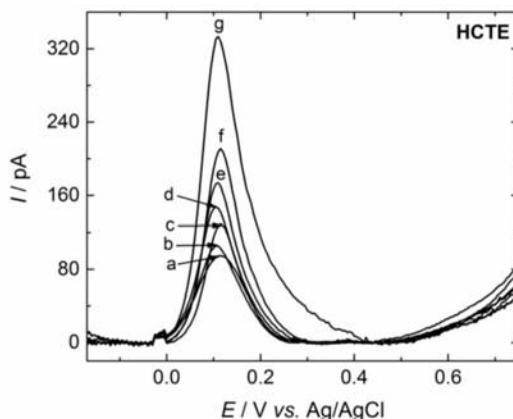
Fig. 2 Differential pulse voltammetry of dopamine at a HCTE in a pH = 7.4 citrate-phosphate buffer (0.1 mol L^{-1}) at concentrations: (a) 1, (b) 2, (c) 4, (d) 6, (e) 8, (f) 10, and (g) 20 μmol L^{-1}.

Table 1
Analytical parameters of concentration dependences of dopamine obtained by differential pulse voltammetry in a pH = 7.4 citrate-phosphte buffer (0.1 mol L^{-1}). All quoted uncertainties represent the 95% confidence interval and the correlation coefficient (R) was found to be statistically significant at the 95% using Student's t-test.

	Small conical-tip electrode	
	As-prepared	Hydrogenated
Linear range / μmol L^{-1}	1–10	1–20
Intercept 10^{-2} / pA μm^{-2}	1.08 ± 0.04	2.73 ± 0.11
Slope 10^{-3} / pA L μm^{-2} μmol^{-1}	1.28 ± 0.07	4.43 ± 0.12
R	0.993	0.998
Limit of detection / μmol L^{-1}	1.00	0.77

Next, HCTEs were incubated in a synthetic fouling solution containing 4% (w/v) bovine serum albumin, 0.01% (w/v) cytochrome C (both are proteins) and 1.0% (v/v) caproic acid (a lipid) for 30 min. Cyclic voltammetry of 1.0 mmol L^{-1} dopamine at these HCTEs was then conducted in a pH = 7.4 citrate-phosphate buffer to evaluate their antifouling property. Notably, a considerable 51.5% (SD = 18.3%, N = 6) decrease in dopamine signal was observed at CTEs. In contrast, only a corresponding 6.9% decrease (SD = 3.5%, N = 40) was estimated at HCTEs, as shown in Fig. 1(D). Clearly, this represents a major improvement in the antifouling capability of HCTEs obtained using diphenylsilane reduction, compared to CTEs and other previously tested hydrogenating agents [9] including n-butylsilane (35% decrease), triethylsilane (23% decrease) and phenylsilane (18% decrease). Therefore, this work has successfully demonstrated the effectiveness of diphenylsilane reduction method in developing antifouling electrodes for dopamine detection.

We have also studied the concentration dependence of dopamine in a pH = 7.4 citrate-phosphate buffer by differential pulse voltammetry. A typical calibration plot obtained is shown in Fig. 2. The analytical parameters and estimated limits of detection are summarised in Table 1. These results show that HCTEs outperformed CTEs because they exhibit a ~3.5× higher sensitivity, a 23% lower detection limit and a wider linear range.

4. Conclusions

In this study, physically small HCTEs with anti-fouling characteristics, achieved by hydrogenation using diphenylsilane reduction, were successfully fabricated and electrochemically characterised using several redox probes. Next, dopamine detection was performed before and after incubation of electrodes in a synthetic fouling solution containing a high concentration of biomolecules. Only a low 6.9% (SD = 3.5%) decrease in dopamine limiting current was achieved at HCTEs obtained by diphenylsilane reduction, indicating their significantly less susceptibility to biofouling than CTEs. These promising results indicate that antifouling HCTEs will potentially benefit the development of biosensors for dopamine detection *in-vivo* in biological media.

References
[1]   Baranwal A., Chandra P.: Clinical implications and electrochemical biosensing of monoamine neurotransmitters in body fluids, *in vitro, in vivo*, and *ex vivo* models. *Biosens. Bioelectron.* **121** (2018), 137–152.
[2]   Cao Q., Puthongkham P., Jill Venton B.: Review: new insights into optimizing chemical and 3D surface structures of carbon electrodes for neurotransmitter detection. *Anal. Methods* **11** (2019), 247–261.
[3]   Lin P.-H., Lin B.-R.: Antifouling strategies in advanced electrochemical sensors and biosensors. *Analyst* **145** (2020), 1110–1120.
[4]   Hanssen B. L., Siraj S., Wong D.K.Y.: Recent Strategies to Minimise Fouling in Electrochemical Detection Systems. *Rev. Anal. Chem.* **35** (2016), 1–28.
[5]   McNally M., Wong D.K.Y.: An *in-vivo* probe based on mechanically strong but structurally small carbon electrodes with an appreciable surface area. *Anal. Chem.* **73** (2001), 4793–4800.
[6]   Siraj S., McRae C.R., Wong, D.K.Y.: Effective activation of physically small carbon electrodes by *n*-butylsilane reduction. *Electrochem. Commun.* **64** (2016), 35–41.
[7]   Park J., Show Y., Quaiserova V., Galligan J., Fink G.D., Swain G.M.: Diamond microelectrodes for use in biological environments. *J. Electroanal. Chem.* **583** (2005) 56–68.
[8]   Shin D., Tryk D.A., Fujishima A., Merkoci A., Wang J.: Resistance to surfactant and protein fouling effects at conducting diamond electrodes. *Electroanalysis* **17** (2005) 305–311.
[9]   Roshni R.: *An Antifouling, Structurally Small Carbon Electrode for Detection of the Neurotransmitter Dopamine.* PhD Thesis, Macquarie University, Sydney, 2019.

A comparative study of covalent glucose oxidase and laccase immobilization techniques at powdered supports for biosensors fabrication

SOFIIA TVORYNSKA[a, b, *], JIŘÍ BAREK[a], BOHDAN JOSYPČUK[b]

[a] *UNESCO Laboratory of Environmental Electrochemistry, Department of Analytical Chemistry, Faculty of Science, Charles University, Hlavova 2030/8, 128 43 Prague 2, Czech Republic*
   ✉ *sofiia.tvorynska@jh-inst.cas.cz*
[b] *J. Heyrovský Institute of Physical Chemistry of the Czech Academy of Sciences, Dolejškova 3, 182 23 Prague 8, Czech Republic*

Keywords
biosensor
covalent immobilization
enzymatic reactor
glucose oxidase
laccase

Abstract
In order to develop the optimal strategy and to deepen the knowledge in the field of enzyme immobilization, three different techniques of covalent binding for two enzymes (glucose oxidase and laccase) at powdered surfaces were compared. Immobilization protocol was optimized by changing supports (two mesoporous silica powders (SBA–15, MCM–41) and a cellulose powder), the functionalized groups introduced at support surfaces ($-NH_2$ and $-COOH$), and the methods of activation (glutaraldehyde and carbodiimide). Amino and carboxyl functionalized mesoporous silica and cellulose powders were prepared by silanization using (3-aminopropyl)triethoxysilane and carboxyethylsilanetriol, respectively. It was found that coupling of both enzymes by their $-NH_2$ groups through glutaraldehyde to $-NH_2$ functionalized supports, in particular SBA15–NH_2 and cellulose–NH_2 for glucose oxidase, MCM41–NH_2 for laccase, showed the highest activity and the best stability.

1. Introduction

The analytical performances of enzymatic biosensors are strongly affected by the enzyme immobilization process. There is no universal technique for enzymes attachment. Therefore, special attention should be paid to the selection of the appropriate support and the development of the optimal binding strategy in order to ensure the best characteristics of immobilized enzyme. Despite a variety of previously reported covalent immobilization methods for different enzymes, the presented procedures can be hardly compared to find the optimal ones because of different analytical methods and experimental conditions used. Up to date, there

is still a lack of the comparative systematic studies focusing on the enzymes immobilization on the various supports using different techniques.

The aim of this work is the systematic comparative study of the different techniques for covalent coupling of the enzymes, which ensures not only the development of the optimal immobilization strategy for the selected enzymes, but also enables to find out some tendencies in enzyme attachment process generally. Thus, this work is focused on a detailed analysis of the effect of the kind of support, its anchor groups, and the activation methods on activity and stability of immobilized enzymes. Two enzymes with different nature (glucose oxidase (GOx) and laccase (Lac)) were chosen as the testing bioreceptors.

2. Experimental

2.1 Reagents and chemicals

All chemicals were of p. a. or better grade. Glucose oxidase from *Aspergillus niger* (GOx, EC 1.1.3.4; 145.2 U mg^{-1}), laccase from *Trametes versicolor* (Lac, EC 1.10.3.2; 12.9 U mg^{-1}), D-(+)-glucose, dopamine, glutaraldehyde (GA, grade II, 25% aqueous solution), *N*-(3-dimethylaminopropyl)-*N*'-ethylcarbodiimide hydrochloride (EDC, ≥98.0%), *N*-hydroxysuccinimide (NHS, ≥97.0%), (3-aminopropyl)-triethoxysilane (APTES), mesoporous silica powder SBA−15 (particle size 2–6 µm, pore size ≈ 7 nm, surface area ≈ 600 m^{2}g^{-1}), mesoporous silica powder MCM−41 (pore size 2.1–2.7 nm, surface area ≈ 1000 m^{2}g^{-1}), cellulose (Cell, microcrystalline powder, particle size 20 µm) were purchased from Sigma Aldrich. Carboxyethylsilanetriol (CEST, 25 % aqueous solution) was purchased from abcr® (Germany).

2.2 Instrumentation

Amperometric measurements were carried out at room temperature using computer-controlled electrochemical stand (Polaro-Sensors, Czech Republic) with MultiElchem v. 3.1 software (J. Heyrovský Institute of Physical Chemistry of the CAS). Flow injection analysis (FIA) with the three-electrode laboratory-made flow-through cell was used: working electrode – tubular detector of polished silver solid amalgam (TD-p-AgSA, laboratory-made, inner diameter 0.5 mm, the amalgam tube length 6.0 mm), reference electrode – a miniaturized saturated calomel electrode based on silver paste amalgam [1] (laboratory-made, it has the same potential as classical saturated calomel electrode), auxiliary electrode – platinum wire (diameter 1.0 mm, length 10 mm). The system for FIA with electrochemical detection comprised of a linear syringe pump, a 2-position 6-port sample injector valve, an injection loop laboratory-made of Teflon® (PTFE) tubing (100 µL), a solenoid operated micro-pump, an enzymatic reactor, and a flow-through cell for TD. The enzymatic reactor consists of a tube filled by the enzymatic powder.

3. Results and discussion

Based on the data reported in the literature [2,3] and on the results of our previous works [4–8], for this study Cell and mesoporous silica powders(namely SBA−15 and MCM−41) have been selected as the potential promising supports for the covalent enzyme immobilization. Because of the high content of surficial –OH groups which are capable of chemical reactions, these supports can be easily functionalized. The well-known and frequently utilized technique of silanization has been used to modify the surfaces of SBA15, MCM−41 and Cell by the desired functionalized groups. Aminosilane APTES was applied to form –NH$_2$ groups on the matrix surfaces, whereas carboxylsilane CEST was used to introduce –COOH groups.

Generally, the procedure of the covalent immobilization of enzyme (either Lac or GOx) on the functionalized support consists of three steps:

I.   Synthesis of the functionalized support, which means the modification of the matrix (MCM−41, SBA−15, and Cell) with suitable anchored groups (–NH$_2$ or –COOH).

II. Activation step of the functionalized support with specific activating agents (glutaraldehyde or EDC/NHS) to make it reactive towards enzyme.

III. Enzyme (Lac or GOx) coupling to the activated support.

To investigate the effect of support, its surface functionalized groups, and the methods of activation on the efficiency of the covalent enzyme immobilization, three different strategies (A, B, and C) for Lac and GOx attachment have been used. The details of the used techniques and the denotations of the prepared enzymatic powders are summarized in Table 1 (next page). To examine the efficiency of Lac and GOx immobilization, the enzymatic reactors (filled by the enzymatic powders prepared with different techniques) coupled with TD were used for amperometric determination of dopamine and glucose, respectively, in flow systems. The principle of glucose detection is based on amperometric measurements of the enzymatically consumed oxygen, whereas dopamine was detected by the reduction of the enzymatically oxidised dopamine.

As depicted in Fig. 1, the biosensors responses are strongly affected by the strategy used for Lac or GOx immobilization. As shown, the responses of Lac and GOx biosensors decrease in the order strategy A > strategy B > strategy C, irrespective of the type of support. It is clearly seen that amino functionalized supports (SBA15−NH$_2$, MCM41−NH$_2$, and Cell−NH$_2$) provide higher activities of the immobilized Lac and GOx than these supports functionalized by carboxyl groups (SBA15−COOH, MCM41−COOH, and Cell−COOH). By comparing activities of immobilized enzymes using strategies A and B, the influence of the activation agent has been evaluated. The best results for both enzymes were obtained for –NH$_2$ functionalized supports activated by GA. It could be explained by the fact that GA, contrary to carbodiimide with none molecular space, provides a long

Table 1
The principles of the covalent immobilization methods of enzymes used in this study.

	Strategy A	Strategy B	Strategy C
Support	SBA–15, MCM–41, Cell	SBA–15, MCM–41, Cell	SBA–15, MCM–41, Cell
Support functionalized group	–NH$_2$	–NH$_2$	–COOH
Activation agent	Glutaraldehyde (GA)	Carbodiimide (EDC/NHS)	Carbodiimide (EDC/NHS)
Enzyme reactive group	–NH$_2$	–COOH	–NH$_2$
Type of bond	secondary amine	amide	amide
Denotations of the prepared enzymatic powders	GOx–NH–CH–(CH$_2$)$_3$–CH–NH–SBA15 GOx–NH–CH–(CH$_2$)$_3$–CH–NH–MCM41 GOx–NH–CH–(CH$_2$)$_3$–CH–NH–Cell Lac–NH–CH–(CH$_2$)$_3$–CH–NH–SBA15 Lac–NH–CH–(CH$_2$)$_3$–CH–NH–MCM41 Lac–NH–CH–(CH$_2$)$_3$–CH–NH–Cell	GOx–C(=O)–NH–SBA15 GOx–C(=O)–NH–MCM41 GOx–C(=O)–NH–Cell Lax–C(=O)–NH–SBA15 Lac–C(=O)–NH–MCM41 Lac–C(=O)–NH–Cell	GOx–NH–C(=O)–SBA15 GOx–NH–C(=O)–MCM41 GOx–NH–C(=O)–Cell Lac–NH–C(=O)–SBA15 Lac–NH–C(=O)–MCM41 Lac–NH–C(=O)–Cell

spacer arm ensuring minimal steric hindrances for enzymes binding. It can be concluded that the covalent immobilization of both enzymes by their –NH$_2$ groups via GA to –NH$_2$ functionalized mesoporous silica powders (strategy A) provided the highest activities. Interestingly, in the similar comparative studies it is reported that among –OH, –COOH, and–NH$_2$ functionalized supports activated by divinylsulfone, carbodiimide, and GA, respectively, the last one was found as the most suitable technique for the covalent binding of Lac [9], invertase [10], and pepsin [11].
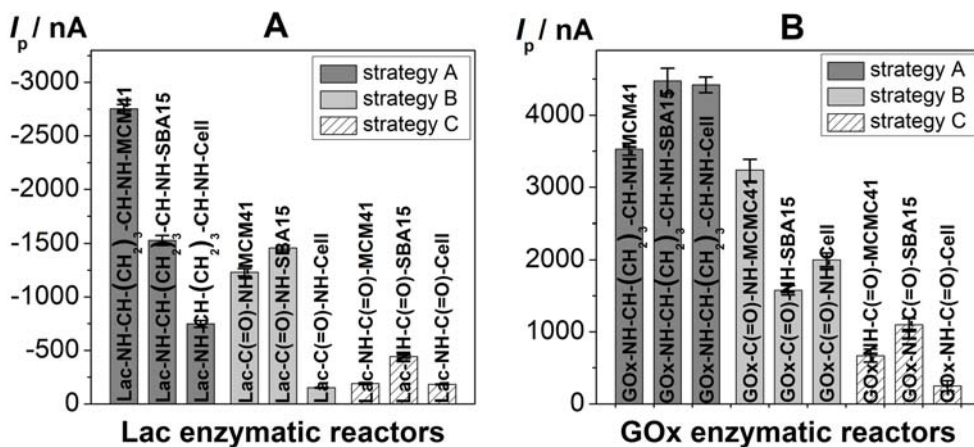
Fig. 1 Effect of the covalent attachment techniques on (A) laccase, and (B) and glucose oxidase biosensor responses. Experimental conditions: (A) c_{DOP} = 500 µmol L^{-1}, E_{det} = −50 mV, v_{flow} = 0.1 mL min^{-1}, V_{DOP}= 40 µL, carrier solution: 0.1 mol L^{-1}acetate buffer , pH = 4.8; (B) c_{Glu} = 500 µmol L^{-1}, E_{det} = −1100 mV, v_{flow} = = 0.1 mL min^{-1}, V_{Glu} = 40 µL, carrier solution: 0.1 mol L^{-1}acetate buffer, 0.001 mol L^{-1} Na$_2$EDTA, pH = 6.5.

When the effect of the method of the covalent enzyme coupling on the biosensor stability was evaluated, it was found that Lac bounded to –NH$_2$ functionalized supports via GA (strategy A) has shown the highest stability (>65% of the initial responses after 1 month) compared to other strategies, whereas GOx immobilized with two strategies (A and B) possessed approximately similar high stability (>80% of the initial responses in 1 month). Both enzymes bounded via –NH$_2$ groups to –COOH functionalized supports through EDC/NHS (strategy C) showed quite low stability.

4. Conclusions

Three different strategies, including the support selection, the anchor surface groups, and the activation method, have been compared for efficient covalent immobilization of Lac and GOx. The results showed that –NH$_2$ functionalized supports (SBA15–NH$_2$, Cellulose–NH$_2$ for GOx and MCM–NH$_2$ for Lac) activated by GA may be used to effectively bind enzymes in terms of high activity and stability.

References

[1]   Yosypchuk B., Barek J., Yosypchuk O.: Preparation and properties of reference electrodes based on silver paste amalgam. *Electroanalysis* **23** (2011), 2226–2231.

[2]   Liu Y., Chen J. Y.: Enzyme immobilization on cellulose matrixes. *J. Bioact. Compact. Polym.* **31** (2016), 553–567.

[3]   Hartmann M., Kostrov X.: Immobilization of enzymes on porous silicas – benefits and challenges. *Chem. Soc. Rev.* **42** (2013), 6277–6289.

[4]   Josypčuk O., Barek J., Josypčuk B.: Electrochemical biosensors based on enzymatic reactors filled by various types of silica and amalgam powders for measurements in flow systems. *Electroanalysis* **28** (2016), 3028–3038.

[5]   Josypčuk O., Barek J., Josypčuk B.: Amperometric determination of catecholamines by enzymatic biosensors in flow systems. *Electroanalysis* **30** (2018), 1163–1171.

[6]   Tvorynska S., Barek J., Josypčuk B.: Amperometric biosensor based on enzymatic reactor for choline determination in flow systems. *Electroanalysis* **31** (2019), 1901–1912.

[7]   Tvorynska S., Barek J., Josypčuk B.: Flow amperometric biosensor based on two enzymatic reactors (acetylcholinesterase-choline oxidase) for the detection of neurotransmitter acetylcholine. In: *Proceedings of the 15th International Students Conference "Modern Analytical Chemistry"*. K. Nesměrák (ed.). Prague, Faculty of Science, Charles University 2019, p. 61–66.

[8]   Tvorynska S., Barek J., Josypčuk B.: Acetylcholinesterase-choline oxidase-based mini-reactors coupled with silver solid amalgam electrode for amperometric detection of acetylcholine in flow injection analysis. *J. Electroanal. Chem.* **860** (2020), 113883.

[9]   Rekuć A., Kruczkiewicz P., Jastrzembska B., Liesiene J., Peczyńska-Czoch W., Bryjak J.: Laccase immobilization on the tailored cellulose-based Granocel carriers. *Int. J. Biol. Macromol.* **42** (2008), 208–215.

[10]   Bryjak J., Liesiene J., Štefuca V.: Man-tailored cellulose-based carriers for invertase immobilization. *Cellulose* **15** (2008), 631–640.

[11]   Szałapata K., Osińska-Jaroszuk M., Bryjak J., Jaszek M., Jarosz-Wilkołazka A.: Novel application of porous and cellular materials for covalent immobilization of pepsin. *Braz. J. Chem. Eng.* **33** (2016), 251–260.

Capillary flow injection analysis with electrochemical detection for carbohydrate analysis

NICOLE HEIGL*, FRANK-MICHAEL MATYSIK

Institute of Analytical Chemistry, Chemo- and Biosensors, Faculty of Chemistry and Pharmacy, University of Regensburg, Universitätsstraße 31, 93053 Regensburg, Germany
✉ *nicole.heigl@chemie.uni-regensburg.de*

Keywords

capillary flow injection analysis
carbohydrates
mass spectrometry
disposable electrodes
pulsed amperometric detection

Abstract

A simple capillary flow injection analysis system with amperometric detection was arranged for the development of a method for fast optimization of detection conditions in the context of the determination of carbohydrates by means of electrochemistry-capillary electrophoresis-mass spectrometry. This setup is free of electrical interference by high voltage and is perfect for studying the oxidation of various analytes. Furthermore, it assures easy coupling to MS and thus is an useful tool to investigate the corresponding oxidation products of an analyte.

1. Introduction

Carbohydrates are crucial for energy, structure and signaling in the human body [1]. There is a variety of carbohydrates, but the most important one for life is glucose as it is fundamental in the metabolism and photosynthesis [2]. Glucose is classified as hexose. These monosaccharides only differ in the position of hydroxyl substituents in some cases. In addition to the structural similarities, these molecules lack a chromophore and are not easily ionizable ($pK_a \sim 12$). Thus, detection in the UV region and separation of analytes by capillary electrophoresis (CE) are challenging [1, 3]. At the moment there are many different techniques for the analysis of carbohydrates commonly including time-consuming derivatization steps or eluents with high pH values (pH > 12) in ion chromatography. A well-established technique for the analysis of carbohydrates is high-performance anion-exchange chromatography with pulsed amperometric detection (HPAE-PAD) [4]. Electrochemical detection like AD is matching miniaturization, simple instrumentation, low cost and robustness, and thus is often used for flow-based systems such as CE and flow injection analysis (FIA) [5].

In this contribution, capillary flow injection analysis (CFIA) with AD will be presented as a method to apply and test AD for the detection of monosaccharides on different disposable thin-film or screen-printed electrodes. CFIA was chosen over conventional FIA for this purpose as the gravity flow in CFIA is stable for a longer time and very low sample consumption can be achieved [6]. The CFIA system was arranged as simple as possible and performed hydrodynamically to avoid any interferences. Furthermore, it assures the coupling of the flow system to a mass spectrometer. Thus, the same setup as used for CFIA can be utilized for capillary electrophoresis-mass spectrometry (CE-MS) experiments by changing the flow through the electrochemical flow cell in opposite direction. In future experiments, the experience in terms of AD on those electrodes will be used to develop electrochemical pretreatment protocols for carbohydrate determination by CE-MS.

2. Experimental

2.1 Reagents and chemicals

The following chemicals were used for this study, all of analytical grade: Ammonium acetate (NH_4OAc) was obtained from Merck (Darmstadt, Germany) and ferrocene methanol (FcMeOH) from ABCR (Karlsruhe, Germany). Milli-Q water (18.2 MΩ/cm) was generated by a Milli-Q Advantage A10® system (Merck Millipore, Darmstadt, Germany). Carrier solution was prepared by dissolving NH_4OAc (50 mmol L^{-1}) in Milli-Q water. FcMeOH solution was prepared by dissolving FcMeOH in carrier solution.

2.2 Instrumentation

Electrochemical measurements were performed using a µAutolab Type III potentiostat/galvanostat (Metrohm Autolab B. V., Utrecht, Netherlands) controlled by NOVA 2.0 software for experimental control and data acquisition. CFIA was performed using the setup illustrated in Fig. 1 (A) consisting of a carrier reservoir, sample vial and two fused silica capillaries (Polymicro Technologies, Phoenix, AZ, USA; inner diameter: 100 µm, length inlet: 40 cm, length outlet: 10 cm) connected to a commercially available flow cell from Micrux Technologies (model ED-FLOW-CELL, Oviedo, Spain). Inside of the flow cell the fused silica capillary was placed in a so-called wall-jet configuration above the working electrode of a disposable thin-film gold electrode (model ED-SE1-Au, Micrux Technologies, Oviedo, Spain) as can be seen in Fig. 1 (B). The thin-film electrodes were based on a three-electrode system with a gold working, auxiliary and quasi-reference electrode. The hydrostatic pressure was achieved by a height difference between inlet and outlet reservoir of 30 cm resulting in a gravity flow of the carrier solution through a fused silica capillary and subsequently through the flow cell.
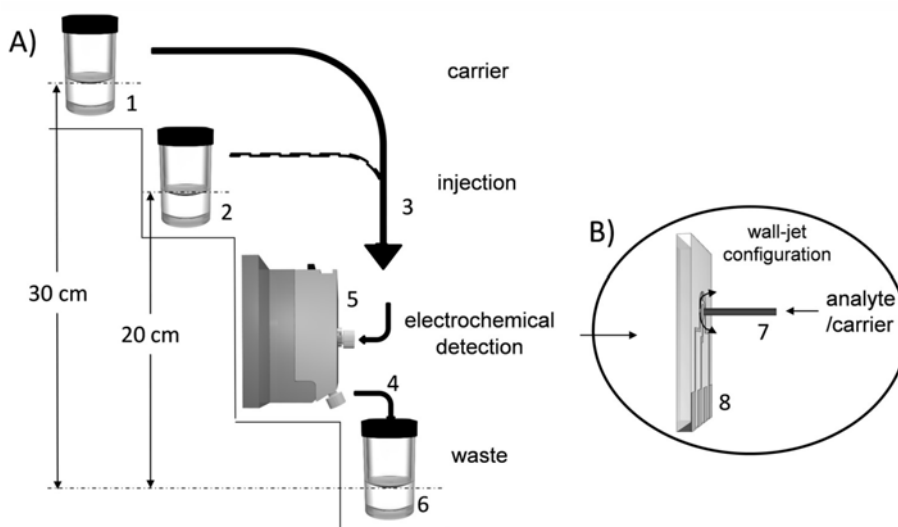
Fig. 1
(A) Scheme of the used capillary flow injection analysis setup: (1) carrier reservoir , (2) sample vial, (3) inlet capillary with a length of 40 cm and an inner diameter of 100 μm, (4) outlet capillary with a length of 10 cm and an inner diameter of 100 μm, both capillaries connected to (5) a commercially available flow cell from Micrux, and (6) a waste vial.
(B) Configuration inside the flow cell: (7) the fused silica capillary was placed in a so-called wall-jet configuration above the working electrode of (8) a disposable thin-film gold electrode.

The injection was carried out by lowering the vial containing the carrier solution to the level of the outlet, exchanging the carrier reservoir with the sample vial and lifting the sample vial to 20 cm for a defined period of time. Re-establishing the carrier reservoir took place the same way.

3. Results and discussion

A simple CFIA-AD system was arranged, where hydrostatic pressure by a height difference between inlet and outlet reservoir resulted in a gravitational flow. To obtain general information about the behavior of the assembled CFIA system preliminary experiments with FcMeOH were performed. To assure compatibility with MS later on, NH_4OAc was chosen as the electrolyte. Various height differences and injection times were tested and the injection at a height difference of 20 cm lasting for 10 s was found to be the optimum concerning feasibility and peak shapes. Injections of several solutions of FcMeOH of different concentrations showed that the concentration dependence of FcMeOH was linear in the investigated range (Fig. 2). Furthermore, experiments revealed that the injection procedure was established with reasonable precision. When repeating the injection of 0.5 mmol L^{-1} FcMeOH in carrier solution for ten times the relative standard deviation was found to be 3% for the manual injection protocol.
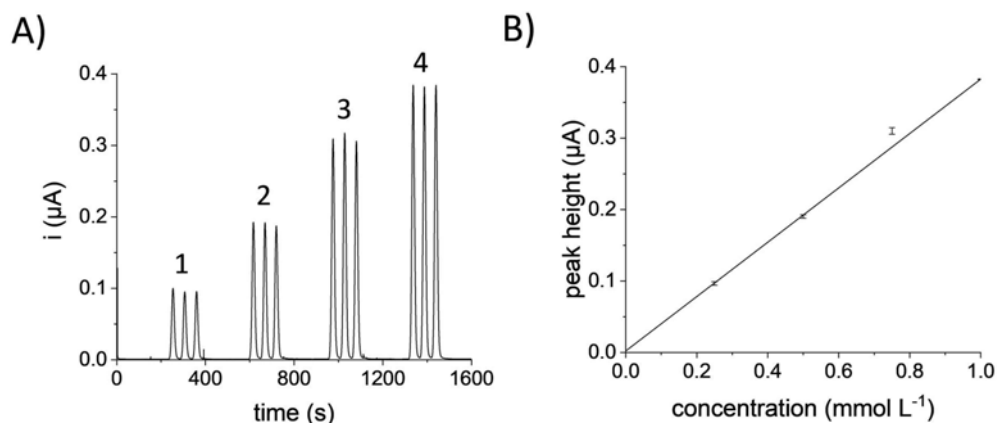
Fig. 2
(A) CFIA-AD recordings of three consecutive injections of (1) 0.25 mmol L^{-1}, (2) 0.5 mmol L^{-1}, (3) 0.75 mmol L^{-1}, and (4) 1 mmol L^{-1} FcMeOH in 50 mmol L^{-1} NH$_4$OAc, detection at a Micrux thin-film Au electrode at a constant potential of 0.3 V in a flow cell. Hydrodynamic injection lasted 10 s at a height difference of 20 cm.
(B) Calibration dependence of FcMeOH for CFIA-AD determination and detection at a Micrux thin-film Au electrode at a constant potential of 0.3 V in a flow cell. The standard deviations of peak heights (n=3) are indicated by error bars.

4. Conclusions

The presented system for CFIA-AD was arranged as simple as possible and represents a useful approach for the development of a method for fast optimization of detection conditions in the context of the determination of carbohydrates by means of electrochemistry-CE-MS. The setup is free of electrical interference by high voltage, compatible with MS and thus promising for studying the oxidation of various analytes.

References

[1]   Lu G., Crihfield C. L., Gattu S., Veltri L. M., Holland L. A.: Capillary electrophoresis separations of glycans. *Chem. Rev.* **118** (2018), 7867–7858.
[2]   Galant A. L., Kaufman R. C., Wilson J. D.: Glucose: Detection and analysis. *Food Chem.* **188** (2015), 149–160.
[3]   Sarazin C., Delaunay N., Costanza C., Eudes V., Gareil P.: Application of a new capillary electrophoretic method for the determination of carbohydrates in forensic, pharmaceutical, and beverage samples. *Talanta* **99** (2012), 202–206.
[4]   Rohrer J.S., Basumallick L., Hurum D.: High-performance anion-exchange chromatography with pulsed amperometric detection for carbohydrate analysis of glycoproteins. *Biochem.* **78** (2013), 697–709.
[5]   Islam M.A., Mahbub P., Nesterenko P.N., Paull B., Macka M.: Prospects of pulsed amperometric detection in flow-based analytical systems – A review. *Anal. Chim. Acta* **1052** (2019), 10–26.
[6]   Matysik F.-M., Werner G.: Trace metal determination in tears by anodic stripping voltammetry in a capillary flow injection system. *Analyst* **118** (1993), 1523–1526.

Application of covalent coatings based on imidazolium cations for separation and on-line preconcentration of basic and neutral analytes in capillary electrophoresis

Anastasia V. Kravchenko[a, *], Ekaterina A. Kolobova[a, b], Liudmila A. Kartsova[a]

[a] *Department of Organic Chemistry, Institute of Chemistry, Saint Petersburg State University, 26 Universitetskii prospect, 198504 St. Petersburg, Peterhof, Russia*
   ✉ *kravchenko161216@gmail.com*
[b] *The Federal State Institute of Public Health "The Nikiforov Russian Center of Emergency and Radiation Medicine", The Ministry of Russian Federation for Civil Defence, Emergencies and Elimination of Consequences of Natural Disasters, 54 Optikov st., 197082 St. Petersburg, Russia*

Keywords

biological active analytes
capillary coating
capillary electrophoresis
imidazolium ionic liquids

Abstract

The method of capillary electrophoresis (CE) is actively developed and more and more attracts scientists attention every year. However, the sorption of analytes on surface of fused-silica capillary walls is one of the significant disadvantages of this approach. The formation of coatings on the inner capillary surface is typical way to prevent sorption and to increase separation efficiency and selectivity of determined analytes. Coatings that covalently bonded to capillary walls is more suitable because they are stable and provides high reproducibility of analysis. The present work is focused on the development of the method of electrophoretic determination of biological active analytes using a covalent coating based on imidazolium cations. The effect of substituent in imidazolium ring on main electrophoretic parameters was examined. It was shown that alkylimidazolium coatings contribute to significant reducing of biogenic amines limits of detection, while β-cyclodextrinimidazolium covalent coating allows to separate both of hydrophobic and hydrophilic analytes in one run.

1. Introduction

To prevent sorption on the capillary surface and improve separation efficiency and selectivity of determined analytes, coatings are formed on the capillary surface. There are two types of ones, namely dynamic and covalently bonded coatings. Despite the simplicity of creation, dynamic coatings cannot provide required reproducibility, while covalent coatings contribute the stable electro-osmotic flow (EOF) and high reproducibility of the analysis. In most cases, the

analytes nature determines type of used modifiers because suitable ones can provide accessorial interaction between the analytes and the stationary phase improving separation selectivity and efficiency [1, 2]. Ionic liquids have been widely used in analytical chemistry [3] and separation techniques particularly in capillary electrophoresis [4]. Early researches [5–9] have shown opportunity of covalently bonded imidazolium ionic liquids for electrophoretic separation. However, the effect of various substituents in imidazolium ring has not been described previously. Thus, the purpose of this study was to create covalent coatings based on ionic liquid with various substituents and to compare their analytical capabilities in the electrophoretic separation of biologically active compounds.

2. Experimental

2.1 Reagents and chemicals

(3-Glycidyloxypropyl)trimethoxysilane (GPTMS), hydrochloric acid, sodium dodecyl sulfate (SDS), imidazole, 2,2-diphenyl-1-picrylhydrazyl (DPPH), *p*-toluen-sulfonyl chloride, β-cyclodextrin, hydrocortisone (F), 11-deoxycortisol (S), Corticosterone (B), *rac*-ketoprofen, (–)-adrenaline (A), L-(–)-norepinephrine (NE), DL-normetanephrine (NMN), dopamine (DA), D,L-metanephrine hydrochloride (Met), serotonin hydrochloride (Ser), homovanillic acid (HVA), 2,4-dihydroxy-benzoic acid (2,4-DHBA), 3,4-dihydroxy-L-phenylalanine (DOPA), L-tryptophan (Trp), L-tyrosine (Tyr) were purchased from Sigma-Aldrich (USA). 1-Bromo-butane, 1-bromooctane were purchased from ReagentPlus (Ukraine). Sodium dihydrogenphosphate dihydrate, acetone, *N,N*-dimethylformamide (DMF) were obtained from Merck (Germany). All reagents used were analytical grade. All solutions were prepared using deionized water.

2.2 Instrumentation

Capillary electrophoresis experiments were carried out using the system of capillary electrophoresis CAPEL'-105 M (Lumex, Russia) with UV-spectrophotometric detector (wavelength range 190–360 nm). Separations were performed using 58 × 49 cm (9 cm to the detector, outside diameter 360 μm, and inner diameter 50 μm) coated silica capillaries (Lumex, Russia). The buffer pH was measured with a pH-meter HI 2210–2216 (Hanna).

2.3 Capillary coating synthesis

Earlier our research team has proposed the synthesis route for the covalent coatings based on imidazolium cation functionalized with alkyl group [10] and β-cyclodextrin [11]. All capillaries were prepared according above-mentioned

manuscripts and characterized by the EOF mobility measurement and scanning electron microscopy. The synthesis consisted of following steps: preparation of a capillary to create a covalent coating (heating capillary filled with 2M NaOH at 90 °C for 1h and drying followed); silylation with GPTMS and functionalization with the imidazole solution followed modification by butyl- and octylbromide or tosyl-β- cyclodextrin (see details in [10] and [11]).

2.4 Solutions

A stock buffer solution in concentration 50mM was prepared by dissolving appropriate amount of sodium dihydrogenphosphate dihydrate in deionized water adjusting pH to 2.0 with 1M hydrochloric acid. This buffer solution was then diluted with deionized water.

All the sample stock solutions were prepared with concentration 1.0 mg mL^{-1}. The stock solutions of the neurotransmitters and their metabolites (adrenaline, noradrenaline, dopamine, normetanephrine, metanephrine, serotonin, homo-vanillic acid), and 2,4-dihydroxybenzoic acid as inner standard, and amino acids (tryptophan, 3,4-dihydroxy-L-phenylalanine, tyrosine) were prepared in 0.1 M hydrochloric acid. The stock solutions of steroids (hydrocortisone, 11-deoxycortisol and corticosterone) were prepared in acetonitrile. The stock solutions of ketoprofen racemate and *S*-ketoprofen were prepared in acetonitrile/water solution (10:90, *v/v*).

Until electrophoretic analysis the stock solutions were stored at −16 °C. The working solutions were prepared by diluting the initial solutions with water just before the experiments.

3. Results and discussion

Covalent coatings based on *N*-alkylimidazolium cation were especially suitable for separation of neurotransmitters and their metabolites (Fig.1). In addition, the combination of covalent coating with on-line preconcentration techniques allows to the significant decrease of these analytes limits of detection (*LOD*). Accessorial interactions positively charged analytes with positively charged imidazole improve separation selectivity (via π-π interaction) and efficiency (concentration in tight zones via electrostatic repulsion). Sodium dodecyl sulfate (SDS) added into background electrolyte (in concentration above critical micelle concentration) strongly interacts with hydrophobic alkyl groups in covalent coating structure. The negatively charged SDS layer is formed on inner capillary surface. The double reversing EOF allows us to carry out electrokinetic injection of sample and on-line preconcentration by sweeping simultaneously. *LOD* were decline to 0.8–2.0 ng mL^{-1}. The length of alkyl substituent also affects the stacking efficiency factor and *LOD*. More hydrophobic octyl groups compare to butyl provide more effective interaction with SDS and, as result, lower *LOD*.
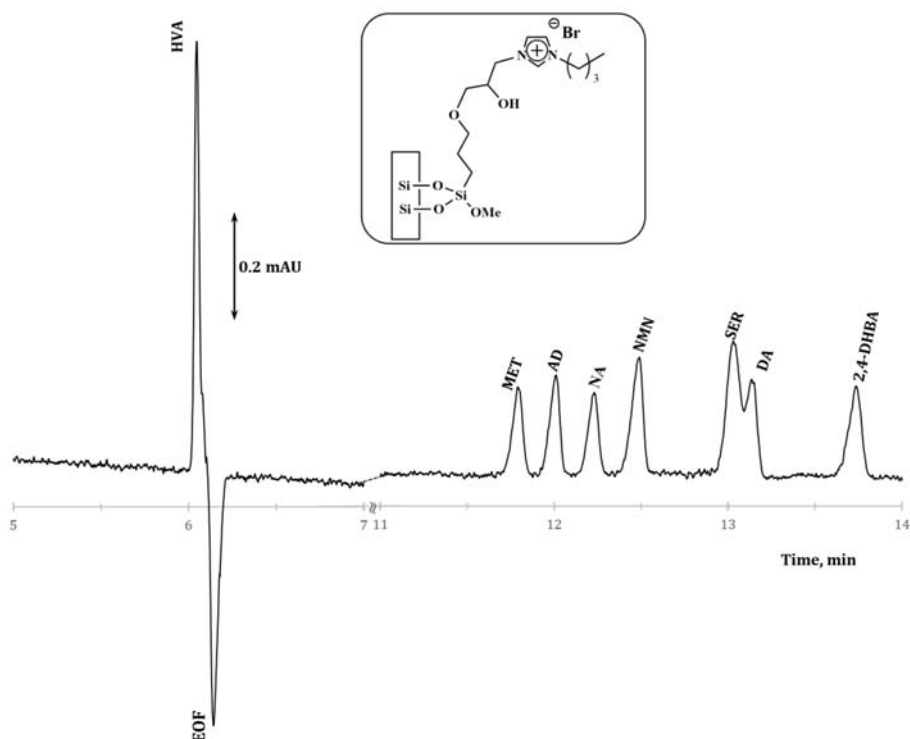
Fig. 1 Electropherogram of mixture of neurotransmitters and their metabolites: adrenaline (A), norepinephrine (NE), normetanephrine (NMN), dopamine (DA), metanephrine (Met), serotonin (SER), homovanillic acid (HVA), and the inner standard 2,4-dihydroxybenzoic acid (2,4-DHBA) on covalently modified with *N*-buthylimidazolium ionic liquids capillary. Conditions: 10 mM NaH_2PO_4 (adjusted to pH = 2.0 by 1 M HCl); injection: 5.0 s×30 mbar; –20 kV; 220 nm; model mixure: $10 \, \mu g \, mL^{-1}$ (MET, AD, NMN, NA, DA, 2,4-DHBA), $5 \, \mu g \, mL^{-1}$ (SER), and $20 \, \mu g \, mL^{-1}$ (HVA).

Covalent coating modified β-CD has not shown sharp reducing of *LOD* by on-line preconcentration. Stacking, sweeping (SDS as micelle reagent), field-enhanced sample injection were examined using different model mixtures of analytes. Nevertheless, this coating allows simultaneous separation of both of hydrophobic steroid hormones and hydrophilic biogenic amines in a single run (Fig 2).

The guest-host interaction hydrophobic cavity of β-cyclodextrin with the hydrophobic steroids leads to the formation of complex which affects steroids electrophoretic mobility. At the same time, β-cyclodextrin can act as a chiral selector and baseline separation of ketoprofen enantiomers has also been achieved.
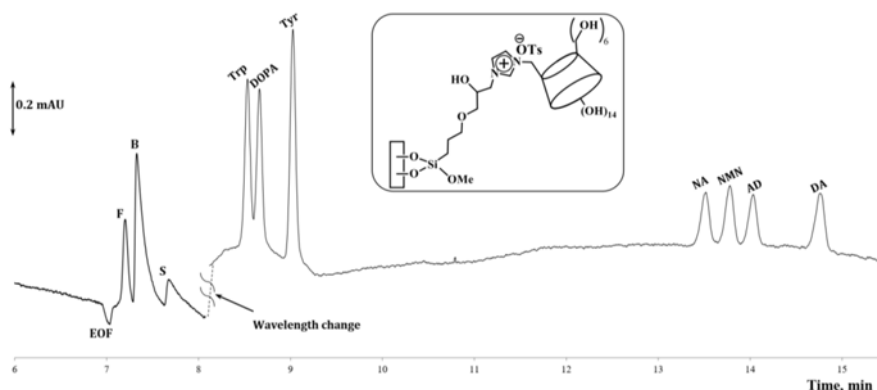
Fig. 2 Electropherogram of simultaneous separation of hydrophobic (steroid hormones) and hydrophilic analytes (amino acids and biogenic amines) in single run with covalent coating based on imidazole and β-CD. Conditions: 10 mM NaH_2PO_4 (adjusted to pH = 2.0 by 1 M HCl); injection: 2.0 s×30 mbar; –20 kV; 254 nm (1–8 min) and 220 nm (8–15 min), 0 mbar (1–10 min) and 40 mbar (10–15 min). Model mixture: corticosterone (B), hydrocortisone (F), 11-deoxycortisole (S) 5 µg mL^{-1}; L-tryptophan (Trp), 3,4-dihydroxy-L-phenylalanine (DOPA) 10 µg mL^{-1}; L-tyrosine (Tyr) 5 µg mL^{-1}; noradrenaline (NA), normetanephrine (NMN), adrenaline (AD), dopamine (DA) 20 µg mL^{-1}.

Table 1
The summation of possibilities of covalent coatings based on imidazolium cation.

Covalent coating type	Electrophoretic separation of				On-line preconcentration
	biogenic amines and their metabolites	amino acids	steroid hormones	ketoprofen enantiomers	
N-β-cyclodextrinimidazolium covalent coatings	yes	yes	yes	yes	the suitable approach was not founded
N-alkylimidazolium covalent coatings	yes	yes	non separated	non separated	the significant reducing for biogenic amines *LOD*

4. Conclusions

It was shown that structure covalent coating affects its analytical characteristics. We compared two types of covalent coating differing substituent in imidazolium ring, namely alkyl group and β-cyclodextrin. The first type is great coupled with on-line preconcentration technic but it is limited to effectively determine of biogenic amines only, while the second type (with β-cyclodextrin) showed the possibilities to separate various analytes but suitable on-line mode has not been found. The main points are summarized in Table 1.

Acknowledgments

References

[1]   Hu L.F., Yin S.J., Zhang H., Yang F.Q.: Recent developments of monolithic and open-tubular capillary electrochromatography (2017–2019). *J. Sep. Sci.* **43** (2020), 1942–1966.

[2]   Kartsova L.A., Kravchenko A.V, Kolobova E.A.: Covalent coatings of quartz capillaries for the electrophoretic determination of biologically active analytes. *J. Anal. Chem.* **74** (2019), 729–737.

[3]   Ho T.D., Zhang C., Hantao L.W., Anderson J.L.: Ionic liquids in analytical chemistry: Fundamentals, advances, and perspectives. *Anal. Chem.* **86** (2014), 262–285.

[4]   Tang, S., Liu, S., Guo, Y., Liu, X., Jiang, S.: Recent advances of ionic liquids and polymeric ionic liquids in capillary electrophoresis and capillary electrochromatography. *J. Chromatogr. A*. **1357** (2014), 147–157.

[5]   Qin W., Li S.F.Y.: Electrophoresis of DNA in ionic liquid coated capillary. *Analyst* **128** (2003), 37–41.

[6]   Qin W., Wei H., Li S.F.Y.: 1,3-Dialkylimidazolium-based room-temperature ionic liquids as background electrolyte and coating material in aqueous capillary electrophoresis. *J. Chromatogr. A* **985** (2003), 447–454.

[7]   Qin W., Fong S., Li Y.: Determination of ammonium and metal ions by capillary electrophoresis–potential gradient detection using ionic liquid as background electrolyte and covalent coating reagent. *J. Chromatogr. A.* **1048** (2004), 253–256.

[8]   Qin W., Li S.F.Y.: An ionic liquid coating for determination of sildenafil and UK-103,320 in human serum by capillary zone electrophoresis-ion trap mass spectrometry. *Electrophoresis* **23** (2002), 4110–4116.

[9]   Borissova M., Vaher M., Koel M., Kaljurand M.: Capillary zone electrophoresis on chemically bonded imidazolium based salts. *J. Chromatogr. A.* **1160** (2007), 320–332.

[10] Kolobova E., Kartsova L., Kravchenko A., Bessonova E.: Imidazolium ionic liquids as dynamic and covalent modifiers of electrophoretic systems for determination of catecholamines. *Talanta* **188** (2018), 183–191.

[11] Kravchenko A., Kolobova E., Kartsova L.: Multifunction covalent coatings for separation of amino acids, biogenic amines, steroid hormones, and ketoprofen enantiomers by capillary electrophoresis and capillary electrochromatography. *Sep. Sci. plus* **3** (2020), 102–111.

Determination of vanillin in smoking mixtures by spectrophotometry

ELIZAVETA EFREMENKO*, ANNA CHERNOVA, OLGA BASTRYGINA

Department of Chemical Engineering, National Research Tomsk Polytechnic University, Lenin avenue 30, 634 050 Tomsk, Russia ✉ eae@tpu.ru

Keywords

smoking mixtures
spectrophotometry
vanillin

Abstract

The research deals with determination of vanillin in smoking mixtures by ultraviolet-visible spectrophotometry. The method showed good linearity in the range of 0.05–$0.12\,\mathrm{g\,L^{-1}}$ with a limit of detection $0.05\,\mathrm{g\,L^{-1}}$. After validation studies, the method was successfully applied to the determination of vanillin in smoking mixtures with satisfactory results. It was shown that the error of this method does not exceed 1%. The developed spectrophotometric procedure for determining vanillin in smoking mixtures can be used as a control.

1. Introduction

Synthetic 4-hydroxy-3-methoxybenzaldehyde (vanillin) is used as a flavoring agent in foods, drinks, perfumes and pharmaceuticals [1]. However, at certain concentrations, the substance may accumulate in the body, have a toxic effect, and at high concentrations may be fatal (lethal dose: LD_{50} (oral, rat) $=2\,\mathrm{g\,kg^{-1}}$, LD_{50}(oral, guinea pig) $= 1.4\,\mathrm{g\,kg^{-1}}$, LD_{50}(intravenous, dog) $= 1.32\,\mathrm{g\,kg^{-1}}$; lethal concentration LC (inhalation, mouse)$= 41.7\mathrm{g\,kg^{-1}}$) [2]. According to Russian State Standart GOST 12.1.005-88, the toxic effects of vanillin in the workplace in the form of vapours or aerosols are observed at concentrations above $1.5\,\mathrm{mg\,m^{-3}}$. Chromatography [3], spectrophotometry [4], capillary electrophoresis are used for vanillin determination in different objects.

Currently, smoking mixtures for hookahs and electronic cigarettes are widely used among young people. These mixtures are not controlled for the content of substances and are freely available, considering them more harmless with respect to ordinary cigarettes. Thus, the development of a method for the determination of 4-hydroxy-3-methoxybenzaldehydein smoking mixtures is relevant.

2. Experimental

2.1 Reagents and chemicals

A sample of vanillin (purity: 98%) was taken as the object of study. As solvents, we used 95% ethanol. All chemicals used were of analytical reagent grade.

2.2 Instrumentation

The optical density of samples was measured in cuvette with an absorbing layer thickness of 10 mm using a Cary 60 spectrophotometer (Agilent, USA). All measurements were carried out at room temperature.

2.3 Sample preparation

Sample preparation of the investigated objects consisted of the preliminary dissolution of the sample in 95% ethanol. The sample 10 mg of tobacco "Adalya – Vanilla" (Turkey) was diluted in 10 µL of 95% ethanol to the concentration of $1 \, g \, L^{-1}$. The sample 10 µL of "Flavoring TPA – Vanilla Custard" (USA) was diluted in 10 µL of 95% ethanol The resulting solution was diluted six times to the concentration of $0.17 \, \mu L \, cm^{-3}$.

3. Results and discussion

To determine vanillin in the samples, the optical properties of vanillin in various solvents were determined. As a result, the 95% ethanol was chosen as the optimal solvent [4].

It has been established that in the UV spectra of the analyte, absorption bonds are observed with maximum values at 230.0, 280.0, and 310.0 nm, which corresponds to published data [4, 5] (Fig.1).

To quantify vanillin the calibration curve of the optical density on the concentration of vanillin in 95% ethanol was obtained at concentrations 0.05, 0.06, 0.07, 0.08, 0.10, and 0.12 $g \, L^{-1}$. Calibration curve of vanillin in 95% ethanol at a wavelength of 280 nm is

$$A_{280} = 8.1914 \, c \, [g \, L^{-1}] + 0.0357 \tag{1}$$
$$R^2 = 1$$

Calibration curve of vanillin in 95% ethanol at 310 nm is

$$A_{310} = 7.3824 \, c \, [g \, L^{-1}] + 0.0301 \tag{2}$$
$$R^2 = 1$$
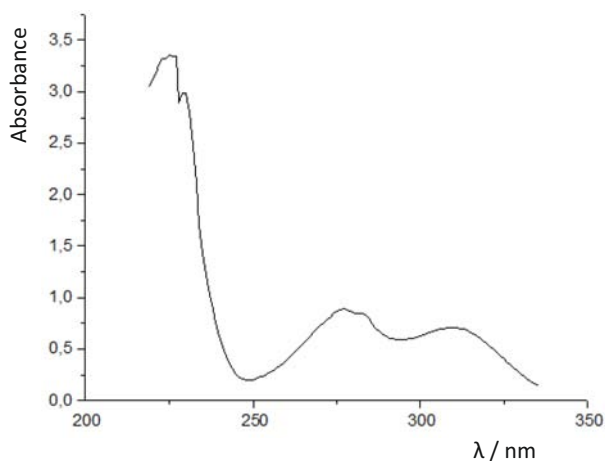
Fig. 1 Absorption spectrum of vanilin solution in 95% ethanol at concentration 0.1 mol L^{-1} (an absorbing layer thickness of 10 mm).

Table 1
Testing methods introduced found of vanillin in the samples at 310 nm by spectrophotometric method ($n = 5$, $p = 0.99$; S – standard deviation, Sx – relative standard deviation; Δx – absolute error; δ – relative error).

Sample	λ / nm	Took / mg	Found / mg	S	Sx	Δx	δ / %
Flavoring TRA – Vanilla Custard	310	10.850	10.4096	0.0024	0.0011	0.0006	0.0306
Adalya – Vanilla	310	10.0000	1.0162	0.0019	0.0009	0.0002	0.0025
Flavoring TRA – Vanilla Custard	280	10.0300	9.6062	0.0033	0.0015	0.0032	0.0042
Adalya – Vanilla	280	10.0000	1.0122	0.0013	0.0006	0.0012	0.0017

In the spectra of the analyzed sample solutions absorption maxima (280.0 nm and 310.0 nm) characteristic for vanillin were observed. The amount of vanillin in the sample was determined using calibration curves at 280 and 310 nm. Weighted least square regression was applied to the calibration curves to improve the accuracy, especially at in low concentration level range. Good linearity was found in the range of 0.05–0.12 g L^{-1} with a detection limit of 0.05 g L^{-1}. The results are presented in the Table 1.

4. Conclusions

The developed method can be used as a control method. The error in the method for determining vanillin in the sample "Flavoring TPA – Vanilla Custard" with a known concentration of vanillin was 0.004%. According to the data obtained, we recommend a wavelength of 280 nm for the determination of vanillin in samples.

Then, the developed method was tasted on the sample "Adalya – Vanilla" sample with a more complex composition and an unknown concentration of vanillin was taken. The vanillin content in the sample was determined according to the developed method, it amounted to 10% of the total mass. Studies have shown the possibility of using spectrophotometric analysis for the qualitative and quantitative determination of vanillin. Also based on preliminary studies, a spectrophotometric procedure was developed for the quantitative determination of vanillin based on absorption in ethanol in the wavelength range 200–400 nm.

References

[1]   https://www.rusnauka.com/43_DWS_2015/Chimia/6_203179.doc.htm (accessed 25th February 2019)

[2]   https://www.cdc.gov/niosh/rtecs/default.htm (accessed 11st April 2020)

[3]   Ali L., Perfetti G., Diachenko G.: Rapid method for the determination of 342 coumarin, vanillin, and ethyl vanillin in vanilla extract by reversed-phase liquid 343 chromatography with ultraviolet detection. *J. AOAC Int.* **91** (2008), 383–386.

[4]   Бастрыгина О.А., Ефременко Е.А., Чернова А.П. Выделение ванилина, исследование его оптических свойств, определение в биологическом материале. В: *Химия и химическая технология в XXI веке. Материалы XX Международной научно-практической конференции имени профессора Л.П. Кулёва студентов и молодых ученых.* Томск, Национальный исследовательский Томский политехнический университет 2019, с. 301–302.

[5]   Weast R.C.: *Handbook of Chemistry and Physics.* 60th ed. Boca Raton, CRC Press 1979, p. 143.

Uranyl ion-selective electrode with solid contact

Karolina Pietrzak*, Cecylia Wardak

Department of Analytical Chemistry, Institute of Sciences, Faculty of Chemistry, Maria Curie-Sklodowska University, Maria Curie-Sklodowska Sq. 3, 20-031 Lublin, Poland
✉ *karolina.pietrzak@poczta.umcs.lublin.pl*

Keywords
ion-selective electrode
solid contact
uranyl

Abstract
New all solid state uranyl ion-selective electrodes with low detection limits (7.1×10^{-7} mol L^{-1}), short response time, good selectivity and stable and reproducible potential were developed. Many types of electrodes with different active ingredient content in ion-selective membrane (bis(2,4,4-trimethylpentyl)phosphonium acid, Cyanex-272) were tested. As an additive, an ionic liquid 1-octyl-3-methyl-imidazole chloride was used. The optimal composition of the ion-selective membrane was chosen from all electrodes based on the determination and comparison of analytical parameters of the sensors.

1. Introduction

Uranium belongs to the group of hazardous elements. It is a highly harmful and radioactive element, toxic to humans and all living organisms [1, 2]. Inhaled with air, it has a particularly destructive effect on the kidneys, and as a result of accumulation in white blood cells, it can also cause impairment of the immune system [2]. Uranium occurs at several degrees of oxidation, however in aqueous solutions the most stable form is uranyl ion ($UO_2(II)$) [1, 2]. The presence of uranium in the environment is caused by, among others natural soil and rock erosion. Environmental pollution with this element is also constantly increasing due to human activity: coal combustion, uranium ore mining and processing, the arms industry, and the use of uranium as nuclear fuel in fission reactors [3]. It is very important to constantly monitor the concentration of uranium both in the natural environment in order to assess its state and safety (especially in the case of drinking water), as well as in all stages of processing processes associated with the nuclear industry to avoid the occurrence of nuclear pollution [1, 3].

Scientists have made many attempts to develop research methods to determine the content of uranyl compounds in liquid samples. Efforts were made to use many analytical methods for this purpose, including spectrophotometry,

plasma spectrometry, luminescence spectroscopy, voltammetry or chromatography methods [2].

Due to many advantages of potentiometric methods (among them lower costs, easier operation of devices, quick response and the ability to perform measurements in flow mode) [3], a number of potentiometric sensors have also been developed that could be successfully used in this type of research. The most popular potentiometric sensors include ion-selective electrodes (ISEs), which are characterized by low-energy consumption, small size and portability and are successfully widely used for the determination of both inorganic and organic ions in clinical analysis, process technology as well as in control the state of the natural environment [4, 5]. Removal of the internal solution containing the same analyte to which the electrode is sensitive resulted in the so-called solid contact ISEs, which are much smaller in size than their predecessors, are more convenient to use and more mechanically resistant. In this type of sensors, however, it is important to achieve satisfactory potential stability, which is necessary to obtain satisfactory results [5]. A very important part of ISEs is the ion-selective membrane, whose composition determines the analytical parameters of the sensors. Researchers are currently focusing on the production and testing of new substances that could be successfully used as membrane components and solid contacts that would allow to obtain new sensors with lower detection limits, longer lifetime and better potential stability, and to determine new, previously unattainable analytes [4].

As the active components of the membrane sensitive to uranyl ion, scientists have already used: Kryptofix 22DD (4,13-didecyl-1,7,10,16-tetraoxa-4,13-diazacyclooctadecane) [2], Cyanex extractants (bis(2,4,4-trimethylpentyl)phosphinic acid, bis(2,4,4-trimethylpentyl)monothiophosphinic acid, and bis(2,4,4-trimethylpentyl)dithiophosphinic) acid [3], DBBP (dibutyl butylphosphonate) and DOPP (di-*n*-octyl phenylphosphonate) [6], DMSO (dimethylsuphoxide) [7], TTPTP (5,6,7,8-tetrahydro-8-thioxopyrido[4',3',4,5]thieno[2,3-*d*]pyrimidine-4(3H)one) [8] or TEHP (tris(2-ethylhexyl)phosphate) and TPTU (*O*-(1,2-dihydro-2-oxo-1-pyridyl)-*N,N,N',N'*-bis(tetra-methylene)uronium hexafluorophosphate) [9].

2. Experimental

2.1 Reagents and chemicals

This paper presents research on the design and properties of ion-selective electrodes with solid contact for the determination of uranyl ions. Bis(2,4,4-trimethylpentyl)phosphonium acid (Cyanex-272) was used as the active component of the membrane, which was described in the literature as a good uranyl extractant [10]. In order to ensure a constant potential of this electrode and reduce the electrode resistance, the ion-sensitive membrane was enriched with a few percent addition of 1-octyl-3-methylimidazole chloride ionic liquid.

Table 1
Quantitative and qualitative composition of electrode membranes: Cyanex-272 (bis(2,4,4-tri-methylpentyl)phosphoric acid), TBP (tri-*n*-butyl phosphate), and OMImCl (1-octyl-3-methyl-imidazole chloride).

Abbreviation of electrode	Membrane composition / % (*w/w*)			
	Cyanex-272	PVC	TBP	OMImCL
ISE-1	0.0	33	62.0	5
ISE-2	0.5	33	61.5	5
ISE-3	1.0	33	61.0	5
ISE-4	3.0	33	59.0	5
ISE-5	5.0	33	57.0	5
ISE-6	10.0	33	52.0	5

Several types of ion-selective electrodes were prepared using an Ag/AgCl electrode as an internal electrode, which differ in the quantitative and qualitative composition of the membranes. All compositions are listed in Table 1.

2.2 Instrumentation

Measurements were made at room temperature using a 16-channel data collection system (Lawson Labs. Inc. USA) coupled to a computer in solutions mixed with a mechanical stirrer. A silver / silver chloride electrode with double junction was used as the reference electrode.

3. Results and discussion

The effect of ion-selective membrane composition on the properties of the obtained potentiometric sensors was examined by determining their basic analytical parameters, including: slope of the electrode characteristics, detection limit, measuring range (concentration range in which the course of the electrode characteristics is rectilinear), pH range (in which it has no effect for electrode potential) and response time. The obtained values of the tested parameters are shown in Table 2.

Figure 1 shows the calibration curves of the tested electrodes determined in $UO_2(NO_3)_2$ solutions in the concentration range 1×10^{-7}–1×10^{-1} mol L^{-1}. As it can be seen in Fig. 1 and Table 2 all electrodes were sensitive to uranyl ions, but in different extend. The best response exhibited ISE-3 containing 1% (*w/w*) of ionophore. Increasing the ionophore content in the membrane shortened the linearity range of the calibration curve and its supernenstian slope.

The selectivity of the tested electrodes was estimated by determining the selectivity coefficients in relation to interfering ions. For this purpose, the separate solution method was used (extrapolating response curves to $a_i = a_j = 1$ mol L^{-1}). Comparison of ISE-1 and ISE-3 electrode selectivity is shown in Fig. 2.

Table 2
Selected parameters and their determined values of tested ion selective electrodes.

Abbreviation of electrode	Slope / mV/$pa(UO_2^{2+})$	Detection limit / mol L^{-1}	Linear range / mol L^{-1}	Response time / s	pH range
ISE-1	29.7	2.5×10^{-5}	$5\times10^{-5}-1\times10^{-1}$	5–8	2.8–4.2
ISE-2	29.2	6.5×10^{-6}	$1\times10^{-5}-1\times10^{-1}$	5–8	2.5–6.0
ISE-3	29.8	7.1×10^{-7}	$1\times10^{-5}-1\times10^{-1}$	5–8	2.4–6.0
ISE-4 (I)	35.7	3.1×10^{-6}	$5\times10^{-4}-1\times10^{-1}$	5–8	n.d.
ISE-4 (II)	24.2	3.1×10^{-6}	$5\times10^{-6}-5\times10^{-4}$	5–8	n.d.
ISE-5 (I)	63.8	n.d.	$1\times10^{-3}-1\times10^{-1}$	5–10	n.d.
ISE-5 (II)	23.4	n.d.	$5\times10^{-5}-1\times10^{-3}$	5–10	n.d.
ISE-6 (I)	73.3	n.d.	$1\times10^{-3}-1\times10^{-1}$	5–10	n.d.
ISE-6 (II)	22.2	n.d.	$5\times10^{-5}-1\times10^{-3}$	5–10	n.d.
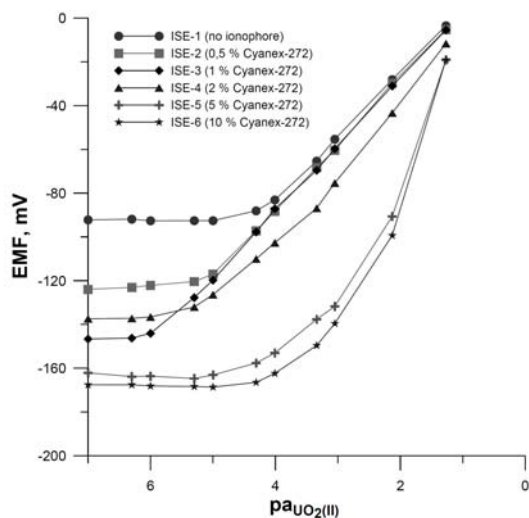
Fig. 1 Calibration curves of the tested electrodes obtained in $UO_2(NO_3)_2$ solutions in the concentration range from 1×10^{-7} to 1×10^{-1} mol L^{-1}.
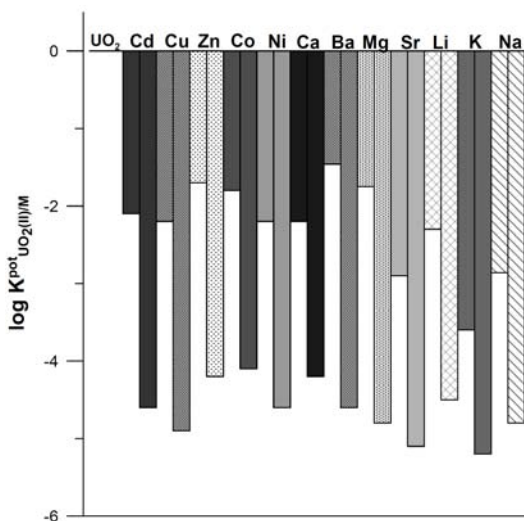
Fig. 2 Comparison of selectivity coefficients (log $K^{pot}(UO_2(II))/M$) for electrodes ISE-1 (1st column) and ISE-3 (2nd column).
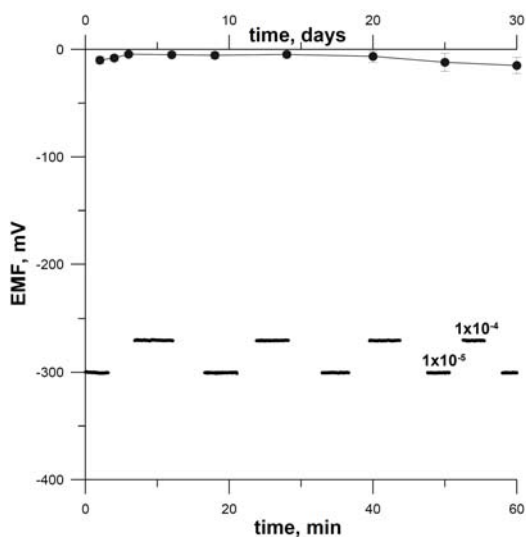
Fig. 3 Stability (●), reproducibility and reversibility (–) of the potential of ISE-3. Standard deviations given on the plot are determined for the same three ISE-3.

In order to examine the reversibility of the potential of the tested electrodes, potential measurements were made alternately in solutions 1×10^{-4} mol L^{-1} and 1×10^{-5} mol L^{-1} of $UO_2(NO_3)_2$. The recorded potential readings are shown in Fig. 3. Long-term potential stability and sensor reproducibility were evaluated by determining the average value of the electrode potential in a 0.1 mol L^{-1} $UO_2(II)$ ion solution over time for three identical ISE-3. These measurements were made to observe changes in the potential of electrodes with the same concentration over a long period of time (30 days). Figure 3 shows the long-term potential stability and reproducibility determined for three identical sensors.

4. Conclusions

As a result of the tests, ion-selective electrode for the determination of uranyl ions was obtained which is easy to design and use. The best analytical parameters exhibited ISE-3 containing 1% ionophore in the ion-selective membrane. For this type of electrodes, the detection limit of 7.1×10^{-7} mol L^{-1}, linearity of the electrode calibration curve in the range 1×10^{-6}–1×10^{-1} mol L^{-1} and response time 5–8 s were obtained. In addition, the manufactured sensors also showed stable, reproducible and reversible potential, and very good selectivity in relation to the tested interferents.

References

[1] Ansari R., Mosayebzadeh Z.: Construction of a new solid-state U(VI) ion-selective electrode based on polypyrrole conducting polymer. *J. Radioanal. Nucl. Chem.* **299** (2014), 1597–1605.
[2] Ghanbari M., Rounaghi G.H., Ashraf N.: An uranyl solid state PVC membrane potentiometric sensor based on 4,13-didecyl-1,7,10,16-tetraoxa-4,13-diazacyclooctadecane and its application for environmental samples. *Int. J. Environ. Anal. Chem.* **97** (2017), 189–200.

[3]   Badr I.H.A., Zidan W.I., Akl Z.F.: Cyanex based uranyl sensitive polymeric membrane electrodes. *Talanta* **118** (2014), 147–155.

[4]   Bieg C., Fuchsberger K., Stelzle M.: Introduction to polymer-based solid-contact ion-selective electrodes: basic concepts, practical considerations, and current research topics. *Anal. Bioanal. Chem.* **409** (2017), 45–61.

[5]   Bobacka J., Ivaska A., Lewenstam A.: Potentiometric ion sensors. *Chem. Rev.* **108** (2008), 329–351.

[6]   Zidan W.I., Badr I.H.A., Akl Z.F.: Development of potentiometric sensors for the selective determination of UO_2^{2+} ions. *J. Radioanal. Nucl. Chem.* **303** (2015), 469–477.

[7]   Saleh M.B., Soliman E.M., Gaber A.A.A., Ahmed S.A.: Novel PVC membrane uranyl ion-selective sensor. *Sens. Actuators B* **114** (2006), 199–205.

[8]   Saleh M.B., Hassan S.S.M., Abdel A.A., Abdel N.A.: A novel uranyl ion-selective PVC membrane sensor based on 5,6,7,8-tetrahydro-8-thioxopyrido[4',3',4,5]thieno[2,3-*d*]pyrimidine-4(3H)one. *Sens. Actuators B* **94** (2003), 140–144.

[9]   Hassan S.S.M., Ali M.M., Attawiya A.M.Y.: PVC membrane based potentiometric sensors for uranium determination. *Talanta* **54** (2001), 1153–1161.

[10]   Prabhu D.R., Ansari S.A., Raut D.R., Murali M.S., Mohapatra P.K.: Extraction behaviour of dioxouranium(VI) cation by two phosphorous-based liquid cation-exchangers in room-temperature ionic liquids. *Sep. Sci. Technol.* **52** (2017), 2328–2337.

Polarographic determination of metronidazole and oxytetracycline hydrochloride in veterinary drug for honey bees

KATERYNA PLOTNIKOVA[a, *], LILIYA DUBENSKA[a], IVAN ZELENYI[b]

[a] *Analytical Chemistry Department, Ivan Franko National University of Lviv, Kyryla i Mefodia Str. 8, 79005 Lviv, Ukraine* ✉ *katerina27pl@gmail.com*
[b] *Drohobych Pedagogical Lyceum, Ivana Franka Str. 36, 82100 Drohobych, Ukraine*

Keywords
electrochemistry
metronidazole
oxytetracycline
    hydrochloride
polarography
veterinary drug

Abstract
We have developed a new polarographic method for the determination of metronidazole and oxytetracycline hydrochloride in the veterinary drug Nozemat for honey bees. The technique is based on the reduction of polarographically active compounds on a mercury droplet electrode. The influence of the components of the veterinary drug Nozemat on the polarographic determination of metronidazole was studied. It was found that the reduction of metronidazole is not affected by glucose and ascorbic acid, but is affected by oxytetracycline hydrochloride, which is reduced to mercury droplet electrode at a potential of −1.45 V. The developed technique is characterized by ease of sample preparation and cost-effectiveness. This technique has the ability to identify simultaneously and determinate metronidazole and oxytetracycline hydrochloride in solution without the use of separation and concentration methods.

1. Introduction

Metronidazole (2-methyl-5-nitroimidazole-1-ethanol) is one of the most widely used nitroimidazole antibiotics. Metronidazole is used for the treatment of inflammatory diseases caused by anaerobic organisms and some protozoa, and for prevention of dysentery, colibacillosis, eimeriosis, balantidiasis, salmonellosis, enteritis, septicemia, post-surgical complications [1–3]. Oxytetracycline hydrochloride is an antibiotic of the tetracycline family. It is one of the most commonly used antibiotics in poultry because of its low cost and effective [4]. These compounds are intensively used in poultry breeding and stockbreeding. Unreasonable use of these drugs can cause serious food safety issues [5].

The veterinary drug Nozemat, which include metronidazole and oxytetracycline hydrochloride , was chosen for the experiments. Nozemat is used to treat

bees, and it can be given in unregulated doses. Because of this, an unknown amount of metronidazole can get into the honey, and it sometimes causes side effects of the human body and it could be of great concern for public health [5, 6]. Medicines for people are more stringent and better tested than veterinary drugs. The problem of the control of the veterinary drugs is urgent nowadays. Veterinary medicines could be unauthorized and the uncontrolled use of medicines exists in retail pharmacies of medicine or imported as contraband from other countries.

The most widespread of these classes in the quality control are chromatographic [6–9], spectrophotometric [10–13], and electrochemical methods [14–17]. Many of the known methods for the determination of metronidazole and oxytetracycline hydrochloride have a number of disadvantages: time-consuming, the use of organic solvents and expensive reagents, the side effects of excipients and other active substances. Electrochemical methods are promising alternative for the determination of the electroactive substances. Their advantages are simplicity, miniaturization, high sensitivity and relatively low cost. Therefore, the search for simple, express and affordable methods for the determination of metronidazole remains relevant. One of the promising methods of determination is voltammetry.

2. Experimental

2.1 Reagents and chemicals

Veterinary drug Nozemat (manufacturer API-SAN, Russia) is a yellow powder with a slight typical odor. Available in laminated bags of 2.5 g. Composition per 1 g of the drug: metronidazole 400 mg; oxytetracycline hydrochloride 400 mg; glucose; ascorbic acid.

Metronidazole and oxytetracycline hydrochloride were purchased from Sigma Aldrich (USA). Stock standard solution of metronidazole for determination was prepared by dissolving the exact amount of standard in 7 mL of 2 M hydrochloric in 50.0 mL volumetric flask. Stock standard solution of oxytetracycline hydrochloride was prepared by dissolving the exact amount of standard in distilled water in 50.0 mL volumetric flask. After that, the solutions were adjusted to the mark with distilled water and mixed thoroughly.

The Britton-Robinson buffer preparation was as follows: 20.2 g of sodium tetraborate decahydrate, 28.7 mL of glacial acetic acid and 17.6 mL of concentrated orthophosphoric acid were dissolved in 1.0 L volumetric flask.

Working solution preparation was as follows: an aliquot of stock standard solution was added into a 25 mL volumetric flask to obtain a solution with the necessary concentration, then 2 mL of Britton-Robinson buffer with necessary pH was added to the flask, and distilled water was added to the mark.

Aqueous solution of Nozemat was prepared as follows: the exact portion of the test veterinary drug was dissolved in a 250 ml volumetric flask. An aliquot of

1.00 ml of the resulting solution was added to a 25.0 ml volumetric flask and made up to the mark with water. An aliquot of 1.00 ml of the resulting solution was added to a 25.0 ml volumetric flask, 2 ml of Britton-Robinson buffer with a pH of 9.6 was added and the volume was adjusted to the mark with distilled water.

2.2 Instrumentation

For polarographic measurements we used digital device MTech OVA-410 [18], temperature-controlled three-electrode, a mercury droplet indicator electrode, a saturated calomel reference electrode and platinum wire auxiliary electrode. The accuracy of the potential measurement is 1 mV. The uncertainty of current measurement is 0.1%. The employed mercury droplet electrode had the following characteristics: $m = 5.94 \times 10^{-4} \, g \, s^{-1}$; $\tau = 10$ min in 0.2 M NH_4Cl. We used cyclic voltammetry for the study of the electrochemical process.

We used MV 870 DIGITAL-pH-MESSERÄT pH-meter for measuring pH of the solutions.

The obtained working solutions were introduced into the cell, and deoxygenated with argon for 10 min. Polarograms were recorded in the range of potentials from 0.0 to –1.6 V.

3. Results and discussion

Previously it was found that using the Britton-Robinson buffer with pH = 9.6, metronidazole is reduced with the formation of a characteristic one irreversible peak at –0.64 V (Fig. 1A). Using polarography with fast potential scan, it was found that metronidazole is reduced on mercury droplet electrode in the range of pH 2.0 to 10.5. The peak recovery current of the metronidazole reaches the maximum value at pH 9–10 against the background of a the Britton-Robinson buffer.
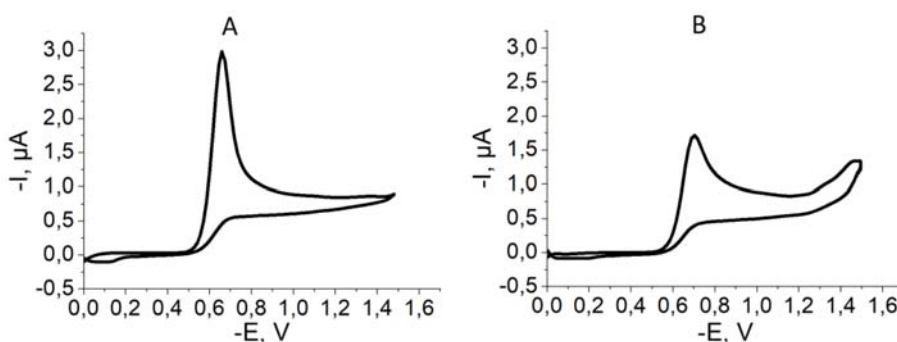

Fig. 1 Polarograms of (A) metronidazole, and (B) metronidazole with oxytetracycline hydrochloride solutions at 0.2 M Britton-Robinson buffer background at pH = 9.6 ($v = 0.5 \, V \, s^{-1}$, c(metronidazole) = $= 4.5 \times 10^{-5}$ M, c(oxytetracycline hydrochloride) = 5.0×10^{-5} M.
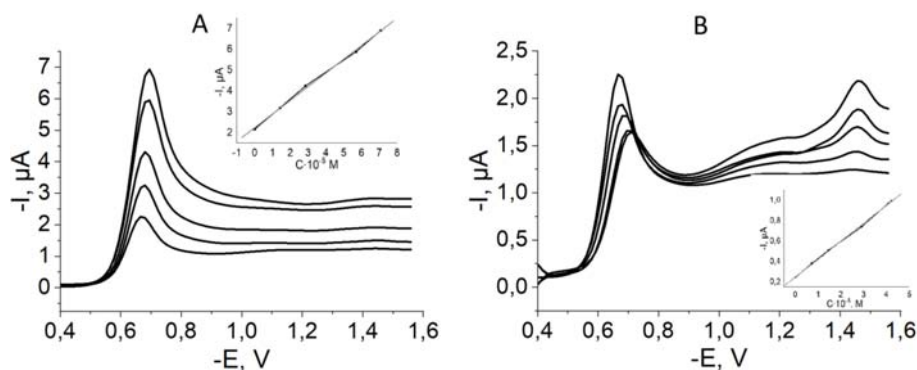
Fig. 2 Polarograms of (A) metronidazole reduction at different metronidazole concentrations, and (B) oxytetracycline hydrochloride reduction at different oxytetracycline hydrochloride concentrations and their corresponding calibration graphs.

Under pre-selected conditions, the effect of some foreign substances on the polarographic determination of metronidazole was investigated. Substances that are components of drugs were studied: glucose, ascorbic acid, oxytetracycline hydrochloride. Glucose and ascorbic acid are not reduced at mercury droplet electrode and do not change the appearance of the polarogram and polarographic characteristics of the recovery of metronidazole. As can be seen from Fig. 1, oxytetracycline hydrochloride is reduced to mercury droplet electrode and changes the appearance of the polarogram and polarographic characteristics of the recovery of metronidazole. With the addition of oxytetracycline hydrochloride, the recovery peak of metronidazole decreases and slightly shifts to more negative potentials.

The composition of the drug is relatively complex; excipients affect the analytical signal of the recovery of compounds, so to take into account the matrix effect used the method of many additives.

Quantitatively transferred the solution of Nozemat to the cell (exact volume), removed dissolved oxygen for 10 min and took polarograms in the range of potentials from 0.0 to −1.6 V. Aliquots of standard metronidazole solution were introduced into the cell to obtain a solution with a given concentration of additive metronidazole 1.0×10^{-5} M to 7.0×10^{-5} M. As with the determination of the metronidazole, aliquots of a standard oxytetracycline hydrochloride solution were added to the cell with solution of Nozemat to obtain a solution with a given additive concentration from 7.0×10^{-6} M to 5.0×10^{-6} M (Fig. 2).

In Table 1 are shown metrological characteristics of the determination of metronidazole and oxytetracycline hydrochloride in veterinary drug. Recovery was calculated. For metronidazole the recovery is 97% and for oxytetracycline hydrochloride the recovery is 103%. Analytical performance of the technique is good for determination veterinary drugs.

Table 1

Validation parameters of the method of metronidazole and oxytetracycline hydrochloride determination in solutions of Nozemat by the method of many additives.

	Metronidazole	Oxytetracycline hydrochloride
Peak's potential / V	−0.65	−1.44
Corelation coefficient, R	0.99892	0.99922
Slope, b / μA M^{-1}	6.56×10^4	1.76×10^4
Δb	1763	400
Intercept, a / μA	2.238	0.219
Δa	0.075	0.009
c / mol L^{-1}	3.42×10^{-5}	1.25×10^{-5}
c / mg g^{-1}	389	413
Recovery / %	97	103

The accuracy was verified by the "added-found" method. Aliquots of standard solution of metronidazole were made in a 25.0 ml volumetric flask to obtain a solution of a given concentration of 3.3×10^{-5} M and the solution of oxytetracycline hydrochloride to obtain a solution of a given concentration of 1.5×10^{-5} M, 2 ml of Britton-Robinson buffer with pH 9.6 was added to flask with stirring and adjusted to the mark with water. The analysis procedure of model solution is similar to analysis procedure of the solution of Nozemat. The calculated amount of metronidazole by the method of multiple additives in the tested model solution is in agreement with the amount that was introduced into the sample.

4. Conclusions

The new polarographic method for the determination of metronidazole and oxytetracycline hydrochloride in the veterinary drug Nozemat for honey bees was developed. We conducted principal component analysis of veterinary drug Nozemat to assess the overall effect for the determination of metronidazole. We found that oxytetracycline hydrochloride is reduced to mercury droplet electrode. This method has the ability to identify simultaneously and determinate metronidazole and oxytetracycline hydrochloride in solution without the use of separation and concentration methods. One more of advantages of technique are fast procedure of analysis, simple sample preparation, low cost, the possibility of miniaturization.

References

[1]   *Antibiotic and Chemotherapy.* Finch R., Greenwood D., Whitley R. (edits.) Amsterdam, Elsevier 2006, p. 292–299.

[2]   Mitrowska K.: Przyczyny i skutki zakazu stosowania 5-nitroimidazoli u zwierząt, których tkanki lub produkty przeznaczone są do spożycia przez ludzi. *Med. Weter*. **71** (2015), 736–742.

[3]   Verma P., Namboodiry V., Mishra S., Bhagwat A., Bhoir S.: A stability indicating HPLC method for the determination of Metronidazole using Ecofriendly solvent as mobile phase component. *Int. J. Pharm. Pharm. Sci.* **5** (2013), 496–501.

[4]   Cervini, P., Ambrozini, B., Machado, L.C.M., Ferreira Garcia, A.P., Cavalheiro Gomes E.T.: Thermal behavior and decomposition of oxytetracycline hydrochloride. *J. Therm. Anal. Calorim.* **121** (2015), 347–352.

[5]   Dang B.N., Anh N.T.K., Ky L.X., Thai P.K.: Antibiotics in the aquatic environment of Vietnam: sources, concentrations, risk and control strategy. *Chemosphere* **197** (2018), 438–450

[6]   Quintanilla P., Hettinga K.A., Beltrán M.C., Escriche I., Molina M.P.: Volatile profile of matured Tronchón cheese affected by oxytetracycline in raw goat milk. *J. Dairy Sci.* **103** (2020), 6015–6021

[7]   Chen F. Yu L., Jingdong P., Xiang W., Huanjun P., Yu C., Yan H.: Study on simultaneous determination of three nitroimidazole residues in honey by high performance liquid chromatography–resonance Rayleigh scattering spectra. *Microchem. J.* **141** (2018), 423–430.

[8]   Hernández-Mesa M., Cruces-Blanco C., Campaña G.A.: Simple and rapid determination of 5-nitroimidazoles and metabolites in fish roe samples by salting-out assisted liquid-liquid extraction and UHPLC-MS/MS. *Food Chem.* **252** (2018), 294–302.

[9]   Xiu-Chun G., Zhao-Yang X., Hai-Hui W., Wen-Yi K., Li-Ming L., Wen-Qing C., Hong-Wei Z., Wen-Hui Z.: Molecularly imprinted solid phase extraction method for simultaneous determination of seven nitroimidazoles from honey by HPLC-MS/MS. Talanta. 166 (2017), 101–108.

[10]   Теплых А.Н., Илларионова Е.А.: Количественное определение метронидазола спектрофотометрическим методом. *Сибирский медицинский журнал* **5** (2009), 48–50.

[11]   Zheltvay O.I., Zheltvay I.I., Spinul V.V., Antonovich V.P.: Spectrophotometric determination of metronidazole and tinidazole using copper (II) complexes. J*. Anal. Chem.* **68** (2013), 663–668.

[12]   Youssef A.K., Saleh M.S., Abdel-Kader D.A., Hashem Facile D.Y.: Spectrophotometric determination of metronidazole and secnidazole in pharmaceutical preparations based on the formatioon of dyes. *Int. J. Pharm. Pharm. Sci.* **6** (2015), 103–110.

[13]   Sversut R.A., Vieira J.C., Rosa A.M., Amaral M.S., Kassab N.M., Salgado H.: Validated spectrophotometric methods for simultaneous determination of oxytetracycline associated with diclofenac sodium or with piroxicam in veterinary pharmaceutical dosage form. *Arabian J. Chem.* **13** (2020), 3159–3171.

[14]   Nikodimos Y.: Electrochemical determination of metronidazole in tablet samples using carbon paste electrode. *J. Anal. Methods Chem.* (2016), 361294.

[15]   Srivastava A.K., Upadhyay S.S., Rawool C.R., Punde N.S., Rajpurohit A.S.: Voltammetric techniques for the analysis of drugs using nanomaterials based chemically modified electrodes. *Curr. Anal. Chem.* **15** (2019), 249–276.

[16]   Sahu G.: Voltammetric behaviour of metronidazole at a composite polymer membrane electrode. *Orien. J. Chem.* **26** (2010), 81–86.

[17]   Yang Y., Yan W., Guo Y., Wang X., Zhang F., Yu L., Guo C., Fang G.: Sensitive and selective electrochemical aptasensor via diazonium-coupling reaction for label-free determination of oxytetracycline in milk samples. *Sensors and Actuators Reports* **2** (2020), 1–7.

[18]   http://chem.lnu.edu.ua/mtech/devices.html (accesed 21st June 2020)

Application of microextraction techniques combined with chromatographic methods for the analysis of complex objects

VLADISLAV DEEV*, ELENA BESSONOVA, LIUDMILA KARTSOVA

Institute of Chemistry, Saint-Petersburg State University, Universitetsky prospect 26, 198504 Peterhof, Saint-Petersburg, Russia ✉ *hitcherv@mail.ru*

Keywords
chemometrics
dispersive liquid-liquid
    microextraction
solid-phase
    microextraction

Abstract
The low concentration of analytes and the prevention of the matrix influence requires a stage for extraction and concentration of the studied compounds. The classical methods of liquid and solid-phase extraction have many limitations that prevent their use in some cases. Microextraction techniques are becoming more widespread. We studied the possibility of using ionic liquids to extract pesticides from water samples with their subsequent HPLS-MS determination. The influence on the degree of extraction of such parameters as a nature of ionic liquids and disperser solvent, their amounts, salt concentration, volume ratio of ionic liquids and water sample, dilution of the ionic liquids extract with methanol was performed. Besides conditions of solid-phase microextraction of volatile organic compounds from urine samples obtained from healthy donors and donors with prostate cancer have been found. The analysis of volatile organic compounds by GC-MS followed by chemometric processing allowed achieving a high value of binary classification accuracy (91%).

1. Introduction

An important part of any analysis that significantly affects the final results is the sample preparation. The low concentration of biologically active compounds and the presence of accompanying components prevent direct analysis of the sample with complex matrix composition. Traditional methods of liquid and solid-phase extraction have a plenty of limitations such as highly time-consuming procedures, large volume of samples, expensive cartridges, toxic organic solvents and challenges in automating the process. Therefore, the application of extraction techniques employing low amount of solvents (microextraction methods) and the low toxicity extractantes has become the main research direction in recent years [1, 2].

Solid-phase microextraction (SPME) was proposed by Pavlishin in 1989 [3]. One variant of this method is to use thin rods with various polymer coatings such

as divinylbenzene, polydimethylsiloxane, polyacrylate, and polyethylene glycol, which applied to the surface [4]. The polymer sorbent is placed in the equilibrium headspace above a condensed phase of the sample and the volatile compounds are extracted.

Liquid microextraction consists of using small amounts of liquid (extractant) in equilibrium with the gas or liquid phase of the sample. Dispersive liquid-liquid microextraction (DLLME) is a variant of liquid microextraction. The essence of the method is as follows: extractant is dissolved in the phase of a dispersing solvent and the mixture is rapidly injected into the sample volume [5]. In this case, the dispersing solvent is dissolved and a "cloud" of extractant is formed. A large surface area contributes to mass transfer processes. The combination of DLLME with the use of ionic liquids (ionic liquids) as extractants reduces the harmful impact on the environment [6].

So, the goal of this study was the application of microextraction methods for the analysis of real samples.

2. Experimental

2.1. Reagents

Deionized water was obtained at the AQUILON D 301 deionizer (Russia). All chemicals and reagents (the highest commercially available purity) were purchased from Reachim, Baker, Acros organics and Sigma Aldrich.

2.2 Instrumentation

HPLC analysis was carried out using an HPLC LCMS-8030 (Shimadzu) with a triple quadrupole mass-selective detector with electrospray ionization. Analysis of volatile organic components (volatile organic compounds) of urine samples was made by GCMS-QP2010 SE (Shimadzu). Chemometric data processing was performed using RStudio.

2.3 Determination of volatile organic compounds in urine samples by GC-MS method

For SPME of volatile organic compounds in urine sample was used fiber coated with a polydimethylsiloxane (PDMS). The volatile organic compounds were extracted onto fiber coating for 20 min at 50 °C. Then the analytes were desorbed into the gas chromatography for 4 minutes at a temperature of 250 °C. Chromatographic separation was carried out on a HP-5 capillary column (30 m × 250 µm × 0.25 µm) using temperature programming mode. The temperature of oven was increased from 50 °C up to 250 °C at a rate of $10\,°C\,min^{-1}$. T ion source was 200 °C. Mass spectrometry was used in SIM mode ($m/z = 35$–900).

2.4 Conditions for LC/MS/MS determination of pesticides

Separation of pesticides was performed by HPLC/MS/MS with positive electrospray ionization on column Zorbax Bonus RP 3.5 μm (2.1 × 100 mm) with 40 mM ammonium acetate, and methanol as mobile phase A and B, respectively. The following gradient elution was applied: 20–85% B (8 min), 85% B (8–15 min), 85–95% B (15.0–15.5 min), 95% B (15.5–18.0 min), 95–20% B (18.0–18.5 min). The velocity of the mobile phase was 0.3 ml min^{-1}. The volume of the injected sample was 20 μl. MS detection: capillary voltage +4.5 kV, spray gas velocity 3 dm^{3}min^{-1}, flow rate and drying gas temperature 15 dm^{3}min^{-1} and 250 °C, respectively.

2.5 Selection of conditions for dispersive liquid-liquid microextraction of pesticides

The influence of the natures of ionic liquids ([C$_4$MIM][PF$_6$], [C$_6$MIM][NTf$_2$], [C$_6$MIM][BF$_4$]) and the dispersing solvent (methanol, acetonitrile, acetone), the weight of the ionic liquids (0.060–0.200 g), the volume of the dispersing solvent (0.2–1.0 ml) on the degree of pesticides extraction were studied. The influence of the pH (5.4; 2.2), the concentration of NaCl (0.040–0.200 g) and extraction time (1-6 min) were investigated.

The effects of different ionic liquids and disperser solvents on DLLME procedures were investigated and optimized by using standard solutions of pesticides. In detail, a solution of ionic liquids in a dispersing solvent was prepared and rapidly injected into the aqueous sample solution (2 ml), followed by treatment for 2 min in an ultrasonic bath, cooling at –4 °C for 10 min, centrifugation for 10 min at 3500 rpm and collection of ionic liquids. The water phase was separated and analyzed by HPLC-MS. The ionic liquids extract was diluted in methanol and analyzed by HPLC-MS.

3. Results and discussion

3.1 Microextraction of pesticides

One of the important tasks of environmental monitoring is to control trace concentrations of pesticides in water samples. Technique of combining several pesticides has become more widespread in agriculture. It allows reducing the total concentration of the applied compounds and to decrease the adaptability of pathogens and insects. Therefore, the analysis of real samples requires a preliminary stage of selective analytes extraction and concentration.

Extracting and dispersing solvents are both important in DLLME of analytes. The influence of the nature of the dispersing solvent (methanol, acetonitrile and acetone) and the extractant (imidazolium ionic liquids [C$_4$MIM][PF$_6$], [C$_6$MIM][BF$_4$] and [C$_6$MIM][NTf$_2$]) on the degree of extraction of pesticides was

studied. This parameter was controlled by the residual concentration of pesticides in the water phase after extraction. The best results were obtained for ionic liquids $[C_4MIM][PF_6]$ as an extractant and acetonitrile as a dispersing solvent.

The next step was to select the amount of ionic liquids (0.060–0.200 g) and the volume of acetonitrile (0.2–1.0 ml). It was found that the highest degree of extraction of analytes was achieved by using 0.20 g of ionic liquids and 0.3 ml of acetonitrile.

It was shown that the degree of extraction of selected pesticides does not depend on pH of the water sample, which confirms the partition mechanism of extraction. The degree of extraction of carbofos increased slightly with an increase in the salt concentration and reach maximum by weight to 4% (0.08 g).

It is known that the high viscosity of ionic liquids have hindered the processes of electrospray ionization. Dilution of the sample with methanol by 3 times gives the best result (the signal intensity was 37.3% to 84.5% of the signal without ionic liquids).

Thus, the conditions of DLLME-ionic liquids extraction of pesticides from water samples were found. The limits of detection for pesticides were from 0.07 to 0.19 ng ml^{-1}; the reproducibility of peak areas were from 3 to 5%, the extraction recovery was close to 100%.

3.2 SPME of volatile organic compounds from urine samples

One of the important directions is the search for criteria of early diagnosis of cancer. Obtaining characteristic profiles of volatile organic compounds from urine samples can help develop a non-invasive method for early diagnosis of the disease.

For this, we studied the influence of a number of factors on the total number of peaks and the total peak area. They were the temperature at which the vapor and condensed phases of urine were balanced (30–60 °C), the preheating time of the sample (10–40 min), NaCl concentration (3.0–13.3%, *w/v*) and the sorption time on the PDMS coating (5–30 min).

An increase in the preheating temperature of the sample to 500 °C led to an increase in the number of signals, which did not change with a further temperature increasing. Next parameter was the time of achievement equilibrium of the vapor and condensed phases. The largest number of peaks was observed at 40 min, but this greatly increased the time of analysis and so we chose 20 min. Also, we studied the desalting effect of sodium chloride on efficiency of extraction. The best volatile organic compounds sorption was achieved by adding 13.3% salting agent. It is also shown that, the number of peaks did not change after 20 minutes of sorption.

Thus, to obtain the characteristic profiles of urine samples, the following conditions were selected: 13.33% NaCl was added to the urine sample (3 ml),
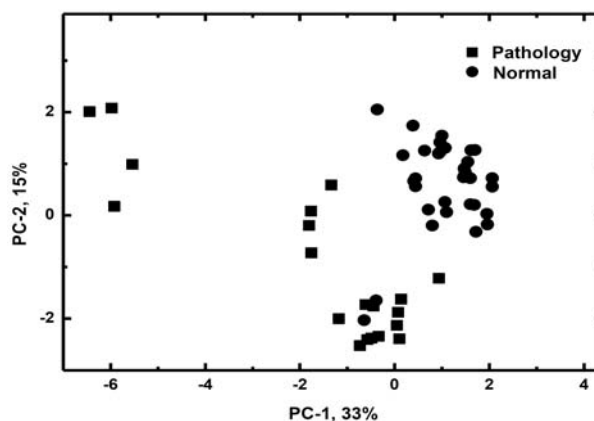
Fig. 1 Scores plot relative to the first and second principal component.

heating for 20 min at 50 °C; then sorption of volatile organic compounds on PDMS fiber coating at 50° C for 20 min.

Under the selected conditions, we obtained vapor-phase profiles of 52 urine samples (32 normal and 20 pathology). Prior to performing chemometric processing of chromatographic profiles of urine samples, preliminary data preparation is necessary [7]. The baseline was removed and the peaks were aligned using dynamic time warping with controlling by mass spectra.

The PCA model was based on 52 aligned characteristic profiles. There is a satisfactory separation of data into two clusters in the scores plot relative to the first and second principal component (Fig. 1).

The original data set (52 samples) was randomly divided into calibration (13 pathology, 21 normal) and test (7 pathology, 11 normal) sets. Then the PLS-DA model was built using the calibration set, and its predictive ability was evaluated using the test set. The procedure was repeated 100 times. The average values of sensitivity, specificity, and accuracy in this case were 95%, 94% and 91%.

4. Conclusions

The possibility of using imidazolium ionic liquids ($[C_4MIM][PF_6]$) as extractants for quantitative extraction and concentration of pesticides under the conditions of DLLME is shown. The degree of concentration was 28–33, which allowed reaching the detection limits (0.06–0.19 ng ml^{-1}) below the maximum permissible concentration. The possibility of non-invasive diagnosis of prostate cancer by SPME of volatile organic compounds in urine is shown. Chemometric processing of gas chromatographic profiles using PLS-DA and PCA methods allowed achieving classification accuracy values more than 90%.

Resource Education Center in Chemistry of St. Petersburg State University for the provided equipment.

References

[1]   Rutkowska M., Płotka-Wasylka J., Sajid M., Andruch V.: Liquid–phase microextraction: A review of reviews. *Microchem. J.* **149** (2019), 103989.

[2]   Jalili V., Barkhordari A., Ghiasvand A.: A comprehensive look at solid-phase microextraction technique: A review of reviews. *Microchem. J.* **152** (2020), 104319.

[3]   Arthur C.L., Pawliszyn J.: Solid phase microextraction with thermal desorption using fused silica optical fibers. *Anal. Chem.* **62** (1990). 2145–2148.

[4]   Schmidt K., Podmore I.: Solid phase microextraction (SPME) method development in analysis of volatile organic compounds (VOCs) as potential biomarkers of cancer. *J. Mol. Biomark. Diagn.* **6** (2015), 1000253.

[5]   Mousavi L., Tamiji Z., Khoshayand M.R.: Applications and opportunities of experimental design for the dispersive liquid–liquid microextraction method – A review. *Talanta* **190** (2018), 225–356.

[6]   Marcinkowska R., Konieczna K., Marcinkowski L., Namiesnik J., Kloskowski A.: Application of ionic liquids in microextraction techniques: Current trends and future perspectives. *TrAC, Trends Anal. Chem.* **119** (2019), 115614.

[7]   Wehrens R.: *Chemometrics with R. Multivariate Data Analysis in the Natural Sciences and Life Sciences.* Berlin, Springer 2011.

The development of reference probe system for tip-enhanced Raman spectroscopy

MARTIN KRÁL*, MARCELA DENDISOVÁ, PAVEL MATĚJKA

Department of Physical Chemistry, Faculty of Chemical Engineering, University of Chemistry and Technology Prague, Technická 5, 166 28 Prague 6, Czech Republic ✉ Martin.Kral@vscht.cz

Keywords

copper(II) phthalocyanine

scanning tunnelling microscopy

resonance Raman spectroscopy

surface-enhanced Raman spectroscopy

tip-enhanced Raman spectroscopy

Abstract

The tip-enhanced Raman spectroscopy (TERS) is a modern analytical technique with an outstanding spatial resolution and chemical sensitivity. These parameters mainly depend on the structural integrity and chemical purity of employed plasmonic scanning probe tips. Usually, each tip is tested before TERS measurements using commercially available reference samples. However, their price and relatively short expiration date must be considered when planning a research budget. We developed a procedure to produce self-made reference probe samples for testing TERS tips using copper(II) phthalocyanine on a Au nanolayer, which is prepared by thermal vacuum evaporation of Au on a Si wafer. Our results show that the prepared system enables repeated detection of well-resolved TERS spectra. The collected TERS spectra and spectral maps exhibit some degree of variability, which may be due to various photo-induced processes, and it must be considered while performing TERS measurements.

1. Introduction

The self-assembled two-dimensional monolayers (2D SAMs) of various molecules (e.g. graphene [1], MoS_2 [2], rubrene [3]) offer beneficial properties for the construction of nano-electronic and nano-optical devices. The topological and chemical characterization of 2D SAMs is crucial to gather information about the arrangement of deposited molecules and their interaction with the substrate. This task requires analytical techniques with (sub)nanometer spatial resolution and up to single-molecular detection sensitivity. Only few techniques meet the requirements, and one of them is tip-enhanced Raman spectroscopy (TERS), which combines the excellent spatial resolution of scanning probe microscopy (SPM) and chemical sensitivity of surface-enhanced Raman scattering (SERS) spectroscopy [4, 5].

The SERS spectroscopy utilizes plasmonic metal nanostructures to cause a high local enhancement of the electric field in their close vicinity via the surface plasmon resonance (SPR) effect. The local electric field causes an increase of the

Raman scattering from molecules bound to the metal by 6–8 orders of magnitude [6]. The enhancement allows SERS spectroscopy to be used for single-molecular detection. However, Raman microscopes have limited spatial resolution by the light diffraction with the achievable resolution being around half of the excitation wavelength. On the other hand, the spatial resolution of SPM techniques is limited only by the dimensions of the apex of the scanning probe tip, which may even be atomically sharp. By utilizing SPM tip and substrate made from plasmonic metals, an artificial "hotspot" may be created with its position and dimensions being defined by the tip. It opens the possibility to collect strongly enhanced Raman spectra from the area precisely localized bellow the tip, and thus overcome the optical diffraction limit. The artificial hotspot may be relocated by moving the sample below the tip, which is the foundation of TERS mapping [5, 7, 8].

A successful TERS experiment requires an optimal combination of various parameters, the most important of which are tip sharpness and purity [7]. A reference sample, consisting of a flat plasmonic nanolayer with attached probe molecules, is frequently used to check the state of the tip before using it for experiments. Unfortunately, commercially available TERS standards are expensive and have an expiration date of several months.

The goal of this study was to find a preparation procedure, which would be able to produce cheap reference samples for repeated detection of intense TERS spectra. A combination of a Au nanolayer on a Si substrate, prepared by thermal vacuum evaporation, with adsorbed copper(II) phthalocyanine (CuPc), which is a molecule with high Raman cross-section, was tested [9, 10]. Copper(II) phthalo-cyanine, known as phthalocyanine blue, is a synthetic blue pigment and is frequently used in paints. It has been studied as a potential material for the construction of organic solar cells and other photoelectronic devices [11]. As indicated by its colour, CuPc exhibits several absorption bands within the visible region. The effects of a transition to excited electronic states and subsequent luminescence may be observable in Raman measurements [12]. Au is a highly suitable metal for the sample as it is both thermally and electrically conductive, which limits the local heating of the sample during the measurements and enables the use of scanning tunnelling microscopy (STM) for tip-surface interaction feedback [13].

2. Experimental

2.1 Reagents and chemicals

The substrate for the sample was prepared by thermal vacuum evaporation of gold on silicon (100) wafer. First, a 5 nm thick Cr adhesion layer was deposited on the wafer, followed by 100 nm of Au. The deposition rate was 4 nm min^{-1} for Cr and 8 nm min^{-1} for Au. The base pressure of the evaporation system was below 5×10^{-6} mbar. Following the preparation procedure described by Jiang et al. [14],

the clean substrate was immersed into a saturated solution of CuPc (>99%, Sigma Aldrich, USA) in dimethylformamide (>98%, Lach-ner, CZ) for at least 12 h at ambient temperature. Subsequently, the sample was removed from the solution, rinsed with Milli-Q water and methanol (p.a., Penta, CZ), and dried with air.

2.2 Instrumentation

The Raman, SERS and TERS spectra were recorded using Raman spectrometer InVia Reflex (Renishaw, UK) equipped with lasers emitting at two different excitation wavelengths: 633 nm (13.6 mW max. power output) and 785 nm (204 mW max. power output). The spectrometer has a thermoelectrically cooled CCD detector with a spectral resolution of 2 cm^{-1} and 4 microscope objectives with 5×, 20×, 50× and 100× magnitude. For TERS experiments, the laser beam was redirected to the SPM platform Innova-IRIS (Bruker, USA) via a system of light guides. Electrochemically etched Au TERS-STM tips (Bruker, USA) were used for all TERS measurements.

The spectra were processed using the Spectragryph software (F. Menges "Spectragryph - optical spectroscopy software", Version 1.2.14, 2020, http://www.effemm2.de/spectragryph/). Using this software, all collected spectra were treated by a Savitzky-Golay noise filter, automatic baseline correction, spike removal and peak normalization.

3. Results and discussion

3.1 Raman measurements of crystalline copper(II) phthalocyanine

At first, the Raman spectra of pure CuPc were collected to provide reference data while using both 633 and 785-nm excitation lasers (Fig. 1). Both spectra exhibit
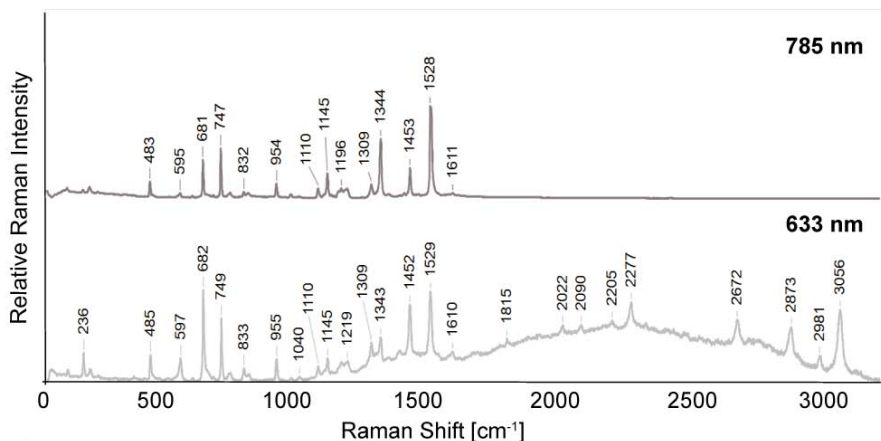

Fig. 1 Raman spectra of Cu(II) phthalocyanine in crystalline form measured at 633 (top) and 785-nm (bottom) excitation. The spectra are offset.
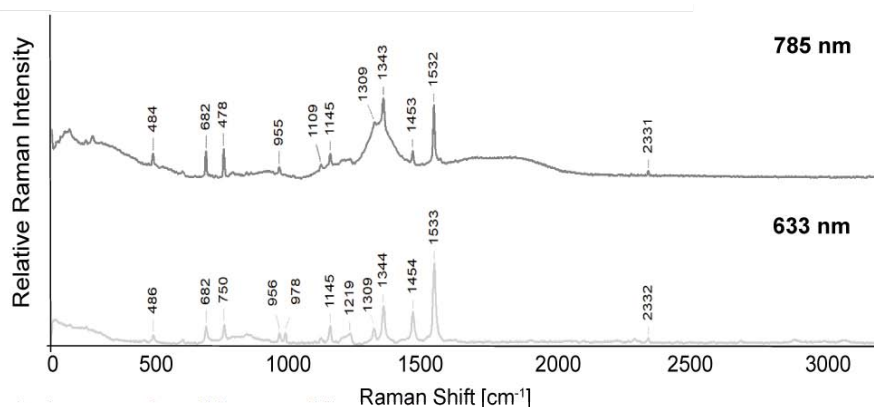
Fig. 2 SERS spectra of Cu(II) phthalocyanine on a Au layer measured at 633 (top) and 785-nm (bottom) excitation. The spectra are offset.

vibration bands in the 500–1600 cm^{-1} region with slight differences in their intensity ratios. The 633-nm excitation allows the observation of additional bands in the 2000–3000 cm^{-1} region (on a luminescence background), which originate from the resonance Raman effect as the excitation energy overlaps with the Q-band of CuPc [12]. Moreover, the process of electronic excitation may lower the D_{4h} symmetry of CuPc during resonance Raman scattering, and previously forbidden bands may become observable [15]. The luminescent background has a maximum around 2200 cm^{-1}, which corresponds to a molecular emission band at 735 nm. Even though the spectra measured with the 785-nm laser line do not exhibit apparent resonance enhancement, a pre-resonance Raman enhancement may occur.

3.2 Surface-enhanced Raman measurements of copper(II) phthalocyanine layer on a gold substrate

The prepared sample of CuPc on a Au layer was analysed using the Raman microscope. Both excitation lasers were used to obtain SERS spectra (Fig. 2), which were compared to the spectra of a pure crystalline CuPc.

The positions of bands in SERS spectra closely match their positions in the spectra of bulk CuPc. However, a slight shift of some spectral bands is observable (e.g. 1528 → 1532 cm^{-1}), which may be attributed to the interaction between CuPc and the Au substrate. The disappearance of luminescence background and resonance-enhanced bands in the spectrum at 633-nm excitation also suggests the molecule-metal interaction and the transfer of energy from CuPc molecules to the substrate. Moreover, there are variations in the relative intensities of bands, which depend on the excitation energy, e.g. the band at 1309 cm^{-1} is enhanced in SERS spectra at the 785-nm excitation, when compared to the spectra of pure CuPc or even SERS spectra at 633-nm excitation.
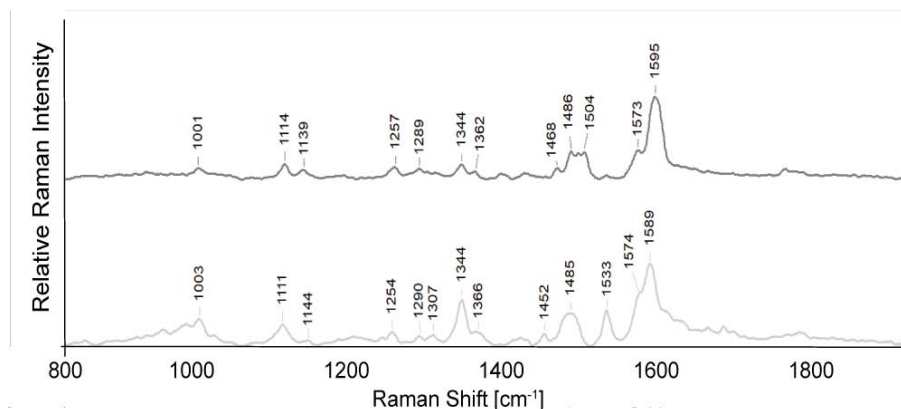
Fig. 3 Two examples of TERS spectra of Cu(II) phthalocyanine, measured at 633-nm excitation. The spectra are offset.

3.3 Tip-enhanced Raman measurements of copper(II) phthalocyanine layer on a gold substrate

SERS microspectroscopy is a diffraction-limited technique as it provides an averaged information about molecules in the illuminated area of several square micrometers. Meanwhile, TERS spectra are collected from an area of tens of nanometers, and they contain specific information about the local molecular arrangement, topography of the underlying metal and properties of the local electric field between the tip and the substrate. Therefore, a higher spectral variability should be expected.

Several TERS mapping experiments were carried out using both 633 and 785-nm excitation with varying experimental parameters such as the number and distance between measured points, acquisition time, number of acquisitions, laser power, etc.

The TERS spectra measured at 633-nm excitation exhibited lower signal to noise ratio and reproducibility. As a consequence, TERS mapping was impossible and only a few one-point TERS spectra were obtained (Fig. 3).

The TERS spectra collected at 785-nm excitation contained a higher number of well-resolved bands. Moreover, the spectra were stable in time and so the TERS mapping was possible. The two presented TERS spectra are averages of TERS maps, which contained 16 and 80 points with 600 and 300-nm spacing, respectively (Fig. 4).

The spectra collected using both excitation wavelengths exhibit a variability in relative intensities and positions of bands between the measured points. The variability may be attributed to the local orientation of CuPc molecules between the tip and the Au surface and the properties of strongly enhanced and non-homogeneous electromagnetic field, which depend on the tip-surface distance, their morphology and relative position. Moreover, the used excitation
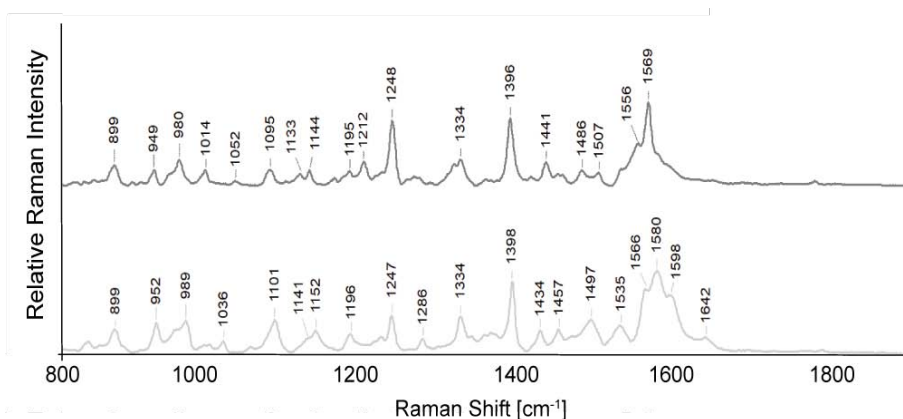
Fig. 4 Two examples of averaged TERS spectra of Cu(II) phthalocyanine measured with 785-nm excitation. The spectra are averages from TERS maps including 16 (top) and 80 (bottom) measured points. The spectra are offset.

wavelengths are close to absorption bands of CuPc and the strong electric field may give rise to photo-induced effects. These effects include the electronic excitation of CuPc to higher states, charge transfer between the Cu atom and the phthalocyanine ring, ionization of the molecule and formation of radicals. The photo-induced processes are likely to play a bigger role in TERS spectra detected at 633-nm excitation due to the overlap with Q-band of CuPc, which may be the cause of their lower signal to noise ratio and reproducibility.

4. Conclusions

The developed reference probe system of CuPc adsorbed on a Au surface has proved to be suitable for the intended use as it enabled the detection of intense and well-resolved SERS and TERS spectra. The Au layer prevents overheating of the sample and allows for the use of STM. The SERS spectra were in a good match with the spectra of pure CuPc. A slight shift of some bands and change in the luminescent background indicated the interaction between CuPc and the Au surface. The TERS experiments resulted in spectral maps with high intensities of individual spectra. Increased variability between measured points was observed. Possible sources of the variability are photo-induced processes that may occur in the strongly enhanced electric field. These effects are a known feature of TERS measurements, and they offer valuable insight into the photophysics and photochemistry of CuPc interacting with the Au surface. The dependence of TERS spectra on experimental parameters and the preparation procedure of the reference sample should be further studied.

References

[1]   Mas-Ballesté R., Gómez-Navarro C., Gómez-Herrero J., Zamora F.: 2D materials: to graphene and beyond. *Nanoscale* **3** (2011), 20–30.

[2]   Zeng H., Cui X.: An optical spectroscopic study on two-dimensional group-VI transition metal dichalcogenides. *Chem. Soc. Rev.* **44** (2015), 2629–2642.

[3]   Schultz J.F., Li L., Mahapatra S., Shaw C., Zhang X., Jiang N.: Defining multiple configurations of rubrene on a Ag(100) surface with 5 Å spatial resolution via ultrahigh vacuum tip-enhanced Raman spectroscopy. *J. Phys. Chem. C* **124** (2020), 2420–2426.

[4]   Whiteman P.J., Schultz J.F., Porach Z.D., Chen H.N., Jiang N.: Dual binding configurations of subphthalocyanine on Ag(100) substrate characterized by scanning tunneling microscopy, tip-enhanced Raman spectroscopy, and density functional theory. *J. Phys. Chem. C* **122** (2018), 5489–5495.

[5]   Shao F., Zenobi R.: Tip-enhanced Raman spectroscopy: principles, practice, and applications to nanospectroscopic imaging of 2D materials. *Anal. Bioanal. Chem.* **411** (2019), 37–61.

[6]   Aroca R.: *Surface-Enhanced Vibrational Spectroscopy.* Hoboken, Wiley 2006.

[7]   Kumar N., Mignuzzi S., Su W., Roy D.: Tip-enhanced Raman spectroscopy: principles and applications. *EPJ Tech. Instrum.* **2** (2015), 9.

[8]   Bailo E., Deckert V.: Tip-enhanced Raman scattering. *Chem. Soc. Rev.* **37** (2008), 921–930.

[9]   Bovill A.J., McConnell A.A., Nimmo J.A., Smith W.E.: Resonance Raman spectra of α-copper phthalocyanine. *J. Phys. Chem.* **90** (1986), 569–575.

[10]   Shaibat M.A., Casabianca L.B., Siberio-Pérez D.Y., Matzger A.J., Ishii Y.: Distinguishing polymorphs of the semiconducting pigment copper phthalocyanine by solid-state NMR and Raman spectroscopy. *J. Phys. Chem. B* **114** (2010), 4400–4406.

[11]   Szybowicz M., Runka T., Drozdowski M., Bała W., Grodzicki A., Piszczek P., Bratkowski A.: High temperature study of FT-IR and Raman scattering spectra of vacuum deposited CuPc thin films. *J. Mol. Struct.* **704** (2004), 107–113.

[12]   Caplins B.W., Mullenbach T.K., Holmes R.J., Blank D.A.: Femtosecond to nanosecond excited state dynamics of vapor deposited copper phthalocyanine thin films. *Phys. Chem. Chem. Phys.* **18** (2016), 11454–11459.

[13]   Sacco A., Imbraguglio D., Giovannozzi Andrea M., Portesi C., Rossi A.M.: Development of a candidate reference sample for the characterization of tip-enhanced Raman spectroscopy spatial resolution. *RSC Adv.* **8** (2018), 27863–27869.

[14]   Jiang S., Chen Z., Chen X., Nguyen D., Mattei M., Goubert G., Van Duyne R.P.: Investigation of cobalt phthalocyanine at the solid/liquid interface by electrochemical tip-enhanced Raman spectroscopy. *J. Phys. Chem. C* **123** (2019), 9852–9859.

[15]   Melendres C.A., Maroni V.A.: Raman spectra and normal coordinate analysis of the planar vibrations of iron phthalocyanine. *J. Raman Spectrosc.* **15** (1984), 319–326.

Determination of heavy metal poisoning antidote 2,3-dimercapto-1-propanesulfonic acid using silver solid amalgam electrode

Marta Choińska[a, b, *], Vojtěch Hrdlička[a, b], Beatriz Ruiz Redondo[b, c], Jiří Barek[b], Tomáš Navrátil[a]

[a] *J. Heyrovský Institute of Physical Chemistry of the Czech Academy of Sciences, Dolejškova 2155/3, 182 23 Prague 8, Czech Republic* ✉ *marta.choinska@gmail.com*
[b] *UNESCO Laboratory of Environmental Electrochemistry, Department of Analytical Chemistry, Faculty of Science, Charles University, Hlavova 2030/8, 128 43, Prague 2, Czech Republic*
[c] *University of Valladolid, Plaza de Santa Cruz, 8, 47002 Valladolid, Spain*

Abstract

2,3-Dimercapto-1-propane-sulfonic acid (DMPS) was investigated using direct current voltammetry (DCV), differential pulse cathodic stripping voltammetry (DPCSV), differential pulse anodic stripping voltammetry (DPASV), and elimination voltammetry with linear scan (EVLS) at a polished (p-AgSAE)and at a meniscus modified silver solid amalgam electrode (m-AgSAE). EVLS confirmed two consecutive reductions with coupled proton/electron transfer. Voltammetric titrations of DMPS with Pb2+ proved complex formation, with limits of quantification (LOQs) and detection (LODs) 0.3 and 0.1 µmol L^{-1} at m-AgSAE and 0.8 and 0.3 µmol L^{-1} at p-AgSAE, respectively. Determination of DMPS in commercial drug Dimaval and human urine samples confirmed practical applicability of the developed method.

1. Introduction

The aim of this work has been development of a new voltammetric method for the determination of 2,3-dimercapto-1-propane-sulfonic acid (DMPS), Fig. 1. Investigation was done to obtain relevant information about complexing behavior of DMPS towards lead ions.

Fig. 1 Chemical structure of 2,3-dimercapto-1-propane-sulfonic acid

Lead is one of heavy metals, which can cause irreversible neurological problems [1, 2]. DMPS is a synthetic antidote with two thiol groups, used for treatment of poisoning by heavy metals [3–6]. Strong complexing properties, high water solubility, and negligible side effects are the most important advantages of DMPS [4, 7].

Voltammetry was chosen as a determination technique due to its high sensitivity and selectivity, speed, low costs [8]. Thiol groups in DMPS can be oxidatively chemisorbed on solid amalgam electrode. It can be used as an accumulation step for cathodic stripping voltammetry [9–11]. Moreover, solid amalgam electrode (SAE) was chosen as the working electrode because of its properties as high signal to noise ratio, wide potential window, and ability to reach low limits of detection (*LOD*) [12–13].

2. Experimental

2.1 Reagents and chemicals

All solutions were prepared using deionized water (Milli-Q-Gradient, Millipore, Prague, Czech Republic) with conductivity <0.05 $\mu S\,cm^{-1}$. Britton-Robinson buffer solutions, pH range from 2 to 12, were prepared by mixing the proper amounts of 0.2 M NaOH (alkaline solution) and of 0.04 M H_3BO_3, 0.04 M H_3PO_4 and 0.04 M CH_3COOH (all Lachema, Czech Republic) acidic solution. The acidic solution was prepared by dissolution of 1.235 g of H_3BO_3, p.a., 0.88 mL of H_3PO_4 (85%), p.a., and 1.435 mL of CH_3COOH (99%), p.a., in 500 mL of deionized water. The alkaline solution was prepared by dissolution of 3.995 g of NaOH, p.a., in 500 mL of deionized water (all Lachema, Czech Republic).

Stock solution of DMPS was prepared by dissolving 10 mg of solid 2,3-dimer-capto-1-propanesulfonic acid monohydrate, p.a. (Merck, Czech Republic) in 100 mL of deionized water. For the preparation of the model sample solution, one capsule of drug Dimaval (Heyl, Germany), contains 100 mg of DMPS, was dissolved in 1.0 L of deionized water, to the DMPS concentration of 0.531 mmol L^{-1}. Two model samples of Dimaval were prepared by dilution of the above-mentioned solution with Britton-Robinson buffer solution, to concentrations 1.0 $\mu mol\,L^{-1}$ and of 10 $\mu mol\,L^{-1}$, respectively. Urine model samples were prepared by mixing Britton-Robinson buffer solution with urine samples obtained from volunteer (man, healthy, 30 years old) in ratio 1:1. Sample pH was adjusted by addition of proper amount of 0.2 mol L^{-1} NaOH. Before each measurement, oxygen was removed for 5 min by nitrogen bubbling (purity class 4.6; Messer Technogas, Prague, Czech Republic).

2.2 Instrumentation

Measurements were performed using two types of working electrodes: meniscus modified silver solid amalgam electrode (m-AgSAE, working surface of 0.382±0.025 mm^2, α < 0.05) and polished silver solid amalgam electrode (p-AgSAE, working surface of 0.196±0.015 mm^2, α < 0.05). Ag|AgCl|3M KCl was used as the reference electrode and platinum wire (Ø1 mm) was used as the auxiliary electrode (both from Elektrochemické detektory, Czech Republic). Measurements were performed at laboratory temperature (25 ± 2 °C).

The pH was measured using pH-meter Jenway 3505 with combined glass electrode, type 924 001 (Bibby Scientific Limited, UK). Voltammetric measurements were performed using the computer-controlled Eco-Tribo Polarograph (Polaro-Sensors, Czech Republic). Software used for measurements was MultiElChem 3.3 for Windows XP/7/8/10 (J. Heyrovský Institute of Physical Chemistry of the Czech Academy of Sciences, Czech Republic).

3. Results and discussion

Optimum conditions for measurements were obtained by series of measurement in wide range of pH values and testing various cleaning procedures. Optimum potential of accumulation (E_{acc}) and time of accumulation (t_{acc}) of DMPS were adjusted for differential pulse cathodic stripping voltammetry (DPCSV) at p-AgSAE and m-AgSAE.

The dependence between peak height and concentration of DMPS at p-AgSAE has a logarithmic shape, which corresponds to the accumulation process at the electrode surface. The linear dependence was observed in the DMPS concentrations from 0.3 µmol L^{-1} to 2.0 µmol L^{-1}. Peak shift towards negative potential with increasing concentration of DMPS corresponds to the metal-thiol bond and influence of electrode surface structure on this bond. On the contrary, signals on m-AgSAE were more stable and the dependence between concentration of DMPS and signal was almost linear in whole tested range of concentrations.

The developed method was tested in model samples of Dimaval and urine. Found amounts of DMPS were in good agreement with declared contents using both electrodes. However, the repeatability of signals registered using p-AgSAE in urine samples were significantly worse than those in Dimaval samples. It can be caused by complicated biological matrices and fouling effects of urine.

ELSV measurements confirmed two consecutive reductions of DMPS in adsorbed state. At m-AgSAE signal were at about −415 mV and −440 mV, respectively and at p-AgSAE at about −790 mV and −830 mV, respectively. Reductions at m-AgSAE at the scan rates from 80 mV s^{-1} to 640 mV s^{-1} have been controlled by a kinetic process at −400 mV.

In anodic scans on m-AgSAE, only one peak was visible at about −390 mV. It corresponds with the oxidation of mercury electrode surface on the electrode in the presence of DMPS and with diffusion from the bulk solution of products. At p-AgSAE no significant anodic signal was found.

The last part of the research revealed voltammetric behavior of DMPS in the presence of Pb^{2+}. Voltammetric titration was investigated by DPCSV and differential pulse anodic stripping voltammetry (DPASV) during consecutive additions of 1 mmol L^{-1} of Pb(NO$_3$)$_2$ into 100 µmol L^{-1} DMPS solution in acetate buffer of pH 5.0. In absence of Pb2+ on the electrode surface, Hg(DMPS) complex is formed during the accumulation step. During the anodic scan, there is only one, well developed reduction peak (Fig. 2A).
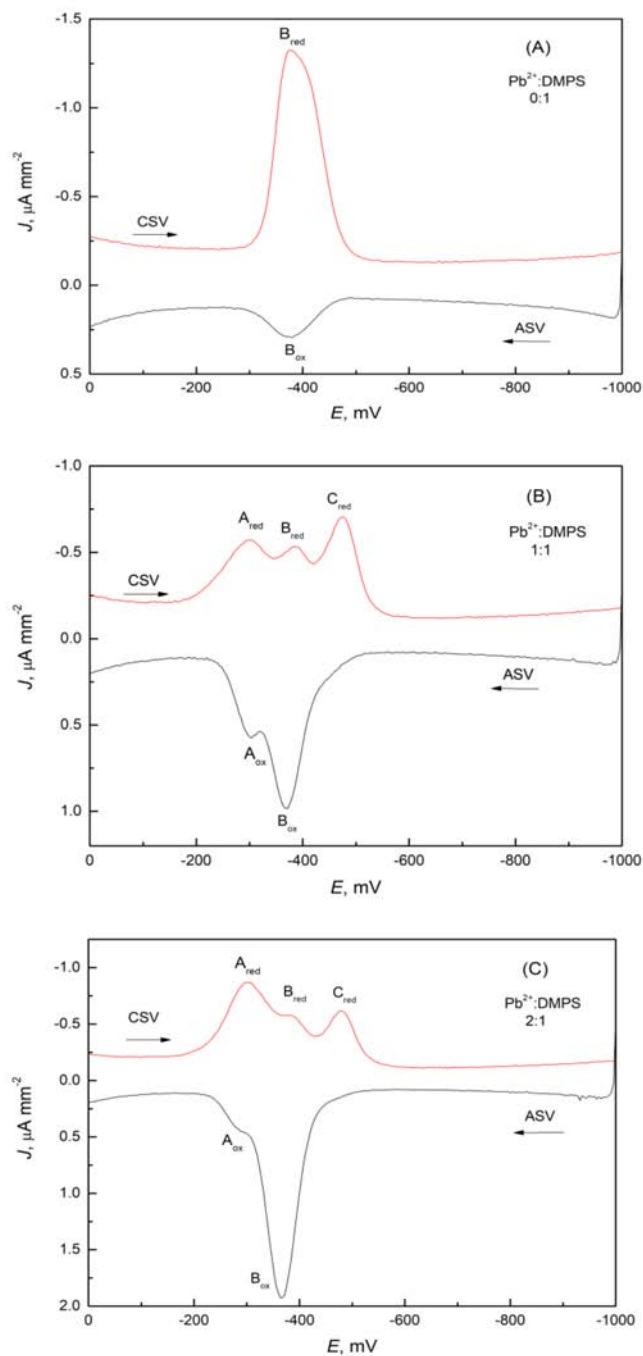
Fig. 2 DP CS and DP AS voltammograms of 10 µmol L^{-1} of DMPS in acetate buffer pH = 5, corresponding to [Pb^{2+}:DMPS] ratios of (A) 0:1, (B) 1:1, and (C) 2:1. Upper curve corresponds to the cathodic scan, E_{acc} = 0 mV, t_{acc} = 15 s. Lower curve corresponds to reverse anodic scan with t_{acc} = 15 s at E_{acc} = −1000 mV, v = 20 mV s^{-1} (Ref. [16]).

Table 1
Comparison of voltammetric methods for DMPS determination (LDR

Method	Working electrode	Linear dynamic range / $\mu mol\ L^{-1}$	LOQ / $\mu mol\ L^{-1}$	LOD / $\mu mol\ L^{-1}$	Ref.
LSV	glassy-carbon electrode modified with multi-walled carbon nanotubes	18–140 260–690	41	14	[14]
DPCSV	p-AgSAE	0.3–2.0	0.8	0.3	this work
DPCSV	m-AgSAE	0.1–1.0 1.0–10.0	0.3	0.1	this work

When Pb^{2+}:DMPS ratio is equal to 1:1, two oxidation and three reduction peaks were registered (Fig. 2B). Peak A_{red} at about –300 mV corresponds to formation of Pb(DMPS) complex. This complex was further reduced to the Pb^0(Hg) at about –500 mV (C_{red}). Reduction peak of free Pb^{2+} was also registered (B_{red}). Oxidation peaks A_{ox} and B_{ox} correspond to reverse processes and C_{ox} is not present, because no free DMPS is present in the solution. At ratio 2:1, there is no free DMPS in the solution, however, excess of lead ions. As a consequence, A_{red} and B_{ox} peak increased. Increase of B_{ox} corresponds to the deposition of Pb^{2+} during the accumulation step. Peaks Bred and Cred remained practically unchanged (Fig. 2C).

Voltammetric titration confirmed the mechanism of formation complexes of Pb(DMPS), Hg(DMPS), and Pb(Hg). It also confirmed possibility of determination Pb^{2+} and DMPS in the same solution.

4. Conclusions

Validation in model sample of drug Dimaval and human urine spiked with DMPS confirmed that this method can be used for clinical purposes. Voltammetric titration of DMPS by Pb^{2+} ions proved that it can be used for simultaneous determination of the drug and heavy metal ions in human urine. Moreover, obtained $LODs$ were two orders lower than those in the previously reported voltammetric method [14] (Table 1).

References

[1] An H.H., Luchak M., Copes R.: Lead toxicity: A systematic review of recently published cases. *Clin. Toxicol.* **53** (2015), 757–758.
[2] Kim Y., Lust M.R., Kreimerbirnbaum M.: 2,3-Dimercaptopropane-1-sulfonate (DMPS) in the treatment of lead-poisoning. *Faseb J.* **2** (1988), A1820–A1820.
[3] Aposhian H.V.: DMSA and DMPS – water-soluble antidotes for heavy-metal poisoning. *Annu. Rev. Pharmacol.* **23** (1983), 193–215.

[4] Bjorklund G., Crisponi G., Nurchi V.M., Cappai R., Djordjevic A.B., Aaseth J.: A review on coordination properties of thiol-containing chelating agents towards mercury, cadmium, and lead. *Molecules* **24** (2019), 3247.

[5] Donner A., Hruby K.: DMPS in the treatment of acute and chronic heavy-metal poisoning. *Acta Med. Aust.* **14** (1987), 10–10.

[6] Donner A., Hruby K., Pirich K., Kahls P., Schwarzacher K., Meisinger V.: Dimercaptopropan-sulfonate (DMPS) in the treatment of acute lead-poisoning. *Vet. Hum. Toxicol.* **29** (1987), 37–37.

[7] Blanusa M., Varnai V.M., Piasek M., Kostial K.: Chelators as antidotes of metal toxicity: Therapeutic and experimental aspects. *Curr. Med. Chem.* **12** (2005), 2771–2794.

[8] Barek J., Moreira J.C., Zima J.: Modern electrochemical methods for monitoring of chemical carcinogens. *Sensors-Basel* **5** (2005), 148–158.

[9] Josypcuk B., Fojta M., Yosypchuk O.: Thiolate monolayers formed on different amalgam electrodes. Part II: Properties and application. *J. Electroanal. Chem.* **694** (2013), 84–93.

[10] Yosypchuk B., Marecek V.: Properties of thiolate monolayers formed on different amalgam electrodes. *J. Electroanal. Chem.* **653** (2011), 7–13.

[11] Alvarez J.M.F., Smyth M.R.: Cathodic stripping voltammetry of pyridine-2-thiol and some related-compounds. *Analyst* **114** (1989), 1603–1605.

[12] Danhel A., Barek J.: Amalgam electrodes in organic electrochemistry. *Curr. Org. Chem.* **15** (2011), 2957–2969.

[13] Fadrna R.: Polished silver solid amalgam electrode: Further characterization and applications in voltammetric measurements. *Anal. Lett.* **37** (2004), 3255–3270.

[14] Ziyatdinova G.K., Grigor'eva L.V., Budnikov G.K.: Electrochemical determination of unithiol and lipoic acid at electrodes modified with carbon nanotubes. *J. Anal. Chem.* **64** (2009), 185–188.

[15] Hrdlicka V., Choińska M., Redondo B.R., Barek J., Navrátil T.: Determination of heavy metal poisoning antidote 2,3-dimercapto-1-propanesulfonic acid using silver solid amalgam electrode. *Electrochim. Acta* doi.org/10.1016/j.electacta.2020.136623

Canagliflozin oxidation study using electrochemical flow cell and comparison with hydrogen peroxide oxidation

Filip Vymyslický[a, *], Tomáš Křížek[a], Jakub Heřt[b]

[a] *Department of Analytical Chemistry, Faculty of Science, Charles University, Hlavova 8/2030, 128 43 Prague 2, Czech Republic* ✉ *f.vymyslicky@gmail.com*
[b] *Zentiva Group, a.s., U Kabelovny 130, 102 37 Prague 10, Czech Republic*

Keywords
canagliflozin
design of experiments
electrochemical flow cell
HPLC
oxidation

Abstract
By standards, the effect on oxidation of an active substance is tested using hydrogen peroxide solution at elevated temperature in a stress chamber for 1–7 days. An alternative way to study the effect of oxidation on an active substance is to use an electrochemical flow cell. Solution with active substance flows at low flow rate into a small reactor, where the active substance is oxidized on working electrode surface. The electrolyte stream with the oxidized active substance is then directed to the sample collector. Products of electrochemical oxidation are analyzed by high performance liquid chromatography with ultraviolet–visible spectrophotometry detection. Canagliflozin has been used because its main degradation pathway is oxidation. The design of experiments approach was used to explore the experimental space and optimize experimental conditions of oxidation. The results of the oxidation study performed in the electrochemical flow cell were statistically compared with the results of a standard study using hydrogen peroxide solution. The most suitable conditions for electrochemical oxidation were found. Electrochemical oxidation produced comparable amounts of impurities as chemical oxidation with hydrogen peroxide.

1. Introduction

Canagliflozin is a selective sodium-glucose cotransporter type 2 inhibitor used for the treatment of type 2 diabetes mellitus. Canagliflozin inhibits sodium-glucose cotransporter type 2 present in proximal tubules of the

Fig. 1 Structure of canagliflozin

kidney, which restricts glucose absorption in the kidney, thereby increasing the urinary excretion of glucose and lowering the level of glucose in the blood [1]. The formula of canagliflozin is $C_{24}H_{25}FO_5S$, the structure of canagliflozin is in Fig. 1. The
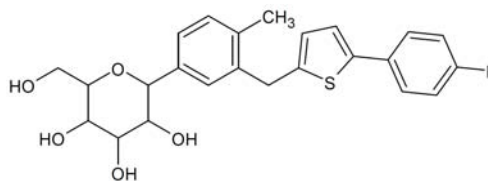
IUPAC name of canagliflozin is (2*S*,3*R*,4*R*,5*S*,6*R*)-2-[3-[5-(4-fluoro-phenyl)-thiophen-2-ylmethyl]-4-methyl-phenyl]-6-hydroxymethyltetrahydro-pyran-3,4,5-triol [2]. Canagliflozin is a white powder, insoluble in water but very soluble in organic solvents like methanol or dimethylsulfoxide. Canagliflozin is sold under tradename INVOKANA.

Many authors have studied the electrochemical properties of active substances in the literature. One example is the study of electrochemical behaviour and oxidation of bromhexine. These properties were studied using differential pulse voltammetry and cyclic voltammetry on a carbon electrode. The results of electrochemical methods were compared with high performance liquid chromatography (HPLC) analysis [3]. Another example is the study of electrochemical behaviour and degradation study performed on the active substance atomoxetine. Degradation was studied using differential pulse voltammetry and cyclic voltammetry on a carbon electrode. The results were also compared with HPLC analysis [4]. Electrochemical methods are used mainly to study the mechanism of oxidation, but in this work, the electrochemical method was used to degrade the active pharmaceutical ingredient.

In the stability studies of active pharmaceutical ingredient properties, the influence of temperature, pH, light, and oxidation is studied [5]. By The International Council for Harmonisation of Technical Requirements for Pharmaceuticals for Human Use (ICH) standards, the influence of oxidation on active pharmaceutical ingredient is studied using hydrogen peroxide at room temperature or increased temperature in the stress chamber during 1–7 days [6]. An alternative way to study the influence of oxidation on active pharmaceutical ingredient is using electrochemical flow cell, where an electrolyte with active pharmaceutical ingredient is driven by low flow rate into the small reactor. In the small reactor, the active pharmaceutical ingredient is oxidized on the surface of the working electrode. The stream of electrolyte with oxidized active pharmaceutical ingredient is driven to the sample collector. Products of electrochemical oxidation are analysed by HPLC UV/VIS. The design of experiments approach was used for development of an alternative method of oxidation of canagliflozin using an electrochemical flow cell. The design of experiments approach was used to explore the experimental space of the method and to find the optimal experimental conditions of electrochemical oxidation of canagliflozin.

2. Experimental

2.1 Material and reagents

Canagliflozin (Zentiva, Czech Republic), 99.9% methanol (Honeywell, Germany), 98% ammonium dihydrogen phosphate (Sigma-Aldrich, Japan), 35% ortho-phosphoric acid (Penta, Czech Republic), 25% ammonia (Lachner, Czech Republic), 30% hydrogen peroxide (Lachner, Czech Republic), water for chromatography
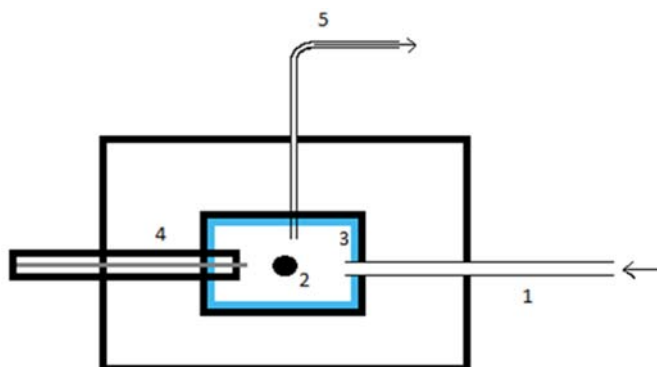
Fig. 2 Scheme of the electrochemical flow cell: (1) input, (2) working electrode, (3) gasket, (4) reference electrode, (5) counter electrode.

was obtained by purifying demineralised water using Millipore type Synergy UV purification instrument.

2.2 Instruments

An Agilent 1290 HPLC system (Agilent Technologies, Germany) with high pressure pump, autosampler, thermostat and DAD detector was used for all experiments. The Pinnacle DB biphenyl column (100×2.1 mm, 1.9 µm; Restek, USA) was used for separation. In the HPLC method 10 mM ammonium dihydrogen phosphate buffer pH = 2.5 was used as component A and methanol as component B of the mobile phase. The gradient program was set as follows: t(min)/% B: 0/15; 5/50; 10/55; 17/90; 22/90; 23/15; 25/15. The flow rate of the mobile phase was 0.4 ml min^{-1} and the injection volume was 2 µl. The detector operated at a wavelength of 220 nm. The autosampler temperature was set at 20 °C and the column temperature at 60 °C. The Empower software was used for evaluation. For electrochemical oxidation, electrochemical flow cell from ALS (Japan) was used. Glassy carbon electrode ($\varnothing$ = 6 mm) and silver/silver chloride electrode were used as working and reference electrode, respectively. The scheme of electrochemical flow cell is in Fig. 2. Electrodes were connected with potentiostat PalmSens 3 from Palmsens (Netherlands). An Elmasonic S15H ultrasonic bath from Elma (Germany) was used for sample preparation. For pH measurements pH meter Jenway 3540 from Jenway (United Kingdom) was used.

3. Results and discussion

At the development of the method for the study of canagliflozin oxidation using electrochemical flow cell, it was first necessary to find the optimal conditions of electrochemical oxidation. The design of experiments approach was used. Chosen
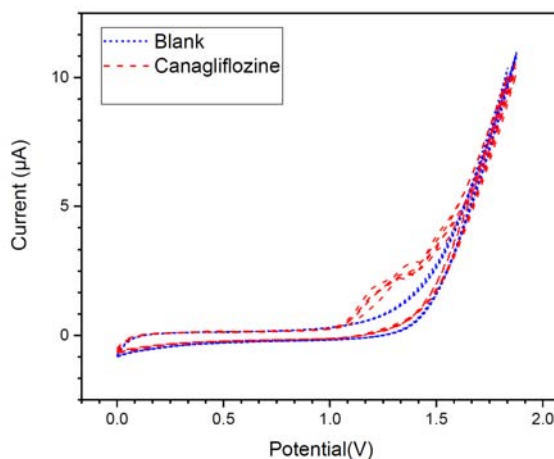
Fig. 3 Cyclic voltammogram of canagliflozin (concentration of canagliflozin 1.1 mg ml^{-1}; electrolyte: 300 mM ammonium dihydrogen phosphate, pH = 4.0 and methanol (1:1, *v/v*) and scan rate 0.01 V s^{-1}).

independent variables and their levels were: concentration of electrolyte (100; 200; 300 mM), pH of electrolyte (4.0; 6.0; 8.0), cell size (50; 100; 200; 500 μm), and flow rate (0.1; 0.25; 0.4 ml h^{-1}). The reduced combinatorial design was used. In the Modde 12 software a worksheet containing 11 experiments was created. The working potential of 1.2 V was selected based on cyclic voltammetry of canagliflozin in Fig. 3. From this figure, it can be seen that the oxidation of canagliflozin occurs in the region from 1.1 V to 1.4 V. All experiments were performed with 1.1 mg ml^{-1} canagliflozin samples. The glassy carbon electrode was used as a working electrode and the silver/silver chloride electrode was used as a referent electrode. The canagliflozin samples oxidized in the electrochemical flow cell under the experimental conditions given by the worksheet were measured by HPLC with UV/VIS detection. Dependent variables peak areas of impurities and percentage of peak areas of impurities obtained from chromatograms were evaluated by the partial least square method in the Modde 12 software. The variable importance in the projection plot tool was used for interpretation of the data as a whole. The significance values of the independent variables were evaluated: buffer pH = 1.37, flow rate of 1.25 ml h^{-1}, buffer concentration 0.61 mM, and cell size 0.4 μm. From this tool it was concluded that the electrochemical oxidation of canagliflozin is the most affected by the pH of the electrolyte and flow rate of the electrolyte. Using the optimizer tool, the most suitable conditions for the oxidation of canagliflozin were evaluated: flow rate 0.1 ml h^{-1}; 300 mM ammonium dihydrogen phosphate; pH of electrolyte 4.0 and cell size 500 μm. Using one factor at the time approach the dependence of the cell size on the total sum of impurities was tested (Fig. 4A).

It is visible from the graph that the smaller the cell we use, the more oxidation products are formed. Based on the graph, the most suitable conditions were
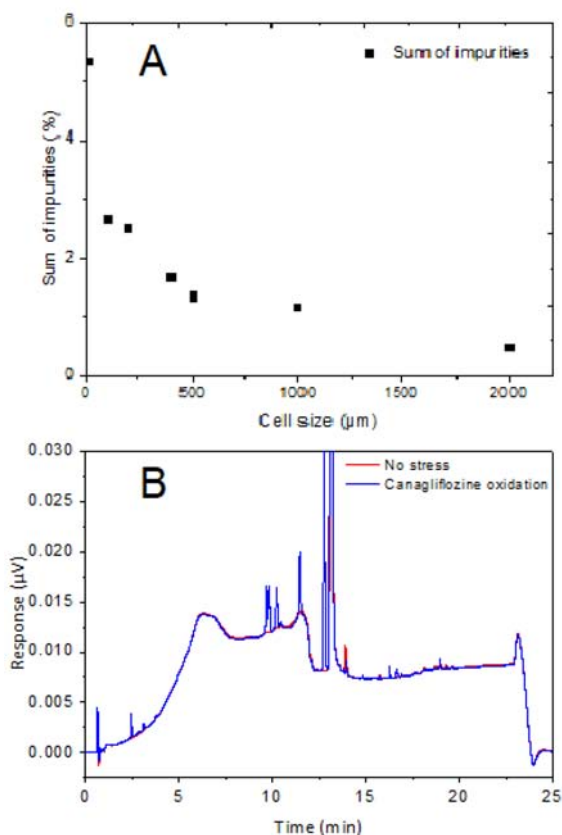
Fig. 4 (A) Optimization of electrochemical oxidation conditions, dependence of sum of impurities on cell size. (B) Chromatogram of a sample oxidized under most suitable conditions.

adjusted to flow rate 0.1 ml h^{-1}; 300 mM ammonium dihydrogen phosphate; pH of electrolyte 4.0 and cell size 12 µm. Under the most suitable conditions, a repeatability test was performed, by ten independent oxidation experiments. The relative standard deviation of the percentage area of canagliflozin was 1.64% at a significant level of 0.95. The chromatogram of sample oxidized under most suitable conditions is in Fig. 4B. The standard study of the effect of oxidation on canagliflozin using hydrogen peroxide according to ICH guidelines was performed. The study was performed under two sets of experimental conditions. In the first case, a solution of 50% methanol with the addition of 3% H_2O_2 was used. In the second case, the conditions in the electrochemical flow cell were simulated. A 300 mM ammonium dihydrogen phosphate, pH 4.0 and methanol in a ratio 1:1 (*v/v*) with the addition of 3% H_2O_2 was used. Samples for the oxidation study were stressed in a stability chamber for 1, 3 and 7 days at the constant temperature of 50 °C.

The total sums of impurities formed during chemical oxidation using hydrogen peroxide in both media were compared as is shown in Fig. 5A. It is obvious that
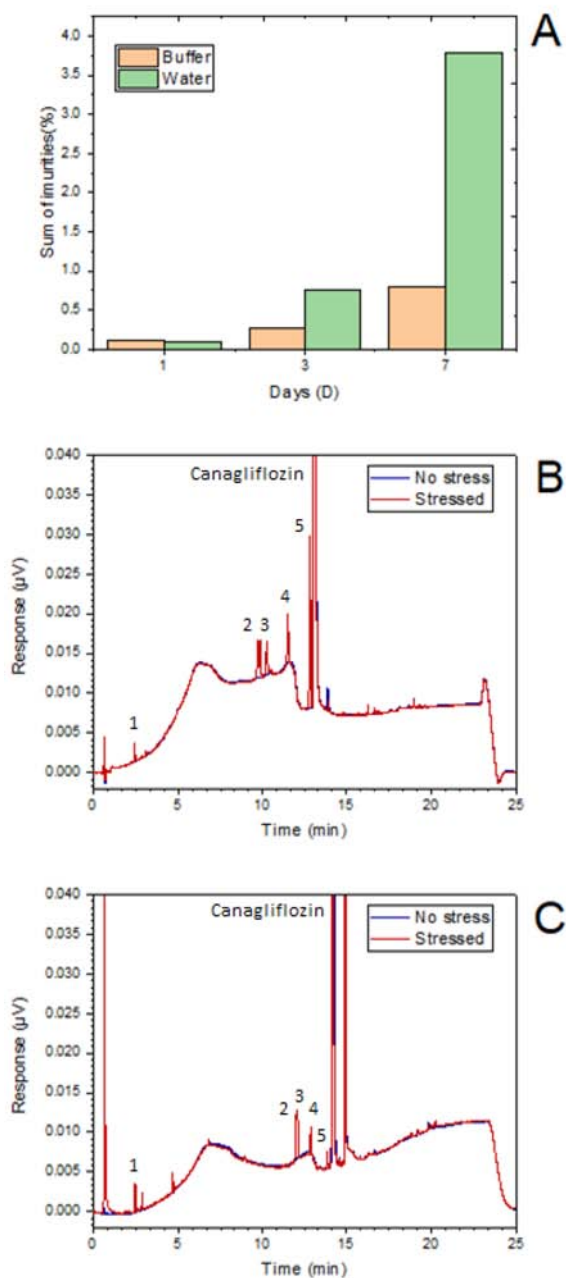
Fig. 5 (A) A comparison of a standard oxidation study using hydrogen peroxide in 50% methanol with added buffer and without them. (B) Chromatogram of sample oxidized electrochemically. (C) Chromatogram of sample oxidized chemically.

ammonium phosphate suppresses oxidation of canagliflozin. The reason of this phenomenon is unknown. Fig. 5B and Fig. 5C show chromatograms of samples oxidized electrochemically and chemically, respectively. It can be seen that five impurities were formed by both types of oxidation, however, in different amounts.

4. Conclusion

An alternative method for the oxidative study of canagliflozin was developed. The design of experiments approach was used in the method development. The developed method works with *RSD* of 1.65% (α= 0.95). Oxidation of canagliflozin by the developed method produced five impurities that are identical with those produced using the standard oxidation study with hydrogen peroxide.

References

[1]   Chao E.C.: Canagliflozin. *Drugs Future* **36** (2011), 351–357.
[2]   Nisly S.A., Kolanczyk D.M., Walton A.M.: Canagliflozin, a new sodium-glucose cotransporter 2 inhibitor, in the treatment of diabetes. *Am. J. Health. Syst. Pharm.* **70** (2013), 311–319.
[3]   Turchan M., Jara-Ulloa P., Bollo S., Nunez-Vergara L.J., Squella J.A., Alvarez-Lueje A.: Voltammetric behaviour of bromhexine and its determination in pharmaceuticals. *Talanta* **73** (2007), 913–919.
[4]   Perez-Ortiz M., Munoz C., Zapata-Urzua C., Alvarez-Lueje A.: Electrochemical behavior of atomoxetine and its voltametric determination in capsules. *Talanta* **82** (2010), 398–403.
[5]   Baertschi S.W., Alsante K.M., Reed R.A.: *Pharmaceutical Stress Testing: Predicting Drug Degradation.* London, Informa Healthcare 2011.
[6]   Rignall A.: ICHQ1A(R2) stability testing of new drug substance and product and ICHQ1C stability testing of new dosage forms. In: *ICH Quality Guidelines: An Implementation Guide.* A. Teasdale, D. Elder, R.W. Nims (Eds.). Hoboken, Wiley 2017, p. 3–44.

Novel hybrid electrochemical DNA biosensor for monitoring oxidative DNA damage via oxidation/reduction signals of low molecular weight double-stranded DNA

MICHAL AUGUSTÍN*, VLASTIMIL VYSKOČIL

UNESCO Laboratory of Environmental Electrochemistry, Department of Analytical Chemistry, Faculty of Science, Charles University, Hlavova 8, 128 43 Prague 2, Czech Republic
✉ *michal.augustin@natur.cuni.cz*

Keywords
biosensor
damage
DNA
graphite
voltammetry

Abstract
Deoxyribonucleic acid (DNA) represents a major target molecule for many damaging agents causing unfavorable changes in a structure of DNA molecule that bind and interact with DNA. Thus, a high demand for reliable tools regarding a better comprehension of the nature of DNA damaging processes still represents one of the main goals in this area. Herein, we describe a development of a novel hybrid electrochemical DNA biosensor based on an "edge-plane" pyrolytic graphite electrode (EPPGE) in connection with an elementary optimization process providing a closer resolution of the redox processes of low molecular weight double-stranded DNA (dsDNA) at the EPPGE. Subsequent analytical application incorporating an employment of the model structure $K_2[IrCl_6]$ (representative of transition metal complexes), and evaluation of its damaging effect in relation to DNA by means of linear sweep voltammetry resp. square-wave voltammetry are also presented.

1. Introduction

Although DNA represents a relatively stable component from the chemical point of view, it remains constantly exposed to a large number of chemical or physical agents causing chemical changes in DNA molecules that occur in the environment or are major or minor products of cellular metabolism [1].

One-electron oxidation of the DNA represents a damaging process where the loss of an electron (oxidation) from duplex DNA results in the formation of a nucleobase radical cation (electron "hole") that is subsequently consumed in chemical reactions that often lead to mutations. A defining characteristic of the one-electron oxidation of DNA is the preferential reaction at the guanine moiety that is detected as strand cleavage following chemical or enzymatic treatment of the oxidized DNA [2–3].

DNA-based electrochemical biosensors are successfully used in various applications such as monitoring and evaluating the mechanisms of interaction between DNA and various drugs or damaging agents, rapid monitoring of trace metals or pollutants present in the environment, or direct monitoring of DNA hybridization processes [4].

The electrochemical activity of nucleic acids (both the native high-molecular ones as well as oligonucleotides) is in general referred to the electroactivity of its components – nucleobases and sugar residues. At mercury-based electrodes, adenine and cytosine residues undergo reduction processes close to –1.4 V (against SCE) in neutral or weakly acidic medium (giving rise to the peak CA). On the other hand, all bases have been reported to be electrochemically oxidized at carbon electrodes, but only adenine and (particularly) guanine oxidation signals have been widely utilized in electrochemical DNA biosensors [5].

In 2017, the electrochemistry of nucleic acids achieved an important milestone as the reduction of the DNA oligonucleotides was performed at a "basal-plane" pyrolytic graphite electrode which provided wide potential window allowing both the electrooxidation as well as the eletroreduction of the nucleobases at a single electrode for the very first time. Despite these findings, utilization of the aforementioned biosensor in terms of analytical applications has yet to be verified and remains unclear up to this date [6].

The aim of the proposed contribution is a presentation of the development process and subsequent testing of a novel type of hybrid electrochemical DNA biosensor and its verification as a reliable analytical tool in terms of monitoring DNA damage.

2. Experimental

2.1 Reagents and chemicals

Low molecular weight double-stranded DNA (dsDNA) derived from salmon sperm was obtained from Sigma-Aldrich, Germany. Stock solutions (0.1 mg/mL) of dsDNA were prepared in a 0.1 mol/L phosphate buffer of pH = 7.4 (PB). Dipotassium hexachloroiridate ($K_2[IrCl_6]$) was purchased from Sigma-Aldrich, Germany. Stock solutions (0.001 mol/L) of $K_2[IrCl_6]$ were prepared in the PB.

2.2 Apparatus

Voltammetric measurements were performed using the µAutolab III/FRA2 potentiostat/galvanostat (Eco Chemie, The Netherlands) driven by a NOVA 1.11 software (Metrohm Autolab, Switzerland). All measurements were carried out in a three-electrode system using an "edge-plane" pyrolytic graphite working electrode (EPPGE) with an electroactive surface diameter of 3 mm (BAS, Japan), a silver|silver chloride reference electrode (Ag|AgCl|sat. KCl), and a platinum

counter electrode (Elektrochemické Detektory, Czech Republic) in a 20 mL glass voltammetric cell at ambient temperature.

2.3 Preparation of the biosensor

Prior to the every measurement, surface of the EPPGE was mechanically cleaned by gentle wiping of the electrode on the soft polishing pad rinsed with distilled water. Afterwards, the electrode was rinsed with distilled water and placed in the PB for the subsequent electrochemical activation. Electrochemical activation was performed in the PB by applying potential of 1.5 V for 240 s without stirring. A potential pulse in working range of potentials (0.0–1.5 V) was then applied.

Additional electrochemical activation was performed in the solution of the redox indicator ($[Fe(CN)_6]^{3-/4-}$) by consecutive cycling in the range of potentials from 1.0 to –0.8 V (15 scans) and from 0.55 to –0.15 V (10 scans).

The electrochemical DNA biosensor based on the EPPGE (dsDNA/EPPGE biosensor) was prepared by the adsorption of dsDNA on the EPPGE. Optimal parameters of the dsDNA adsorption were: a concentration of 0.1 mg/mL in the PB ($c_{g(dsDNA)}$), a deposition potential of 0.7 V (E_{dep}), and an adsorption time of 5 min (t_{ads}) without stirring the solution.

At last, the electrode was immersed in the solution of the redox indicator and the consecutive cycling in the range of potentials from 0.55 to –0.15 V (20 scans) was performed in order to secure the stability of the oxidation/reduction signals of dsDNA at the EPPGE.

2.4 Procedures

The experimental parameters were as follows: square wave voltammetry (SWV) in the PB with a pulse amplitude of 20 mV, a frequency of 50 Hz, a scan rate of 750 mV/s, and a potential step of 15 mV; linear sweep voltammetry (LSV) in the PB with scan rates of 0.2–1.0 V and a potential step of 2.4 mV. All curves were recorded three times ($n = 3$).

3. Results and discussion

Since the closest resolution of the processes associated with the electroreduction of single DNA components at pyrolytic graphite has been performed with the "basal-plane" pyrolytic graphite electrode (BPPGE), we have decided to take over corresponding experimental technique and conditions (LSV; scan rate of 1.0 V/s, step potential of 2.4 mV) at the very beginning of our optimization process with the EPPGE [6].

In this particular case, it is possible to notice the occurrence of the two mixed voltammetric peaks at the default experimental conditions (green line, Fig. 1A) selected for the reduction of dsDNA at the EPPGE. By gradually decreasing the
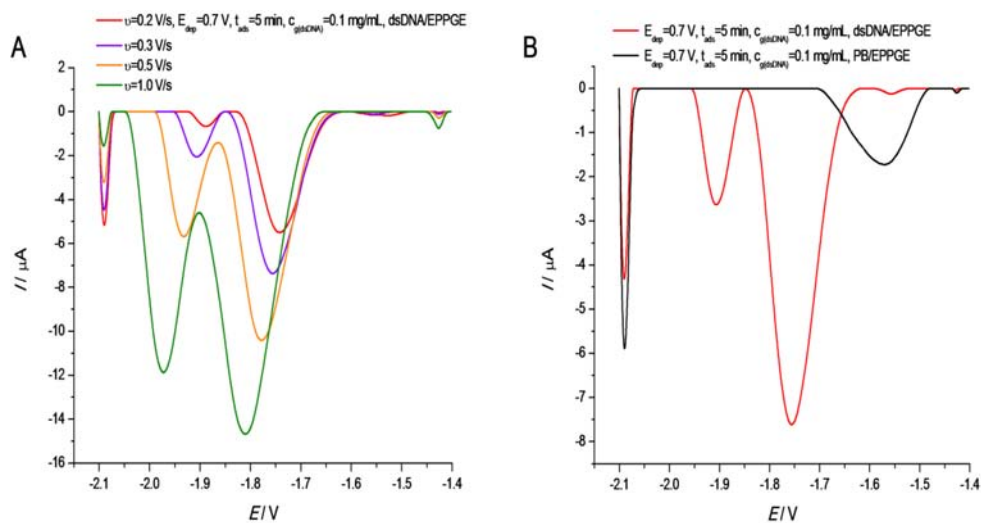
Fig. 1 Baseline-corrected LSV recordings corresponding to the reduction of dsDNA at the EPPGE for different values of scan rate (0.2–1.0 V/s, Fig. 1A), resp. baseline-corrected LSV recordings corresponding to the reduction of dsDNA at the EPPGE and the negative test performed under the same experimental conditions within the blank solution (phosphate buffer) at the bare EPPGE (0.3 V/s, Fig. 1B).

scan rate, the optimal conditions ($v \leq 0.3$ V/s) were found and the mutual separation of the signals was allowed – characterized by the presence of two single well-developed voltammetric peaks at potentials of –1.75 V resp. –1.90 V (0.3 V/s, orange line, Fig. 1A). Taking into account previous work regarding processes associated with the reduction of DNA at the mercury electrodes resp. BPPGE, we can assume that the peak appearing at the potential of –1.75 V corresponds to the mixed peak for the reduction of the cytosine and adenine residues within dsDNA (peak CA) [5–6].

Closer resolution of the second voltammetric peak appears to be far more problematic. Regarding our previous study, we have discovered that the utilization of different E_{dep} for the adsorption of dsDNA ($E_{dep} < 0.7$ V) is connected with an appearance of the third oxidation signal (besides the oxidation signals of guanine resp. adenine moieties) at a potential of 0.73 V corresponding to the oxidation of free guanine bases (FGBs) present within the solution of dsDNA. In this case, we can assume that the peak appearing at a potential of –1.90 V can possibly represent the reduction counterpart of FGBs present within the solution of dsDNA. This assumption can also be supported by the aforementioned study and by the fact that the reduction signal at such a high negative potential can be observed for the oligodeoxynucleotides containing guanine residues [6].

Additionally, in order to verify the true nature of the reduction signals depicted at Fig. 1B and to exclude the option that the related signals do not represent the products of prior electrochemical activation of the EPPGE (various C–O based chemical species), we have decided to perform a negative (control) test within the
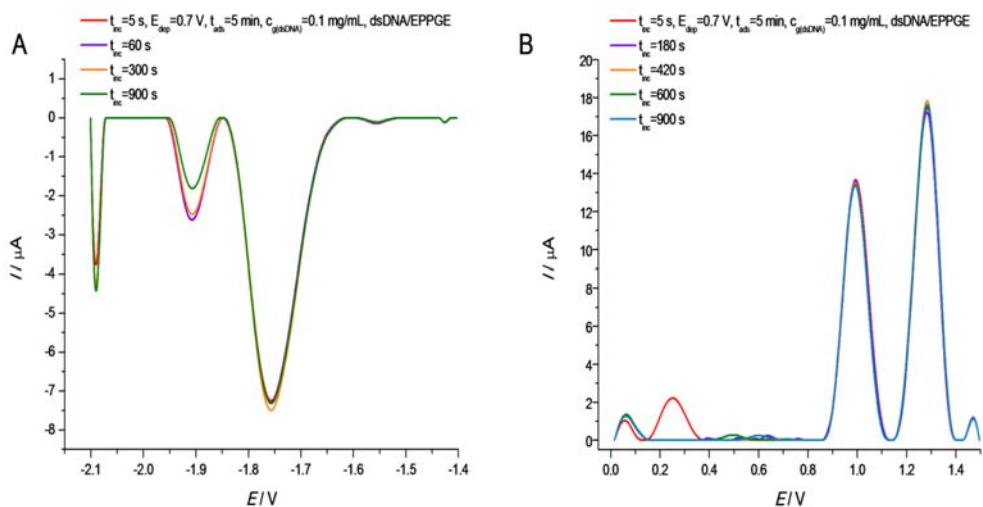
Fig. 2 Baseline-corrected LSV recordings corresponding to the reduction of the dsDNA (0.2 V/s, Fig. 2A) resp. baseline-corrected SWV recordings corresponding to the oxidation of the guanine (0.98 V) resp. adenine (1.28 V) moieties (0.75 V/s, Fig. 2B) at the EPPGE after its incubation in the phosphate buffer for a defined time period (60–900 s).

blank solution (PB) employing the same protocol as for the dsDNA adsorption at the EPPGE. In this case, it is possible to observe the absence of any pronounced voltammetric peaks linked to the dsDNA adsorption and only the presence of one irreversible peak at a potential of –1.53 V corresponding to the electroreduction of the C–O based moiety/moieties, which drops after the dsDNA adsorption to one tenth of its original value (approximately).

Perhaps the most important parameter regarding further optimization process represented the time-dependent stability of the corresponding signals of dsDNA, which can be specifically important in relation to the study of the time-dependent oxidative damage of dsDNA.

As it has already been proved, a single electrochemical activation of the EPPGE in the PB does not represent a satisfying technique regarding stability of dsDNA oxidation signals at the EPPGE, and the additional stabilization is achieved by further electrochemical activation in the solution of a redox indicator (Fig. 2B) [7]. Based on this, a verification of the proposed stabilization protocol in terms of the time-dependent stability of dsDNA reduction signals in the solution of the PB within the defined time period (60–900 s) appeared as a reasonable next step.

From the results depicted in Fig. 2A, it is possible to notice that within the first 300 s, dsDNA reduction signals remain stable in relation to the current response as well as in terms of the potential value. With an additional incubation time (t_{inc}) (900 s, orange line), the peak current of the voltammetric signal present at more negative potentials decreased, which can probably be addressed as a slow progressive elimination of the weak (electro)chemical forces related to the unspecific adsorption of the FGBs at the EPPGE.
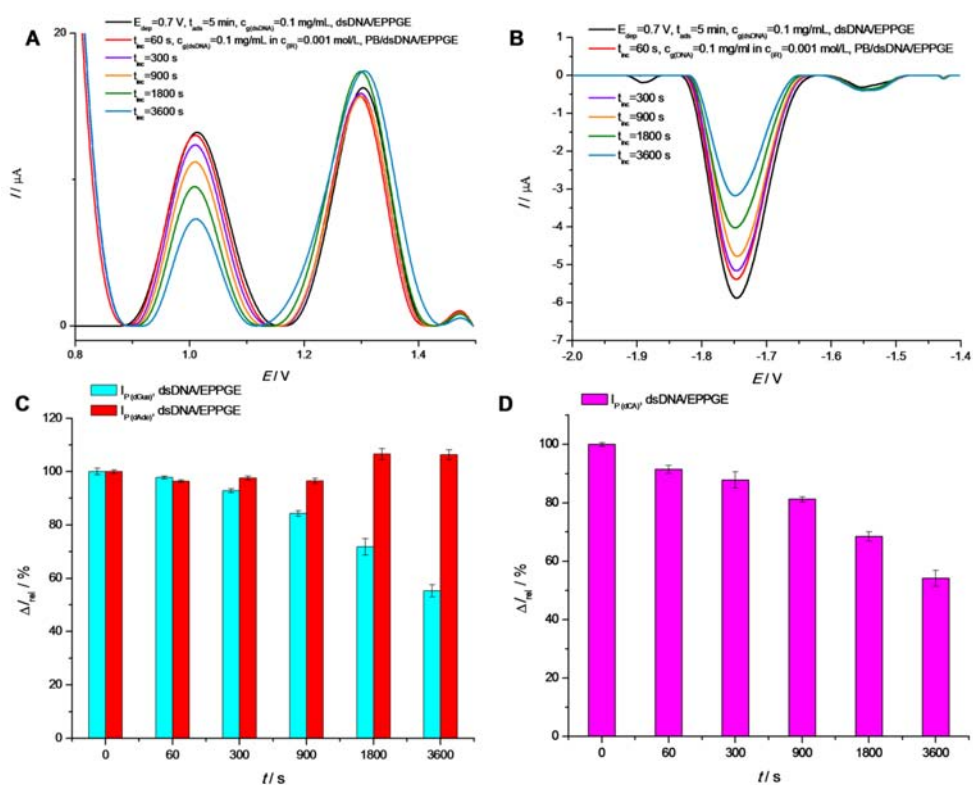
Fig. 3 Baseline-corrected SWV recordings corresponding to the oxidation of the guanine resp. adenine moieties at the EPPGE after its incubation in the solution of $K_2[IrCl_6]$ (IR) for a defined time period (60–3600 s) (0.75 V/s, Fig. 3A) and the corresponding relative biosensor responses (ΔI_{rel}) evaluated using the guanosine (turquoise) and adenosine (red) peaks plotted versus the incubation time (Fig. 3C). Baseline-corrected LSV recordings corresponding to the reduction of dsDNA at the EPPGE after its incubation in the solution of $K_2[IrCl_6]$ (IR) for different time periods (60–3600 s) (0.2 V/s, Fig. 3B) and the corresponding relative biosensor responses (ΔI_{rel}) evaluated using the peak CA (dark pink) plotted versus the incubation time (Fig. 3-D).

Additionally, we have decided to test the applicability of the presented hybrid biosensor in terms of monitoring dsDNA damage caused by a representative of one-electron oxidants – $K_2[IrCl_6]$. In this case, the prepared dsDNA/EPPGE biosensor was immersed into the solution of $K_2[IrCl_6]$ (0.001 mol/L) for the defined time period (60–3600 s).

In the case of the oxidation path (SWV recordings depicted in Fig. 3A), it is possible to observe a time-dependent decrease of the oxidation signal of the guanine moieties, whereas the oxidation signal of the adenine moieties remains unaffected for the most of the incubation period. This phenomenon is in good correlation with the theoretical knowledge regarding oxidative damage of dsDNA caused by one-electron oxidants [3]. Simultaneously with this, LSV recordings depicted in Fig. 3B followed the similar behavior (decrease in relation to the

current response of the dsDNA reduction signal – peak CA) as in the case of the signal regarding oxidation of guanine moieties. In addition, according to the portion of the preserved DNA (Fig. 3C/3D), it is possible to assume that the pronounced oxidative damage of dsDNA can be monitored quite precisely not only directly via the dsDNA oxidation signal of the guanine moieties, but even indirectly through the dsDNA reduction signal – peak CA.

4. Conclusions

In this contribution, we have presented development of an unorthodox hybrid electrochemical DNA biosensor based on an EPPGE. Optimization process concerning some important parameters was performed as well as closer resolution of the nature of the reduction processes of dsDNA at the EPPGE was achieved. In order to confirm the results of the optimization process, applicability of the proposed biosensor had been probed in terms of monitoring DNA damage caused by $K_2[IrCl_6]$. In this case, the final results had proved that the prepared hybrid biosensor can be considered as a versatile analytical tool for monitoring oxidative DNA damage (via oxidation/reduction signals) and is presented as a fine alternative in comparison with conventional electrochemical DNA biosensors prepared within the group of traditional transducer materials (mercury- or carbon-based).

References

[1]   Fojta M., Daňhel A., Havran L., Vyskočil V.: Recent progress in electrochemical sensors and assays for DNA damage and repair. *TrAC Trends Anal. Chem.* **79** (2016), 160–167.
[2]   Giese B., Spichty M., Wessely S.: Long-distance charge transport through DNA. An extended hopping model. *Pure Appl. Chem.* **73** (2001), 449–453.
[3]   Burrows C.J., Muller J.G.: Oxidative nucleobase modifications leading to strand scission. *Chem. Rev.* **98** (1998), 1109–1151.
[4]   Diculescu V.C., Chiorcea-Paquim A.-M., Oliveira-Brett A.M., Applications of a DNA-electrochemical biosensor. *TrAC Trends Anal. Chem.* **79** (2016), 23–36.
[5]   Paleček E., Jelen F.: Electrochemistry of nucleic acids. In: E*lectrochemistry of Nucleic Acids and Proteins – Towards Electrochemical Sensors for Genomics and Proteomics.* Paleček E., Scheller F., Wang J. (edits.). Amsterdam, Elsevier 2005, p. 74–174.
[6]   Špaček J., Daňhel A., Hasoň S., Fojta M.: Label-free detection of canonical DNA bases, uracil and 5-methylcytosine in DNA oligonucleotides using linear sweep voltammetry at a pyrolytic graphite electrode. *Electrochem. Commun.* **82** (2017), 34–38.
[7]   Augustín M., Vyskočil V.: Novel electrochemical DNA biosensor based on edge-plane pyrolytic graphite for DNA interaction studies. In: *Proceedings of the 15th International Students Conference "Modern Analytical Chemistry".* Nesměrák K. (edit.). Prague, Faculty of Science, Charles University 2019, p. 263–268.

Chemical vapor generation of cadmium for analytical atomic spectrometry

Linda Sagapova[a, b, *], Barbora Kodríková[a, b], Milan Svoboda[a], Stanislav Musil[a],
Jan Kratzer[a]

[a] *Institute of Analytical Chemistry of the Czech Academy of Sciences,*
     Veveří 97, 602 00 Brno, Czech Republic ✉ sagapova@iach.cz
[b] *Department of Analytical Chemistry, Faculty of Science, Charles University,*
     Hlavova 8/2030, 128 43 Prague 2, Czech Republic

Keywords
atomic absorption
    spectrometry
atomization
cadmium
chemical vapor
    generation

Abstract
Chemical vapor generation of cadmium volatile compounds was optimized in order to determine trace Cd concentrations by atomic absorption spectrometry (AAS). Several reaction modifiers based on inorganic salts and complexes of Cr^{III+}, Co^{II+}, Ti^{III+}, Ti^{IV+} were tested to improve analytical performance and generation efficiency. The use of these reaction modifiers resulted in 4–5 times enhancement in sensitivity, reflected also in corresponding increase of generation efficiency and better repeatability. Generation efficiency was determined from a comparison between sensitivities obtained with chemical vapor generation and conventional solution nebulization, both simultaneously coupled with inductively coupled plasma mass spectrometry. The identity of the generated cadmium compounds will be discussed.

1. Introduction

Cadmium is one of the most toxic metals and its widespread industrial uses result in increased environmental pollution. Hence, the development of sensitive methodology for Cd determination is still highly desirable. Chemical vapor generation (CVG) of Cd by the tetrahydroborate reduction in acidic medium is a suitable alternative sample introduction technique, compatible with atomic spectrometric detectors and offering improved detection capability. Compared to common liquid nebulization, CVG offers several advantages such as significantly higher analyte introduction efficiency and also analyte separation from sample matrix.

In comparison to CVG of common hydride forming elements, there is a lack of literature dealing with mechanistic aspects of CVG of Cd [1] as well as with stability and identity of its volatile species (free atoms, hydride, other species). Very little information is also available on achieved generation efficiency. Moreover, there are many discrepancies in the literature regarding optimum

Table 1
Optimum conditions for chemical vapor generation of Cd in the presence of modifiers and their absence.

	No additives	Cr^{3+}/KCN	Co^{2+}/CH_4N_2S, $C_6H_8O_6$	Ti^{3+}/KCN	Ti^{4+}/KCN
Carrier (HCl) / mol dm^{-3}	0.1	0.2	1.2	0.48	0.1
Modifier I / mol dm^{-3}	–	1×10^{-3} $Cr(NO_3)_3$	1×10^{-6} $CoCl_2.6H_2O$ in 0.5% $C_6H_8O_6$	1.5×10^{-2} $TiCl_3$ in 0.5% H_2SO_4	7.5×10^{-3} $TiOSO_4$ in 0.5% H_2SO_4
Modifier II	–	0.1 M KCN	0.5% CH_4N_2S	0.16 M KCN	0.08 M KCN
NaBH$_4$	5% in 0.4% KOH	5% in 0.4% KOH	5% in 0.5% KOH	3% in 0.1% KOH	5% in 0.4% KOH

conditions for CVG of Cd. Although strong acid (HCl or HNO_3) is always employed as a carrier and $NaBH_4$ as a reductant, some authors reported various additives (modifiers) based on transition metal ions (Cr^{III+}, Ti^{III+}, Ti^{IV+}) in the presence of KCN [2, 3] or Co^{II+} in the presence of thiourea and ascorbic acid [4] to improve Cd signals significantly.

The aim of this work was to investigate CVG of Cd in a comprehensive way. Firstly, CVG of Cd without and with selected modifiers was optimized employing atomic absorption spectrometry (AAS) as a detector and externally heated quartz tube (QTA) as the atomizer. Secondly, the effect of atomization temperature on Cd signal was studied allowing thus to deduce the atomic or molecular structure of generated Cd species. Thirdly, generation efficiency of Cd volatile species was quantified.

2. Experimental

2.1 Reagents and chemicals

Boiled and bubled (Ar per 30 min) deionized water (< 0.1 µS cm^{-1}, Ultrapur, Watrex, USA) was used to prepare all solutions. Working Cd standards were prepared from 1000 mg L^{-1} Cd stock solution (Astasol, Analytika, Czech Republic) by dilution in 0.1–0.48 mol L^{-1} HCl (based on the modifier employed) from 37% HCl (p.a., Merck, Germany). The optimum generation conditions, being different for each modifier tested, are listed in Table 1. The reductant was a solution of $NaBH_4$ (≥ 97%, Sigma-Aldrich, Germany) in 0.4% (*m/v*) KOH (p.a., Merck, Germany) prepared fresh daily. The solutions of modifiers were prepared as follows: Co^{2+} was prepared from $CoCl_2.6H_2O$ (≥ 99.0% PENTA, Czech Republic), the solution of Cr^{3+} from $Cr(NO_3)_3.9H_2O$ (≥ 99.99% trace metal basis, Sigma-Aldrich, Germany), the solution of Ti^{3+} from $TiCl_3$ solution (about 15% in 10% HCl, Sigma-Aldrich, Germany) and the solution of Ti^{4+} from $TiOSO_4$ (≥ 99.9%, Sigma-Aldrich, Germany). To stabilize the latter solution, 1% H_2SO_4 was used prepared by dilution of 96% H_2SO_4 (p.a., Lach-Ner, Slovakia). Solution of KCN (≥ 97.0%, Fluka, Switzerland) was used as a second modifier when working with Cr^{3+}, Ti^{3+} or Ti^{4+} as modifiers, its concentration varied from 0.08 to 0.16 mol dm^{-3} depending
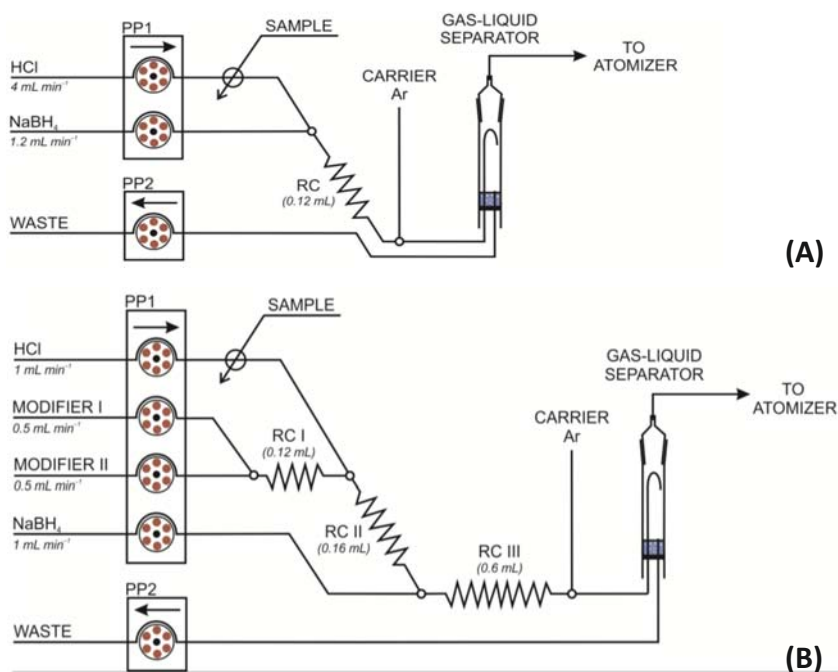
Fig. 1 Schemes of the chemical vapor generation flow injection system with (A) two channels (no modifiers), and (B) four channels (modifiers employed).

on the metal ion. Thiourea (CH_4N_2S, ≥ 98.0%, Lachema, Brno) and ascorbic acid ($C_6H_8O_6$, ≥ 99.7%, Riedel-de Haën, Germany) were used as modifiers combined with Co^{2+}.

2.2 Instrumentation

2.2.1 Chemical vapor generation systems

Two CVG flow injection systems were employed, either a two channel system without addition of a modifier (see Fig. 1A), or a four channel system allowing addition of modifiers (see Fig. 1B).

The flow rates of HCl and $NaBH_4$ were 4.2 and 1.0 mL min^{-1}, respectively, in a two channel system (Fig. 1A) while they were both kept at 1.0 mL min^{-1} in the four channel system (Fig. 1B). The flow rates of modifiers in the four channel system were 0.5 mL min^{-1}. The volume of the sample loop was 0.15 mL in both systems. Carrier gas flow rate of 75 mL min^{-1} Ar was controlled by a mass flow controler (Cole-Parmer, USA).

2.2.2 Atomic absorption spectrometry

The Perkin-Elmer model 503 atomic absorption spectrometer (Bodenseewerk, Germany) was equipped with a Cd electrodeless discharge lamp (Perkin-Elmer, USA) operated at 228 mA. The measurements were performed at 228.8 nm using a 0.7 nm slit width. The Shimadzu model AA-7000 atomic absorption spectrometer (Shimadzu, Japan) was also used. A Cd hollow cathode lamp (Photron, Australia) operated at 228.8 nm line with 0.7 nm spectral bandpass and a lamp current of 12 mA. Signals were recorded for 2 minutes and peak areas were taken for evaluation. The QTA was heated electrically to the temperature required by furnace (Perkin Elmer) and an in-house made furnace controlled by the REX-C100 controller (Syscon, Indiana, USA) with the K-type thermocouple sensor (Omega Engineering, USA).

2.2.3 Quantification of CVG efficiency by ICP-MS

Overall CVG efficiency of Cd was quantified by means of inductively coupled plasma mass spectrometry (ICP-MS) from comparison of the slopes of calibrations obtained with nebulization liquid Cd standards to those obtained with CVG. The efficiency of liquid nebulization was quantified using a modified waste collection method (see reference [5] for details). The Agilent 7700x ICP-MS instrument (Agilent, USA) was operating at 1600 W of RF power. The signal was monitored at ^{111}Cd isotope and corrected for the signal of internal standard (^{125}Te, 1000 ng mL^{-1} Te in 2% HNO_3). Nebulizer and dilution Ar gas flow rates were 1150 and 0 mL min^{-1}, respectively.

3. Results and discussion

3.1 Chemical vapor generation conditions

Univariate optimizations were performed to find optimum conditions for CVG of Cd in presence and absence of modifiers. The parameters to be optimized were: carrier acid (HCl) concentration, reductant (NaBH$_4$) concentration, modifier I and modifier II concentrations, carrier gas flow rate (Ar), length of reaction coils RC I-III (see Fig. 1B). The optimum conditions for individual modifiers are summarized in Table 1.

3.2 Identity of Cd species

The peak areas of generated Cd species were, for a given modifier, measured in the QTA heated to 900 °C and non-heated QTA subsequently. Optimum CVG conditions were employed as summarized in Table 1. This simple experiment allows distinguishing between atomic (free atoms) and molecular forms of generated
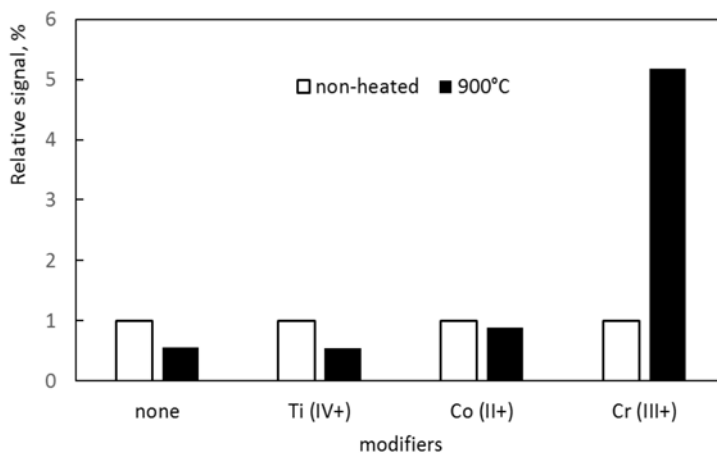
Fig. 2 Relative signal of generated Cd species measured in the QTA heated to 900 °C (black bars) and non-heated QTA (white bars) without or in the presence of modifiers.

species. Only free atoms can be detected in non-heated QTA, similarly as in case of mercury cold vapors. On the contrary, molecular analyte species are atomized at 900 °C. As a consequence, the signal registered in the heated QTA corresponds to both atomic and molecular species generated. It must be highlighted that the residence time of free atoms in the atomizer is dependent on QTA temperature due to gas expansion. As a consequence, the signal in QTA heated to 900 °C should reach 25% of the signal at ambient temperature taking into account that only free atoms are generated. Since the temperature along the optical arm of QTA is not distributed homogeneously decreasing to both end, the effective temperature of the atomizer is lower. Our experiments with CVG of Hg revealed signal in heated QTA is around 40% [6]. The results reached for CVG of Cd are depicted in Fig. 2. The signal of Cd in heated QTA is around 50% of the signal detected in non-heated QTA when no modifier is employed or using Ti^{4+} as the modifier indicating clearly free Cd atoms are the dominant volatile species generated. On the contrary, almost no difference in peak areas was observed for Co^{2+} as the modifier while the signal in heated QTA was even 5 times higher in heated QTA compared to non-heated atomizer with Cr^{3+} as the modifier suggesting the dominant contribution of molecular structures to Cd signal, especially in case of Cr^{3+}/KCN reaction system.

3.3 Generation efficiency

The overall CVG efficiency was estimated from a comparison between sensitivities obtained with CVG sample introduction and conventional solution nebulization ICP-MS under the same experimental conditions. Nebulization efficiency for a MicroMIST nebulizer was determined as 7.9±0.1%. The generation efficiency of Cd was derived from the sensitivity enhancement between CVG and liquid nebulization. The results are summarized in Table 2 indicating that CVG without

Table 2
Generation efficiency of chemical vapor generation of Cd as quantified by ICP-MS.

Modifiers	Generation efficiency / %
No modifiers	15±1
Cr^{3+}/KCN	–
Co^{2+}/thiourea, ascorbic acid	–
Ti^{3+}/KCN	58±2
Ti^{4+}/KCN	61±2

modifiers is only ca two times more sensitive compared to liquid nebulization. Generation efficiency of Cd increases to 60% in the presence of Ti^{3+} and Ti^{4+} modifiers.

4. Conclusions

CVG of Cd was thoroughly optimized in the presence of selected modifiers reported previously in the literature. Generation efficiency of Cd in the absence of any modifiers was quantified to 15% while it can be increased up to 60% in the presence of Ti^{3+}/KCN or Ti^{4+}/KCN as modifiers. Free Cd atoms seem to be the dominant Cd form generated in the absence of any modifiers or using Ti^{4+}/KCN modifier while rather molecular Cd structures are generated in Cr^{3+}/KCN and Co^{2+}/thiourea, ascorbic acid reaction systems.

    Experiments are in progress to finish this comprehensive study. Only the best modifier will be further used for CVG of Cd, to be coupled with other spectrometric detectors and applied to certified reference materials and real samples.

References

[1]   Pitzalis E., Angelini D., Mascherpa M.C., D´Ulivo A.: Insight into the mechanisms controlling the chemical vapor generation of cadmium. *J. Anal. At. Spectrom.* **33** (2018), 2160–2171.

[2]   Arslan Z., Yilmaz V., Rose L.: Efficient generation of volatile cadmium species using Ti(III) and Ti(IV) and application to determination of cadmium by cold vapor generation inductively coupled plasma mass spectrometry. *Microchem. J.* **123** (2015), 170–178.

[3]   Yilmaz V., Rose L., Arslan Z., Little M.D.: On-line chemical vapour generation of cadmium in the presence of hexacyanochromate(III) for determination by inductively coupled plasma mass spectrometry. *J. Anal. At. Spectrom.* **27** (2012), 1895–1902.

[4]   Y. Lu, Sun H.W., Yuan C.G., Yan X.P.: Simultaneous determination of trace cadmium and arsenic in biological samples by hydride generation-double channel AFS. *Anal. Chem.* **74** (2002), 1525–1529.

[5]   Vyhnanovský J., Strugeon R.E., Musil S.: Cadmium assisted photochemical vapor generation of tungsten for detection by inductively coupled plasma mass spectrometry. *Anal. Chem.* **91** (2019), 13306–13312.

[6]   Migašová M., Matoušek T., Schrenková V., Žídek R., Petry-Podgórska I., Kratzer J.: Mercury volatile species generation from HCl and TRIS buffer media. *Anal. Chim. Acta.* **1119** (2020), 68–76.

Photochemical vapour generation of bismuth coupled with atomic fluorescence spectrometry

BARBORA ŠTÁDLEROVÁ[a, b, *], JAROMÍR VYHNANOVSKÝ[a, b], JIŘÍ DĚDINA[a], STANISLAV MUSIL[a]

[a] *Institute of Analytical Chemistry of the Czech Academy of Sciences,*
    Veveří 97, 602 00 Brno, Czech Republic ✉ stadlerova@iach.cz
[b] *Department of Analytical Chemistry, Faculty of Science, Charles University,*
    Hlavova 8/2030, 128 43 Prague 2, Czech Republic

Keywords

atomic fluorescence
    spectrometry
bismuth
hydride generation
photochemical vapour
    generation

Abstract

Photochemical vapour generation of bismuth was successfully coupled with non-dispersive atomic fluorescence spectrometry for the first time. Volatile species of Bi were generated, using a standard mercury low-pressure tube lamp and a coiled reactor, from a reaction medium which was composed of acetic and formic acid, Co^{2+} ions were used as a sensitizer. Optimization of atomization conditions in a flame-in-gas-shield atomizer was performed. This methodology was compared to the commonly employed hydride generation approach. Absolute limit of detection of 6.8 pg was achieved with photochemical vapour generation, which is still about 7 times worse than with hydride generation. The developed methodology was successfully verified by Bi determination in a reference material of water.

1. Introduction

Atomic fluorescence spectrometry (AFS) coupled with vapour generation is an ultrasensitive analytical method for determination of various elements. Its analytical performance can be comparable to ICP-MS with liquid nebulization but at substantially lower cost [1]. Sample introduction to AFS is a crucial step of the analytical procedure since the analyte has to be introduced to the atomizer in the form of its volatile species.

Hydride generation (HG) is a mature technique of sample introduction during which volatile analyte hydrides are formed by reaction with a reducing agent, typically sodium borohydride. A new emerging technique, photochemical vapour generation (PVG), employs UV irradiation of the analyte in liquid phase in the presence of a photochemical agent (usually a low molar mass organic acid: formic or acetic acid). Highly reducing radical species (H•, R•, and COO•⁻) and aquated electrons are formed during irradiation and react with the analyte to form its
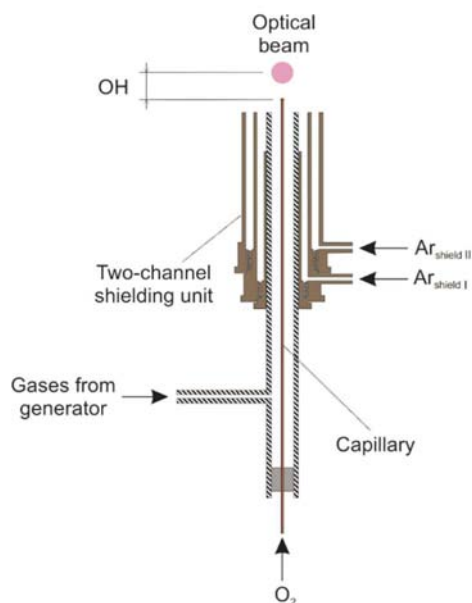
Fig. 1 Flame-in-gas-shield atomizer; OH – observation height.

volatile species. In both cases, the generated volatile species of the analyte have to be separated from the liquid phase in the gas-liquid separator and are carried to the atomizer by a carrier gas [2].

In this work, an atomizer designed specifically for AFS, the flame-in-gas-shield atomizer, was used (Fig. 1). It consists of a vertical quartz tube supplied with argon and hydrogen together with the analyte volatile species. Moreover, a capillary is inserted in the vertical axis of the vertical tube through which oxygen is introduced. A hydrogen-oxygen microflame burns on top of the capillary. The microflame is shielded from the ambient atmosphere by a flow of argon which is introduced through a shielding unit fitted around the vertical tube [3, 4].

The aim of this work was to optimize atomization conditions in the flame-in-gas-shield atomizer using PVG as a sample introduction technique and to compare the analytical characteristics of PVG and HG for ultrasensitive determination of bismuth by AFS.

2. Experimental

2.1 Reagents and chemicals

Deionized water (Ultrapur, Watrex, USA) was used for preparation of all the solutions. Working Bi solutions were prepared fresh daily by serial dilution of stock 1000 mg l^{-1} Bi standard for AAS (Sigma-Aldrich, Germany). Regarding HG, 0.5% (m/v) $NaBH_4$ in 0.4% (m/v) KOH was used as a reductant. A solution of 1 mol l^{-1} HCl was used as a carrier and blank.

Regarding PVG, formic acid (98%, p.a., Lach-Ner, Czech Republic) and acetic acid (99.8%, p.a., Lach-Ner, Czech Republic) were used for preparation of the reaction medium, they were purified in a Teflon BSB-939-IR sub-boiling distillation apparatus (Berghof, Germany). The composition of the reaction medium (40% (*v/v*) acetic, 1.25% (*v/v*) formic acid) was optimized earlier [5]. The 5000 mg l^{-1} Co stock solution was prepared from cobalt(II) acetate tetrahydrate (p.a., Lach-Ner, Czech Republic) and used as a sensitizer of photochemical reaction. The optimal concentration of Co in the standard, samples and blank solutions corresponded to 50 mg l^{-1} (ref. [5]).

A certified reference material (CRM) - 1643f Trace Elements in Water (National Institute of Standards and Technology, USA) was used to check the precision of the developed methodology.

2.2 Instrumentation

2.2.1 Atomic fluorescence spectrometer

An in-house assembled non-dispersive atomic fluorescence spectrometer constructed at our laboratory was used for Bi determination and is described in detail elsewhere. [3] The detector output provided signals in μV. Peak area corrected to baseline and mainly signal to noise ratio were the parameters used to evaluate the data.

2.2.2 Hydride generator, photochemical vapour generator and atomizer

A flow injection hydride generator was employed (Fig. 2a). The reductant (1.2 ml min^{-1}) and the carrier (4 ml min^{-1}) were pumped by a peristaltic pump. The sample was injected through a 1 ml sample loop into the flow of carrier. A glass gas-liquid separator (5 ml) with forced waste removal was employed for separating the gas phase containing bismuthane, which was then carried to the atomizer by argon.

The photochemical vapour generator (Fig. 2b) consisted of the photoreactor constructed with a 15 W low-pressure Hg germicidal lamp (Cole-Parmer, USA) wrapped around with 6 m of PTFE tubing (1 mm i.d.; internal volume 4.71 ml). The reaction medium (3 ml min^{-1}) was pumped by a peristaltic pump. The sample was injected through a 0.56 ml sample loop. A polypropylene gas-liquid separator (15 ml) with forced waste removal immersed in an ice bath [6] was employed for separating the gas phase containing Bi volatile species subsequently carried to the atomizer by argon.

The flame-in-gas-shield atomizer is depicted in Fig. 1, detailed description is given in Ref [3]. The observation height (OH) is defined as the distance from the top of the capillary to the centre of the optical beam.
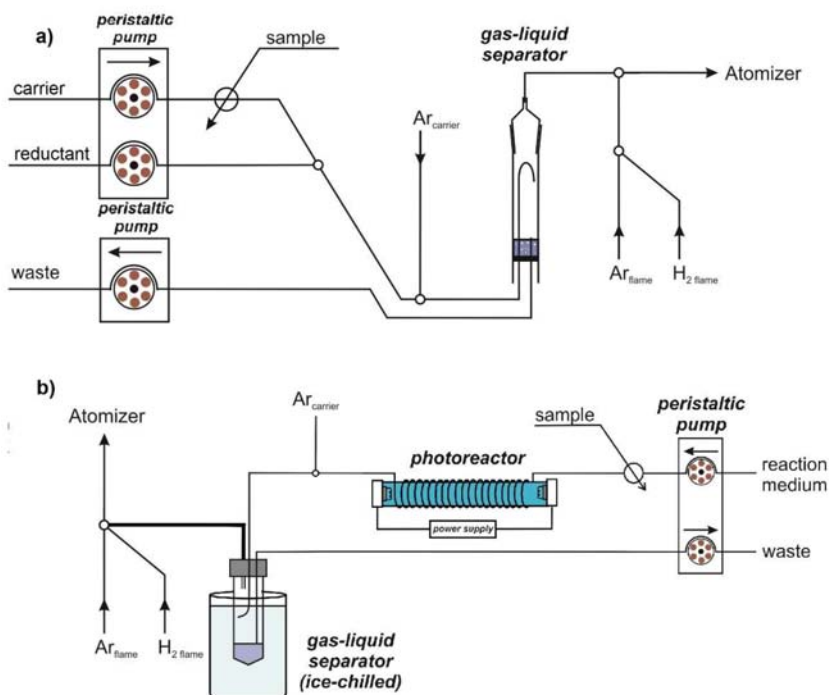
Fig. 2 (a) Hydride, and (b) photochemical vapour generator.

2.3 Sample preparation

CRM NIST 1643f was diluted with 1M HCl 80-fold for Bi determination by HG-AFS. Regarding Bi determination by PVG-AFS, the sample needed to be evaporated to dryness in order to get rid of nitric acid that seriously interferes at mM level [5]. A volume of 3 ml of CRM were pipetted into a 40 ml quartz vial, evaporated (temperature: ≈100 °C; two replicates) and subsequently diluted ca. 33-fold. A sample preparation blank, 3 ml of deionized water, was prepared as well.

3. Results and discussion

The atomization conditions for HG-AFS were optimized in our previous work [3]. These conditions were used as initial to find the optimum conditions for PVG-AFS with the flame-in-gas-shield atomizer with respect to sensitivity and signal to noise ratio. Firstly, the hydrogen fraction in the range 10–16% was optimized at constant total gas flow rate (sum of total argon and total hydrogen) of 500 ml min^{-1}: the lower the hydrogen fraction, the better. However, at 10% hydrogen fraction, the flame was not stable enough and went often out, hence it was opted for 12% hydrogen fraction.

Table 1
Atomization conditions for flame-in-gas-shield atomizer.

Parameter	HG-AFS (ref. [3])	PVG-AFS
Ar total / ml min^{-1}	440	528
H$_2$ total / ml min^{-1}	60	72
O$_2$ / ml min^{-1}	7	20
OH / mm	6	9
Ar shield / l min^{-1}	1.5; 1.5	1.5; 1.5

Table 2
Analytical figures of merit of HG-AFS and PVG-AFS.

Parameter	HG-AFS (ref. [3])	PVG-AFS
LOD / pg	0.9	6.8
LOQ / ng l^{-1}	0.9	12
Repeatability / %	< 1	6

The oxygen flow rate through the capillary was optimized in the range 5–30 ml min^{-1}. The highest signal to noise ratio was achieved with the flow rate of 20 ml min^{-1}.

The total gas flow rate was optimized at constant 12% hydrogen fraction in the range 500–800 ml min^{-1}. The optimum observation height varies with total gas flow rate, so it had to be optimized as well. The optimum conditions are summarized and compared to those achieved with HG in Table 1.

The analytical figures of merit of PVG-AFS with the flame-in-gas-shield atomizer were determined. The calibration function constructed with 0.10, 0.25, 0.50, 1.00 and 2.00 µg l^{-1} Bi standards was linear (R^2 = 0.9998). The repeatability, expressed as the relative standard deviation (n = 10), was 6% at 1 µg l^{-1} and the relative and absolute limits of detection (3σ, n = 10) achieved were 12 ng l^{-1} and 6.8 pg, respectively (Table 2). The absolute limit of detection achieved with HG was 7.6 times lower which can be attributed to several aspects. Firstly, the generation efficiency for PVG approach was around 53% while 100% is expected for HG [3]. Secondly, a full width at half maximum of the measured peaks was ca. 2-fold greater which necessitated longer integration time and was thus reflected in higher noise of the signals. Finally, the limit of detection for PVG approach was affected by serious contamination (around 10 ng l^{-1}), most probably from the sensitizer solution that contained Bi as impurity.

To validate the proposed methodology, Bi content was determined in CRM NIST 1643f (Table 3) and the results were compared to those measured with HG-AFS [3]. Due to severe interferences from inorganic acids, especially nitric acid [5], the sample needed to be evaporated to dryness and then filled up with the reaction medium containing Co^{2+} as the sensitizer (NIST 1643f is stabilized in

Table 3
The determined content of Bi in CRM NIST 1643f presented as median value ± combined uncertainty (n = 3) and recoveries.

Certified value / µg l^{-1}	HG-AFS		PVG-AFS	
	value obtained / µg l^{-1}	recovery^a / %	value obtained / µg l^{-1}	recovery^a / %
12.62 ± 0.11	12.8 ± 0.1	102 ± 1	12.1 ± 0.9	97 ± 5

^{a} Spiked recovery = slope of standard additions (no addition and two spiked concentrations to a sample)/slope of external calibration.

0.32 mol l^{-1} nitric acid). The results obtained by both methodologies are in good agreement with the certified value.

4. Conclusion

Photochemical vapour generation of Bi was successfully coupled with non-dispersive atomic fluorescence spectrometry for the first time and its applicability was verified by determination of Bi in certified reference material of water. Compared to hydride generation, conditions of atomization differ in an optimal observation height and supply of oxygen, which may be needed to "burn out" the organic vapours that are released from the reaction medium to the gas phase, however this remains to be verified. Although there are still some limitations regarding the limits of detection, repeatability and interferences, this new sample introduction approach seems to be promising.

References

[1]   Musil S., Matoušek T., Currier J.M., Stýblo M., Dědina J.: Speciation analysis of arsenic by selective hydride generation-cryotrapping-atomic fluorescence spectrometry with flame-in-gas-shield atomizer: achieving extremely low detection limits with inexpensive instrumentation. *Anal. Chem.* **86** (2014), 10422–10428.
[2]   Sturgeon R.E.: Photochemical vapor generation: a radical approach to analyte introduction for atomic spectrometry. *J. Anal. At. Spectrom.* **32** (2017), 2319–2340.
[3]   Štádlerová B., Kolrosová M., Dědina J., Musil S. Atomic fluorescence spectrometry for ultrasensitive determination of bismuth based on hydride generation – the role of excitation source interference filter and flame atomizers. *J. Anal. At. Spectrom.* **35** (2020), 993–1002.
[4]   Dědina J.: Atomization of volatile compounds for atomic absorption and atomic fluorescence spectrometry: On the way towards the ideal atomizer. *Spectrochim. Acta, Part B* **62** (2007), 846–872.

[5] Vyhnanovský J., Yildiz D., Musil S.: Effect of metal sensitizers on photochemical vapor generation of bismuth for analytical atomic spectrometry. In: *Proceedings of the 15th International Students Conference "Modern Analytical Chemistry".* K. Nesměrák (ed.). Prague, Charles University 2019, p. 257–262.

[6] Vyhnanovský J., Sturgeon R.E., Musil S.: Cadmium assisted photochemical vapor generation of tungsten for detection by inductively coupled plasma mass spectrometry. *Anal. Chem.* **91** (2019), 13306–13312.

Separation of liquid crystals using non-aqueous capillary electrokinetic chromatography

Kateřina Čokrtová*, Tomáš Křížek

Department of Analytical Chemistry, Faculty of Science, Charles University, Hlavova 8/2030, 128 43 Prague 2, Czech Republic ✉ katerina.cokrtova@gmail.com

Abstract

Liquid crystals are widely used in electronics, medicine and other fields. Analytical separations are important in the development of new liquid crystals to control the purity of synthesized substances. The sample analysis is important for detection of impurities formed during synthesis. Liquid crystal-forming substances cannot be separated by capillary zone electrophoresis due to the absence of readily ionizable groups. Therefore electrokinetic chromatography was used in this work. Another problem complicating the analysis was the very low solubility of analytes in water. Separations in this work were therefore carried out under non-aqueous conditions in acetonitrile with acetic acid to adjust the pH and hexadecyltrimethyl-ammonium chloride as a detergent to mobilize the non-ionized analytes. Under these conditions, it was possible to separate impurities from synthesized analytes in samples.

1. Introduction

Liquid crystals are organic substances that form a mesomorphic phase in solution [1]. They are liquid like liquids but have an internal configuration as solids. Their light transmittance changes in the electric field, which is used in liquid crystal displays (LCDs). Cholesteric liquid crystals are temperature sensitive. The color of reflected light changes with small temperature change. This is used in medicine as a sensitive temperature indicator for disease-infected tissues.

High performance liquid chromatography or supercritical fluid chromatography [2,3] are used to separate and determine liquid crystal compounds. An electrophoretic method could be complementary to these commonly used methods. To our best knowledge no study dealing with liquid crystal purity control by electrokinetic chromatography was published until now.

Electroneutral substances move in capillary zone electrophoresis at the same speed corresponding to the speed of the electroosmotic flow (EOF) and therefore
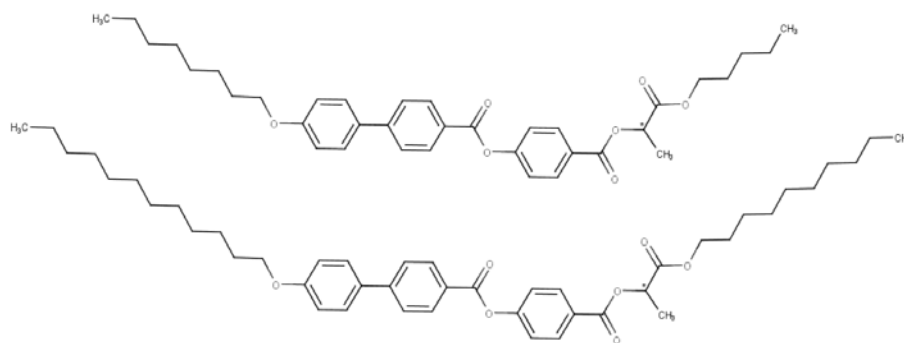
Fig. 1 Structures of liquid crystals 4-({[1-oxo-1-(pentyloxy)propan-2-yl]oxy}carbonyl)phenyl 4'-(octyloxy)-[1,1'-biphenyl]-4-carboxylate (ZL 8/5) and 4-({[1-(decyloxy)-1-oxopropan-2-yl]oxy}carbonyl)phenyl 4'-(dodecyloxy)-[1,1'- biphenyl]-4-carboxylate (ZL 12/10). Optical isomerism sites are marked with an asterisk. Structures created in MarvinSketch [11].

it is not possible to separate them. Due to this, an electrokinetic chromatography method was developed. In this method, a surfactant is added to the background electrolyte. Molecules aggregate and form spherical formations called micelles [4] if the substance is added in sufficient concentration, i.e., higher than the critical micellar concentration (CMC). Separation is possible due to interactions of nonpolar molecule parts with the nonpolar micelle inside. Although water is the most used solvent in electrophoretic methods, for separation of water-insoluble substances organic solvents are selected. However, such solvent must meet certain criteria to be suitable for use in capillary electrophoresis. All components must be soluble in the solvent [5]. It should not be flammable, toxic, or reactive, for practicality it should be liquid at room temperature, and also its price is taken into account. The value of its relative permittivity, which describes the strength of interactions between ions, should be around 30. Low dynamic viscosity is also preferred to allow faster migration of analytes. No organic solvent meets all parameters of the ideal solvent. In practice, methanol, acetonitrile, and their mixtures are the most used. The separation parameters can be influenced by using an organic solvent of the background electrolyte. This topic has already been widely explored [6–8]. It was generally assumed that in anhydrous conditions micelles are not created despite sufficient surfactant concentration. However, it was found out that dodecyl sulfate can form stable micelles when the background electrolyte is dissolved in formamide [9]. For the analysis of active substances in medicinal plants, Chen et al. developed a method in which sodium cholate dissolved in methanol is used as a surfactant [10]. The added pseudostationary phase does not always form micelles but can still affect mobilization and separation of analytes if the analytes interact differently with free molecules of surfactant. In this study, water-insoluble liquid crystals were separated (Fig. 1). Therefore nonaqueous electrokinetic chromatography method was developed.

2. Experimental

2.1 Reagents and chemicals

Acetonitrile ≥99.9% from Sigma-Aldrich (Germany), acetic acid 99% from Lach-Ner Neratovice (Czech Republic) and hexadecyltrimethylammonium chloride 25% (*w/w*) in water from Sigma-Aldrich (USA) were used for preparation of background electrolyte. Mesyloxide p.a. (MO) supplied by Lach-ner Neratovice (Czech Republic) was used as a reference substance.

2.2 Instrumentation

For experiments G7100A Capillary Electrophoresis Instrument (Agilent Technologies, Germany) was used with UV-VIS detector operating at 235 nm and 254 nm wavelength. Measurements were conducted in a fused-silica capillary of 50 μm inner diameter with the total length 50.0 cm and effective length 41.5 cm (Polymicro Technologies, USA).

2.3 Method

Capillary was flushed for 3 minutes with 1 M HCl and for 2 minutes with the background electrolyte. Background electrolyte was prepared by mixing acetic acid (10 mM) and hexadecyltrimethylammonium chloride (40 mM) in acetonitrile. Samples were introduced hydrodynamically by a pressure of 5 kPa for 1 second. Samples were first dissolved in acetonitrile and then diluted two times with the background electrolyte. A voltage of 20 kV was applied during the separation.

3. Results and discussion

Liquid crystal samples were practically insoluble in water, their solubility was tested at a concentration level of 1 mg cm^{-3} in methanol and acetonitrile. While samples were not sufficiently soluble in methanol, they were successfully dissolved in acetonitrile.

Because all analytes are substances that do not have easily ionizable functional groups, the electrokinetic chromatography method was chosen for separation. A suitable surfactant was sought. Commonly used sodium dodecyl sulfate (SDS) is insoluble in acetonitrile. Therefore, hexadecyltrimethylammonium chloride (CTAC), which had sufficient solubility for further experiments, was chosen. Although a suitable buffer was sought to ensure a stable pH, due to problems with precipitation of buffer components in the non-aqueous environment, acetic acid was used to adjust and maintain pH of background electrolyte solution. As the addition of cationic surfactant such as CTAC leads to EOF reversal, the dependence
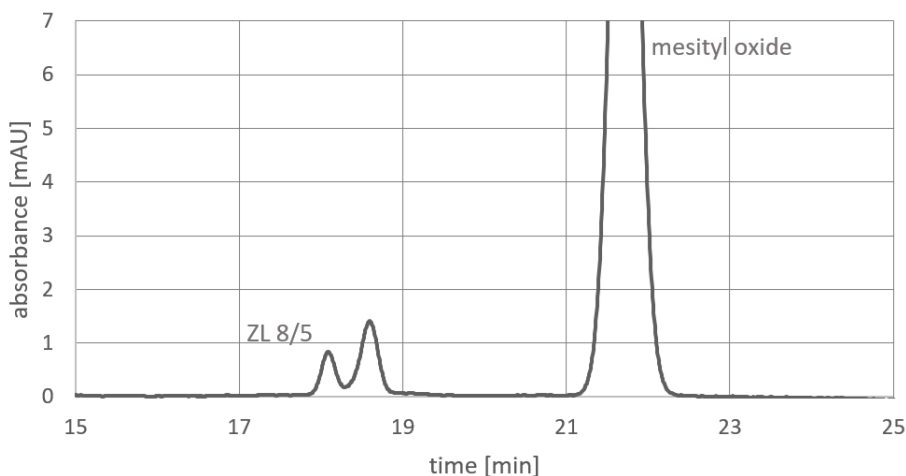
Fig. 2 Electropherogram obtained when a sample of ZL 8/5 liquid crystal with lower purity was introduced. Sample was introduced in 0.1 mg cm^{-3} concentration and with added mesityl oxide (1.0 mg cm^{-3}). Capillary with inner diameter of 50 μm, total length of 50.0 cm, 41.5 cm effective length. The background electrolyte was acetonitrile with 10 mM acetic acid and 40 mM hexadecyltrimethylammonium chloride. A voltage of 20 kV with positive polarity was applied. Detection at 254 nm.

of EOF mobility on the concentration of CTAC in the background electrolyte was measured. Contrary to what is observed in aqueous background electrolytes, EOF was not reversed. Its mobility decreased with increasing CTAC concentration but no major changes occurred above 40 mM concentration. The capillary wall was probably already saturated by CTAC and the further increase in concentration had no signifficant effect on the condition of the capillary wall. Therefore, a CTAC concentration of 40 mmol dm^{-3} was chosen as sufficient for further measurements with respect to the increasing current with increasing ionic strength of the background electrolyte.

The optimized method was used for separation of several liquid crystal samples of different purity. In the sample of the ZL 8/5 liquid crystal with 99% purity, one zone of the analyte was detected. Impurities were separated from this analyte when the sample with lower purity was introduced. The peak of the analyte was identified based on relative migration time related to mesityl oxide. Separation of the analyte from an impurity in the sample ZL 8/5 76% is shown in Fig. 2. The relative migration time of the first peak is 0.834; therefore, it was identified as the ZL 8/5 analyte. The standard deviation of the relative migration times in five measurements was 0.002 min (0.1%).

Using the available high purity sample, it was possible to measure the calibration line for quantification of the analyte in less pure samples. Limit of detection was determined as 0.009 mg cm^{-3} and limit of quantification as 0.031 mg cm^{-3}. From the calibration line concentration of ZL 8/5 in the sample with lower purity was calculated. The concentration was determined as 48 % (*w/w*), standard deviation 5% (*w/w*).
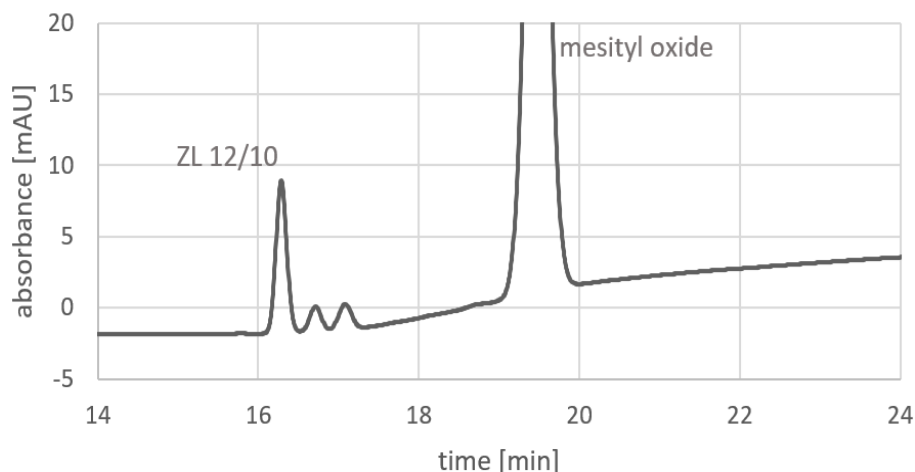
Fig. 3 Electropherogram of sample ZL 12/10 59% at a concentration of 0.5 mg cm^{-3} with mesityl oxide at a concentration of 1.0 mg cm^{-3}, capillary with inner diameter of 50 μm, total length of 50.0 cm, effective length 41.5 cm. The background electrolyte was acetonitrile with 10 mM acetic acid and 40 mM CTAC. Applied voltage 20 kV, positive polarity. Detection at 235 nm.

For sample ZL 12/10 99%, only the analyte and mesityl oxide were detected. In the sample ZL 12/10 59%, several impurities were separated and detected (Fig. 3). According to the relative migration time, the analyte of interest corresponds to the first peak. Peak resolution is sufficient. The resolution of the analyte peak and the second peak is 2.84 and the resolution of the other two peaks is 2.30.

4. Conclusions

In this study, a new method for analysis of newly synthesized liquid crystals was developed. Some parameters of the method were optimized – optimum concentration of hexadecyltrimethylammonium chloride was searched. The identification of analytes was based on a comparison of relative migration times. In samples ZL 8/5 and ZL 12/10 with lower purity, the impurities were separated from the peaks of liquid crystals, the content of analyte was determined in the ZL 8/5 sample according to the calibration line.

References

[1]   Gennes P.G., Prost J.: *The Physics of Liquid Crystals.* 2nd ed. New York, Oxford University Press 1993

[2]   Vaňkátová P., Kalíková K., Kubíčková A.: Ultra-performance supercritical fluid chromato-graphy: A powerful tool for the enantioseparation of thermotropic fluorinated liquid crystals. *Anal. Chim. Acta* **1038** (2018), 191–197.

[3]   Vaňkátová P., Kubíčková A., Cigl M., Kalíková K.: Ultra-performance chromatographic methods for enantioseparation of liquid crystals based on lactic acid. *J. Supercrit. Fluids* **146** (2019), 217–125.

[4]   Terabe S., Otsuka K., Ichikawa K., Tsuchiya A., Ando T.: Electrokinetic separations with micellar solutions and open-tubular capillaries. *Anal. Chem.* **56** (1984), 111–113.

[5]   Riekkola M. L.: Recent advances in nonaqueous capillary electrophoresis. *Electrophoresis* **23** (2002), 3865–3883.

[6]   Wright P.B., Lister A.S., Dorsey J.G.: Behavior and use of nonaqueous media without supporting electrolyte in capillary electrophoresis and capillary electrochromatography. *Anal. Chem.* **69** (1997), 3251–3259.

[7]   Porras S.P., Kenndler E.: Capillary zone electrophoresis in non-aqueous solutions: pH of the background electrolyte. *J. Chromatogr. A* **1037** (2004), 455–465.

[8]   Porras S.P., Riekkola M.L., Kenndler E.: The principles of migration and dispersion in capillary zone electrophoresis in nonaqueous solvents. *Electrophoresis* **24** (2003), 1485–1498.

[9]   Guo X., Wang K., Chen G.H., Shi J., Wu X., Di L. L., Wang Y.: Determination of strobilurin fungicide residues in fruits and vegetables by nonaqueous micellar electrokinetic capillary chromatography with indirect laser-induced fluorescence. *Electrophoresis* **38** (2017), 2004–2010.

[10]   Chen A.J., Li C., Gao W.H., Hu Z.D., Chen X.G.: Application of non-aqueous micellar electrokinetic chromatography to the analysis of active components in radix *Salviae miltiorrhizae* and its medicinal preparations. *J. Pharm. Biomed. Anal.* **37** (2005), 811–816.

[11]   MarvinSketch [computer program], version 19.9.0, ChemAxon, https://chemaxon.com/-products/marvin

Electrochemistry of Sudan I and its derivates in aqueous media

Anna Ondráčková[a, d, *], Marie Stiborová[b], Luděk Havran[a], Karolina Schwarzová-Pecková[c, d], Miroslav Fojta[a, d]

[a]　*Central European Institute of Technology, Masaryk University,*
　Kamenice 753/5, 625 00 Brno, Czech Republic ✉ *anna.ondrackova@ceitec.muni.cz*
[b]　*Department of Biochemistry, Faculty of Science, Charles University,*
　Hlavova 8/2030, 128 43 Prague 2, Czech Republic
[c]　*UNESCO Laboratory of Environmental Electrochemistry, Department of Analytical Chemistry,*
　Faculty of Science, Charles University, Hlavova 8/2030, 128 43 Prague 2, Czech Republic
[d]　*Institute of Biophysics, Czech Academy of Sciences,*
　Kralovopolska 135, 612 65 Brno, Czech Republic

Keywords
boron doped diamond
　　electrode
cytochrome P450
electrochemical analysis
Sudan I

Abstract
Sudan I is an aromatic azo-compound that has been proven to be a carcinogen. During its metabolization by cytochrome P450 in liver a few main derivates can be identified. This work sets out to assess the mechanism of electrochemical reduction and oxidation of Sudan I, its hydroxylation derivatives featuring metabolites in the Sudan I detoxification pathway and to introduce their selective voltammetric analysis on boron-doped diamond electrode. We show successful differentiation among these compounds, thanks to the differences in the electrochemical oxidation of their phenolic groups.

1. Introduction

Sudan dyes are synthetic azo-based aromatic compounds. They are traditionally used in various industries, such as chemical, textile, and woodworking as dyes to colour waxes, plastics, oils, polishes and so forth. They have been categorized as class 3 carcinogens by the International Agency for Research on Cancer and their use is therefore forbidden in the food industry. They are known for their bright colours and easy and cost-effective manufacture. They are nearly insoluble in water, but soluble in various organic solvents, such as methanol or trichloromethane [1].

　　Sudan I, 1-phenylazo-2-naphthol, (Fig. 1A) is a dye used as an orange colouring agent. It's sometimes also sold under names Solvent Orange R or CI Solvent Yellow 14. It is formed as a secondary product in the manufacture of the Sunset Yellow dye.
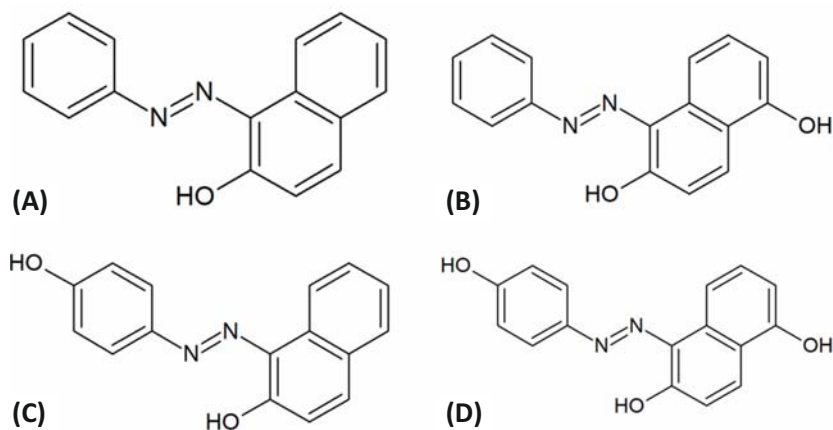
Fig. 1 Chemical structure of (A) Sudan I, (B), 1-(phenylazo)-naphtalene-2,6-diol (SI-6-OH), (C) 1-(4-hydroxyphenylazo)-2-hydroxynaphtol (SI-4'-OH), and (D) 1-(4-hydroxyphenylazo)-naphtalene-2,6-diol (SI-4',6-diOH).

In mammalian organisms, Sudan I is metabolized by the microsomal detoxifying system with a central role of cytochrome P450 hydroxylation activity in liver [2]. During the oxidative process of metabolizing Sudan I, several metabolites were identified by previous tests. These are> 1-(phenylazo)-naphtalene-2,6-diol (further abbreviated: SI-6OH), 1-(4-hydroxyphenylazo)-2-hydroxynaphtol (further abbreviated: SI-4'OH), and 1-(4-hydroxyphenylazo)-naphtalene-2,6-diol (further abbreviated: SI-4',6-diOH); the structures are presented in Fig. 1.

The main method currently used to identify Sudan I among other dyes with similar structure is high-performance liquid chromatography (HPLC). It is recommended as the standard method to identify the level of Sudan I in food [3].

Compared to HPLC, electrochemical methods are proving to be faster, cheaper and comparably precise. Unfortunately, a comprehensive electrochemical study of Sudan I, and particularly of its hydroxylated metabolites, has not been completed yet. The dye can be detected through electrochemistry either by the oxidation of its phenolic group or via reduction of the azo group present in its molecule. In both cases other electrochemically active moieties are formed. The derivates of Sudan I can be detected and recognized from Sudan I through analogous processes [4]. In this study we focused on comparison of electrochemical behaviour of Sudan I and its hydroxylated metabolites on boron doped diamond electrode to address the possibilities of their recognitions in mixtures based on differences in anodic and cathodic signals.

2. Experimental

2.1 Reagents and chemicals

Sudan I (Merck, analytical standard grade) was dissolved in ethanol (Merck) and kept at room temperature. Chemicals for Britton-Robinson buffer preparation (acetic acid, boric acid, orthophosphoric acid, sodium hydroxide) were from Merck with purity ≥99%, pH of the buffer was adjusted by mixing of the acids and sodium hydroxide solution at different ratios. The Sudan I metabolites were synthetized at the Department of Biochemistry, Faculty of Science, Charles University and kept in methanol at temperature 3 °C.

2.2 Instrumentation

Cyclic voltammetric (CV) measurements were carried out in Britton-Robinson buffer of pH = 7.0 at room temperature. Sudan I and its derivatives were added to the solution of Britton-Robinson buffer to final concentration of $5\,\mu mol\,L^{-1}$ and stirred. Before the measurement, oxygen was removed from the solution by purging with argon for 3 minutes. Autolab analyzer PGSTAT 20 (Ecochemie, The Netherlands) in connection with VA-Stand 663 (Metrohm, Switzerland) GPES 4.9 (Metrohm, Switzerland) and a three-electrode setup (with boron doped diamond (Windsor Scientific, UK; disk diameter 3 mm, A = 7.07 mm^2) as working electrode, $Ag/AgCl/3\,mol\,L^{-1}$ KCl as reference electrode and platinum wire as auxiliary electrode). Five cycles were performed for each measurement at scan rate of $1\,V\,s^{-1}$.

3. Results and discussion

For each compound two separate CV measurements were performed, each with five cycles performed in rapid succession. For both measurements, the initial potential was set at 0 V. The anodic scan continued to +1 V, turned towards –1 V and finished at 0 V. In the other setup, cathodic scan was performed first from the starting point to –1 V, turned towards +1 V and returned to 0 V. This way we were able to observe the behaviours of Sudan I and compare it to that of its derivatives while first being reduced and then oxidised or vice versa.

In the anodic scan of Sudan I and its derivatives (Fig. 2) differences in the positions of the oxidation peaks in each compound can be observed. While Sudan I with only one phenol group is oxidized at +0.67 V, the derivatives with two phenol groups, i.e. SI-4'OH and SI-6OH give oxidation peaks at remarkably less positive potential of ca +0.5 V. SI-4',6OH with the presence of overall 3 hydroxy groups yields two oxidation peaks. In the reverse cathodic scan (vertex potential +1 V) probably thanks to the presence reduction peaks appear, which can be further used to differentiate between Sudan I and the derivatives: SI-4'OH and SI-6OH
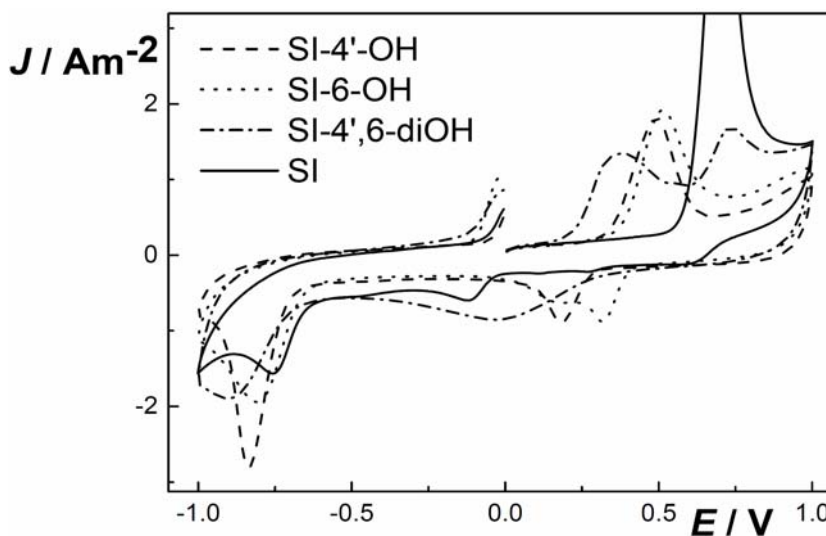
Fig. 2 Cyclic voltammogram of Sudan I and its derivates: SI-4'-OH, SI-6-OH, and SI-4',6-diOH. 1st scan in anodic direction from 0 V, vertex potentials +1 V and −1 V. The measurements were performed in Britton-Robinson buffer (pH = 7) with the concentration of each compound at 5 μM and at scan rate $1\,V\,s^{-1}$.
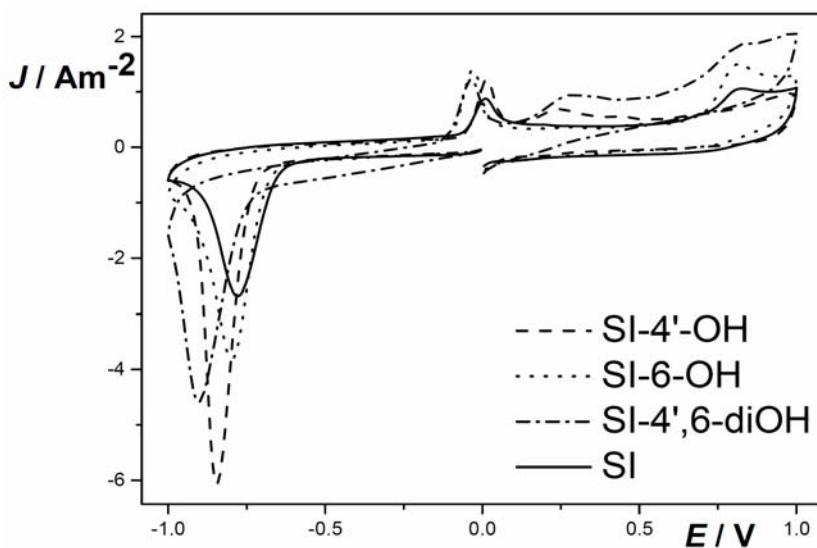

Fig. 3 Voltammetric scan of Sudan I and its derivates: SI-4'-OH, SI-6-OH, and SI-4',6-diOH. 1st scan in cathodic direction from 0 V, vertex potentials −1 V and +1 V. The measurements were performed in Britton-Robinson buffer (pH = 7) with the concentration of each compound at 5 μM and at scan rate $1\,V\,s^{-1}$.

possess two conjugated hydroxyl groups, which can be regarded as hydroquinone structures and thus undergoing quasireversible redox process due to oxidation/reduction of the hydroquinone to quinone moiety. This is well visible at the CVs, as the anodic signal is followed by cathodic one at the potential of +0.23 V for SI-4'OH and +0.3 V for SI-6OH . The oxidation of Sudan I proceeds by mechanism typical for phenolic compounds at more positive potentials, leading by $1e^-/1H^+$ exchange to naphthoxy-type –O· radical [5]. This species undergoes further reactions leading to formation of dimers and polymers. The cathodic peak in the reverse scan at –0.2 V arises from reduction of these reaction products and its origin needs to be further investigated. SI-4',6OH with the presence of overall three hydroxyl groups yields two oxidation peaks. The first one is a result of oxidation of two of them being in conjugation and thus being oxidized to quinone moiety. The second signal at the same potential as the oxidation signal of 2OH on naphthalene ring of Sudan I is consequence of oxidation of the third hydroxyl group of phenolic type. A single wide peak at 0 V in the reverse scan is presumably an overlap of signals arising from reduction of the quinonic moiety and by-products formed during oxidation processes. Thanks to differences of these processes specific for individual compounds, it is possible to differentiate among all four of them via proper setting-up of the initial and vertex potential values.

The cathodic scan of Sudan I and its derivatives (Fig. 3) shows a dominant reduction peak around –0.8 V, which is due to reduction of the azo group in their structures accompanied by cleavage of their molecules to separate the benzene and naphthalene rings [4]. The peaks in the subsequent anodic scans (vertex potential –1 V) are therefore the result of the electrochemical reaction of moieties that are products of the division of the aromatic circles. These products include aniline, 4-aminophenol, 1-amino-2-naphthol, and 1-amino-2,5-naphthalenediol with irreversibly oxidizable amino moieties or (quasi)reversibly oxidizable amino-hydroxyl system on the benzene or naphthalene ring and t is possible to differentiate between them. The obtained oxidation peaks (+0.2 V for SI-4'-OH, +0.73 V for Sudan I and SI-6-OHand +0.25 V and +0.75 V for SI-4',6-diOH) make it possible to differentiate between all compounds with the exception of Sudan I and SI-6-OH. For the reliable recognition of these two compounds another measurement with different parameters is needed.

4. Conclusions

The structures of Sudan I and its hydroxy derivates, that are the main products of the metabolization of Sudan I by cytochrome P450, are similar and their recognition when present in mixture in solution is demanding. Herein, we present a simple approach based on comparison of signals obtained in cathodic and anodic scan in CV measurements, without the need of time-demanding chromatographic separation step. Further work will be devoted to identification of observed redox processes and application of the method for monitoring of metabolic transformations of Sudan I *in vitro*.

Acknowledgments

References

[1]   Chailapakul O., Wonsawat W., Siangproh W., Grudpan K., Zhao Y.F., Zhu Z.W.: Analysis of Sudan I, Sudan II, Sudan III, and Sudan IV in food by HPLC with electrochemical detection: Comparison of glassy carbon electrode with carbon nanotube-ionic liquid gel modified electrode. *Food Chem.* **109** (2008), 876–882.

[2]   Stiborova M., Martinek V., Rydlova H., Hodek P., Frei E.. Sudan I is a potential carcinogen for humans: Evidence for its metabolic activation and detoxication by human recombinant cytochrome P450 1A1 and liver microsomes. *Cancer Res.* **62** (2002), 5678–5684.

[3]   Gomez M., Arancibia V., Aliaga M., Nunez C., Rojas-Romo C.: Determination of Sudan I in drinks containing Sunset yellow by adsorptive stripping voltammetry. *Food Chem.* **212** (2016), 807–813.

[4]   Prabakaran E., Pandian K.: Amperometric detection of Sudan I in red chili powder samples using Ag nanoparticles decorated graphene oxide modified glassy carbon electrode. *Food Chem.* **166** (2015), 198–205.

[5]   Enache T. A., Oliveira-Brett A. M.: Phenol and para-substituted phenols electrochemical oxidation pathways. *J. Electroanal. Chem.* **655** (2011), 9–16.

Group detection of aminoglycosides using ELISA for control of food contamination

Konstantin Burkin[a, b, *], Inna Galvidis[a], Maxim Burkin[a]

[a] *Department of Immunology, I. Mechnikov Research Institute of Vaccines and Sera, Malyj Kazionnyj per. 5a, 105064 Moscow, Russian Federation* ✉ *burkin-kost@yandex.ru*
[b] *Department of Chemical Enzymology, Faculty of Chemistry, Lomonosov Moscow State University, Leninskie Gory 1, 119991 Moscow, Russian Federation*

Keywords	Abstract
aminoglycosides ELISA honey	The growing threat of global antibiotic resistance is forcing to reduce non-target consumption of antibiotics and to monitor contamination of food and environmental objects. In this work, ELISA was developed for group detection of aminoglycosides. To obtain group-specific antibodies, a new immunogen based on ribostamycin was used. The developed indirect competitive format of assay allowed the recognition of 9 aminoglycosides namely, neomycin, ribostamycin, neamin, paromomycin, gentamicin, sisomicin, kanamycin, tobramycin and apramycin with a detection limit ranged between 0.02–0.20 $ng\,mL^{-1}$. The effectiveness of the proposed assay was evaluated in honey as a foodstuff model. To neutralize a strong honey matrix effect and to avoid a laborious sample pre-treatment a new matrix imitator was suggested: 5% sucrose solution imitated the influence of 50-fold diluted honey. The proposed assay allowed us to reveal any of the 9 mentioned aminoglycosides in honey at a $10\,\mu g\,kg^{-1}$ level.

1. Introduction

Aminoglycosides are a large group of natural and semi-synthetic antibiotics with a wide spectrum of antimicrobial activity against most gram-positive and gram-negative microorganisms. Currently, multiple representatives of aminoglycoside family – gentamicin (GM), neomycin B (NM), paromomycin (PM), kanamycin (KM), apramycin (AP), and streptomycin (STM), Fig. 1 – are approved to treat infectious diseases in animals. Maximum residue limits for these aminoglycosides in products and tissues from edible animals are established [1], hence an effective and robust assay is necessary for control of aminoglycosides contamination.

In this study, enzyme-linked immunosorbent assay for the detection of aminoglycosides in food products and environmental objects was developed. Group-specific antibodies were produced owing to immunogen based on ribostamycin (RS), which exposed the common fragment of most aminoglycosides, 2-deoxy-streptamin (2-DOS); Fig. 1. The developed assay was made suitable for the detection of residual aminoglycosides in honey [2].
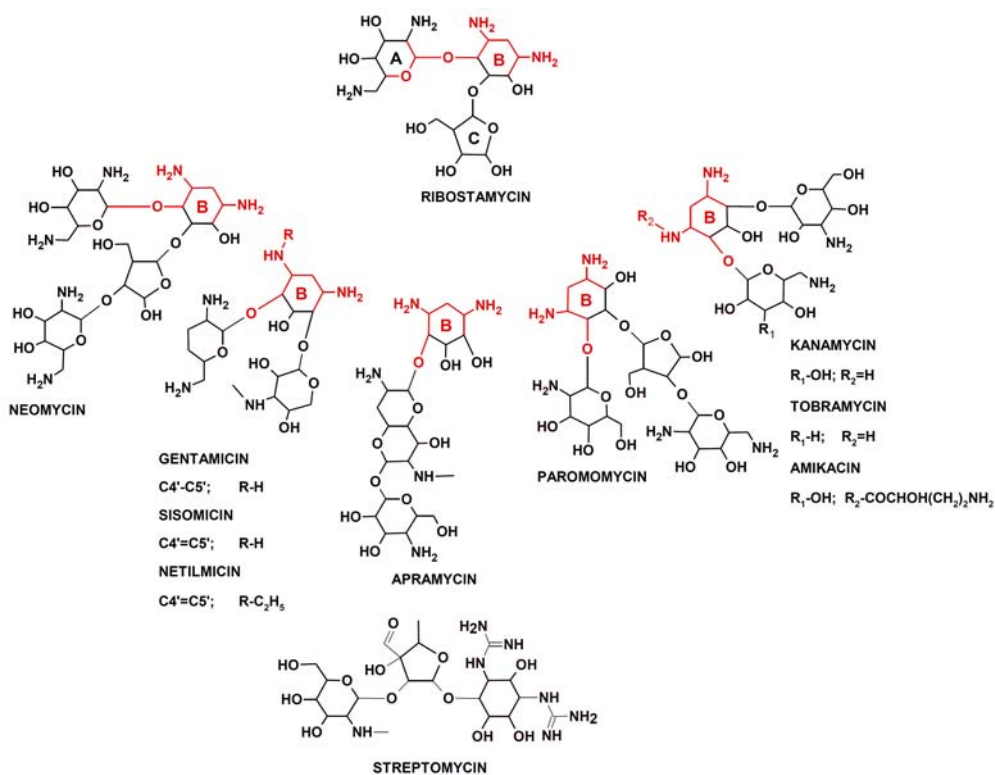
Fig. 1 Structural formulas of studied aminoglycosides.

2. Experimental

2.1 Reagents and chemicals

Neomycin B, ribostamycin, neamin (NA), paromomycin, kanamycin, tobramycin (TM), amikacin (AM), gentamicin, netilmicin (NTM), sisomicin (SSM), geneticin (GC), apramycin and streptomycin were purchased from Chimmed (Moscow, Russia). Bovine serum albumin (BSA), complete Freund adjuvant, 1,6-hexane-diamine, 1-ethyl-3-(3-dimethylaminopropyl)carbodiimide (EDC), sodium perio-date, and sodium borohydride were the products of Sigma-Aldrich (USA). Gelatin (Gel) was from Bio-Rad (USA), sucrose from Serva (Germany), two-component tetramethylbenzidine (TMB) substrate solution was from Bioservice (Russia), and goat anti-rabbit IgG antibodies conjugated to horseradish peroxidase (anti-rIgG-HRP) were from IMTEK (Russia). Honey samples were purchased from local outlets.

2.2 Preparation of conjugated antigens

Two types of conjugates were prepared based on RS and BSA using zero-length and C6 spacer arm between hapten and protein carrier. RS was treated with sodium periodate to oxidize hydroxyls of ribose fragment to reactive aldehyde groups and then coupled to BSA amines through reductive amination. To remove uncoupled RS, an exhausting dialysis was carried out using dialysis membrane tubes (MWCO 14 kDa). Using the same procedure Gel-RS conjugate was synthesized.

For preparation of BSA-C6-RS, we firstly modified BSA with 1,6-hexanediamine. The mixture of BSA and EDC in water were stirred for 30 min. Then, 1,6-hexanediamine was added and stirred for 2 h. The modified protein was dialyzed from the excessive reagents and resultant BSA-C6-NH2 was coupled to RS in reductive amination process as described above.

2.3 Immunization and antibody preparation.

BSA-RS and BSA-C6-RS were used as immunogens. Chinchilla rabbits (2.0–2.5 kg) were subcutaneously injected at 10–15 points on the back with 0.1 mg of immunogens emulsified in the complete Freund adjuvant. The same doses of immunogens in saline were administered monthly for booster immunizations. A week after each injection a blood sample from ear veins was taken for the control of immune response. The antisera in glycerol (1:1, *v/v*) were stored at –15 °C until testing in ELISA.

2.4 The ELISA procedure

A competitive assay was conducted according to classical procedure. Gel-RS was coated overnight on polystyrene 96-well Costar plates. Non-adsorbed conjugate washed out using PBS with 0.05% of tween 20 (PBS-T). The next competitive step included the addition of 0.1 mL standard aminoglycoside solutions (1 pg mL^{-1} to 1 µg mL^{-1}, (B) and 0 µg mL^{-1}, (B_0)) in PBS-T or 0.1 mL of tested sample and 0.1 mL of antibodies in working dilution (1 h, 25 °C). After washing, the antibodies bound to immobilized Gel-RS were detected using anti-rIgG-HRP (1 h, 37 °C). Colored product formed as a result of enzymatic reaction with TMB substrate mixture (0.5 h, 25 °C) was read at 450 nm using a StatFax 2100 plate reader (Awareness Technologies, USA).

Relative antibody binding (B/B_0) vs. the analyte concentrations was plotted as standard curves fitted to a four-parameter logistic function. The cross-reactivity (CR) for every aminoglycoside representative was calculated as ratio of half-inhibition concentrations IC_{50} NM/IC_{50} aminoglycoside. The dynamic range of assay was accepted as IC_{20}–IC_{80} and the limit of detection (*LOD*) was calculated as $B_0 - 3 \times SD$.

3. Results and discussion

3.1 Immunogen synthesis and antibody preparation

In the majority of publications devoted to immunoassay of aminoglycosides, the immunogens, coating antigens, enzyme conjugates or tracers were prepared by carbodiimide or glutaraldehyde methods involving aminoglycosides' amino groups. [3–7] Due to several amino groups in aminoglycoside molecules the formation of conjugates with a variable orientation of the hapten occurs.

In present study, RS was chosen as an immunizing hapten due to the following advantageous features: Being a trisaccharide, RS has the size of a molecule comparable to the most of aminoglycosides; It has three identical rings A-B-C similar to those in NM; Using a periodate oxidation, we could involve a ribose site of RS in coupling to protein that provided a strict orientation of hapten on the carrier with a favorable presentation of the 2-DOS fragment. The resultant immunogens, BSA-RS and BSA-C6-RS were compared to reveal which design is better for presentation of a common fragment of aminoglycoside molecule and generation of group-specific antibody.

Antibodies to the BSA-RS demonstrated moderate sensitivity (NM, $IC_{50} = 10\,\mathrm{ng\,mL^{-1}}$) and high selectivity towards NM with relatively low cross-reactivity (<5%) for GM, KM and AP. The application of the spacer in the immunogen, BSA-C6-RS contributed to a prominent presentation of the 2-DOS determinant and the induction of antibodies with recognition of broad spectrum of different aminoglycosides. In addition, anti-BSA-C6-RS exhibited significantly better sensitivity (NM, $IC_{50} = 0.2\,\mathrm{ng\,mL^{-1}}$). Thus, all subsequent studies were conducted using anti-BSA-C6-RS.

3.2 Examination of assay specificity and selection of immunoreagents

The indirect competitive format of assay was developed. For evaluation of assay specificity, a panel of following aminoglycosides was studied and their cross-reactivity was determined: NA (625%), RS (250%), NM (100%), KM (47.5%), PM (17.3%), GM (9.0%), TM (7.8%), AP (1.7%), SSM (1.2%), AM (<0.1%), GC (<0.1%), STM (<0.1%), and NTM (<0.1%). The most of these analytes are used in medical and veterinary areas, however only NM, PM, GM, KM, AP and STM are applied in animal husbandry [1].

3.3 Determination of aminoglycosides in honey and selection of the matrix imitator

Honey is a complex product consisting of carbohydrates (75–80%), vitamins, proteins, enzymes, organic acids, trace elements, inclusions and other components. These components might interfere immunochemical reaction. Therefore, the isolation of aminoglycosides from honey is a laborious and time-consuming
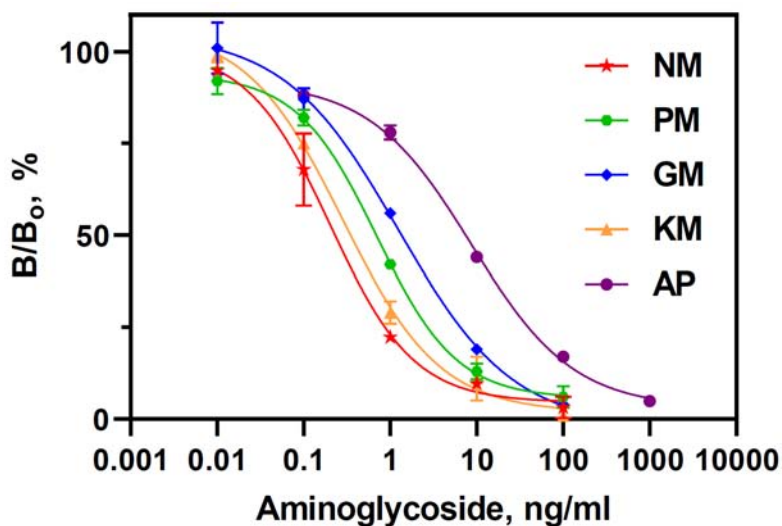
Analyte	IC_{50}/ ng mL^{-1}	Dynamic range IC_{20}–IC_{80}/ng mL^{-1}	LOD/ng mL^{-1}	LOD in honey/μg kg^{-1}
NM	0.2	0.03–2.1	0.02	1.0
PM	0.7	0.08–7.1	0.05	2.5
GM	1.5	0.15–13.3	0.11	5.5
KM	0.35	0.05–3.9	0.04	2.0
AP	6.8	0.5–96.8	0.23	11.5

Fig. 2 Standard curves and analytical parameters of the ELISA-system for group determination of aminoglycosides in honey. Interaction of anti-BSA-RS with coating antigen Gel-RS in 5% sucrose solution as the honey imitator. The detection limit in 5% sucrose solution was determined according to $LOD = B_0 - 3 \times SD$.

procedure. To avoid this step, honey matrix imitators were applied to mimic the influence of honey matrix on antibody binding. Sucrose was chosen as the honey imitator since it exposed a strong honey-matrix-like effect on antibody binding. The adequacy was found between solutions of honey and solutions of sucrose expressing an equal matrix effect. Two pairs with equivalent matrix effect were 1/20 honey = 20% sucrose, and 1/50 honey = 5% sucrose. The latter conditions were chosen as more preferable due to inconvenience of operating with high viscous 20% sucrose solution.

The determination of aminoglycosides in honey could be carried out quantitatively if the analyte to be detected is known. For quantification of aminoglycoside in honey, a sample was diluted 50 times in PBS-T, and aminoglycoside standard curve was generated in 5% sucrose-PBST (Fig 2). If analyte is unknown, the developed group-specific ELISA can be used as a screening test. In this case, the analyzed sample can be considered as contaminated if it caused a relative antibody binding below the cut-off level (Fig 3). Thus, the developed test was
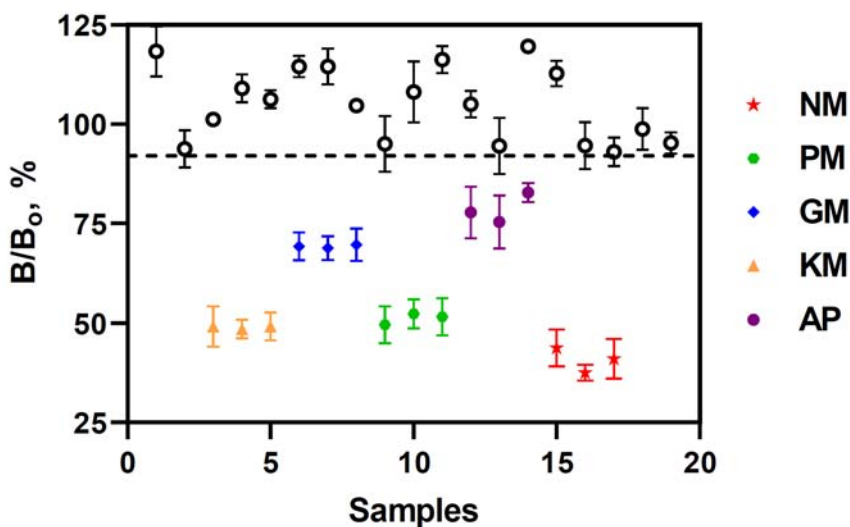
Fig. 3 Detection of aminoglycosides spiked in honey samples at a 40 ppb level using group-specific ELISA. Each symbol corresponds to the average relative binding and the error is *SD* obtained for an individual honey sample analyzed in triplicate. Empty characters represent individual blank honey samples (lime, buckwheat and flower), and filled symbols represent the same samples fortified with aminoglycosides at a 40 mg kg^{-1} (level established only for STM in several countries). The cut-off level corresponds to the limit of assay detection obtained by the matrix imitator (5% sucrose-PBS-T).

capable to reveal the contamination of honey with 9 aminoglycosides, 5 aminoglycosides approved for veterinary (NM, PM, GM, KM, and AP) at a 10 µg kg^{-1} level and also NA, RS, SSM, and TM.

4. Conclusions

A novel indirect competitive ELISA for the detection of aminoglycosides was developed. RS was used as a new immunizing hapten to produce group-specific antibodies against 2-DOS, a common moiety of a large number of aminoglycoside antibiotics. A wide spectrum of aminoglycoside representatives could be detected, including NM, RS, NA, PM, GM, SSM, KM, TM, and AP. The developed assay was capable to detect these analytes with a *LOD* up to 0.02–0.20 ng mL^{-1}. For analysis of honey, a matrix imitator was developed to avoid honey interferences on immunoassay. The analysis of the honey sample allowed us to reveal any of the mentioned aminoglycosides in honey at a 10 µg kg^{-1} level.

References

[1]   Council Regulation (EU) N 37/2010. *Off. J. Eur. Communities: Inf. Not.* **L15** (2009), 1–72.
[2]   Galvidis I.A., Burkin K.M., Eremin S.A., Burkin M.A. : Group-specific detection of 2-deoxy-streptamine aminoglycosides in honey based on antibodies against ribostamycin. *Anal. Meth.* **11** (2019), 4620–4628.

[3]   Thompson S.G., Burd J.F.: Substrate-labeled fluorescent immunoassay for amikacin in human serum. *Antimicrob. Agents Chemother.* **18** (1980), 264–268.

[4]   Li C., Zhang Y., Eremin S.A., Yakup O., Yao G., Zhang X.: Detection of kanamycin and gentamicin residues in animal-derived food using IgY antibody based ic-ELISA and FPIA. *Food Chem.* **227** (2017), 48–54.

[5]   Galvidis I.A., Burkin M.A. Monoclonal antibody-based enzyme-linked immunosorbent assay for the aminoglycoside antibiotic kanamycin in foodstuffs. *Russ. J. Biorgan. Chem.* **36** (2010), 722–729.

[6]   Haasnoot W., Stouten P., Cazemier G., Lommen A., Nouws J.F., Keukens H.J.: Immunochemical detection of aminoglycosides in milk and kidney. *Analyst* **124** (1999), 301–305.

[7]   Peng J., Wang Y., Liu L., Kuang H., Li A., Xu C.: Multiplex lateral flow immunoassay for five antibiotics detection based on gold nanoparticle aggregations. *RSC Adv.* **6** (2016), 7798–7805.

Photochemical vapor generation of cobalt for detection by inductively coupled plasma mass spectrometry

Jaromír Vyhnanovský[a, b, *], Stanislav Musil[a]

[a] Department of Trace Element Analysis, Institute of Analytical Chemistry of the Czech Academy of Sciences, Veveří 97, 602 00 Brno, Czech Republic ✉ jaromir.vyhnanovsky@gmail.com
[b] Department of Analytical Chemistry, Faculty of Science, Charles University, Hlavova 8/2030, 128 43 Prague 2, Czech Republic

Keywords
cobalt
inductively coupled
    plasma mass
    spectrometry
photochemical vapor
    generation

Abstract
This work focused on the photochemical vapor generation of cobalt. Volatile species were generated in a flow-injection system, employing a high-efficiency flow-through UV photoreactor and a formic acid based medium, and were introduced by an argon carrier into an inductively coupled plasma mass spectrometer for detection. Optimal generation conditions were found as 10% (v/v) formic acid and $4\,mol\,L^{-1}$ ammonium formate with a $4\,mL\,min^{-1}$ flow rate which corresponds to irradiation time of around 13 s. The influence of various metal sensitizers of photochemical reaction was investigated and only Cu^{2+} ions exhibited a positive effect on generation efficiency. Interferences from common inorganic anions (NO_3^-, Cl^-, SO_4^{2-}) were also examined. Lastly, the limit of detection and repeatability (at $250\,ng\,L^{-1}$) were determined to be $1.3\,ng\,L^{-1}$ and 4.1%, respectively.

1. Introduction

Photochemical vapor generation is an alternative sample introduction technique for analytical atomic spectrometry. This technique is based around a source of UV-radiation that irradiates a low molecular weight organic acid medium (most commonly formic acid, acetic acid, or their combinations) with an analyte. Highly reducing radicals and aquated electrons are produced and convert the analyte into a volatile species which is then transported into a detector [1]. So far the use of PVG has been described for hydride-forming elements (As, Bi, Te, Sb, Pb, Se, Sn, and Tl) and mercury [1, 2], transition metals (Fe, Co, Ni, Cu, Mo, W, Cd, Ag, Au, Ir, Pd, Pt, Rh, and Os) [1, 3–6] and even non-metals (Br, I, Cl, F, and S) [1, 6–9].

A first successful photochemical vapor generation of cobalt was described by Guo et al. in 2004 [6] which was followed by more systematic studies by Grinberg et al. in 2008 [10] and Deng et al. in 2010 [11]. Later works by de Quadros et al. [12] and de Jesus et al. [13] focused on the analysis of real samples. In the latter work,

the authors also presented a systematic study on generation conditions and achieved a generation efficiency of around 40%.

The main aim of this work was to optimize the conditions of generation with inductively coupled plasma mass spectrometry (ICP-MS) detection, examine the effect of various metal sensitizers to achieve the highest generation efficiency possible and reach the lowest limit of detection possible.

2. Experimental

2.1 Reagents and chemicals

Deionized water (DIW, $< 0.2\,\mu S\,cm^{-1}$, Ultrapur, Watrex, USA) was used for the preparation of all solutions. Formic acid (98%, p.a., Lach-Ner, Czech Republic) and ammonium hydroxide (≥25%, p.a., Sigma-Aldrich, USA) were used for the preparation of the reaction medium. A 1000 $mg\,L^{-1}$ Co stock solution (Sigma-Aldrich, USA) was used for the preparation of all sample solutions. The following compounds were used as potential metal sensitizers: cadmium(II) acetate dihydrate (p.a., Lach-Ner, Czech Republic), zinc(II) acetate dihydrate (p.a., Sigma-Aldrich, USA), copper(II) acetate monohydrate (p.a., Merck, Germany), nickel(II) acetate tetrahydrate (p.a., Sigma-Aldrich, USA), sodium tungstate dihydrate (p.a., Carl Roth, Germany) and iron(II) sulphate heptahydrate (p.a., Lachema, Czech Republic). Nitric acid (65%, semiconductor grade, Sigma-Aldrich, USA), hydrochloric acid (37%, p.a., Merck, Germany) and sulfuric acid (98%, p.a., Lach-Ner, Czech Republic) were used for an interference study.

2.2 Instrumentation

A schematic diagram of the PVG system coupled to ICP-MS is shown in Fig. 1 and a more detailed description can be found in reference [5]. Briefly, a single quadrupole ICP-MS Agilent 7700x (Agilent Technologies, USA) was used as a detector. Deionized water was mixed with a $10\,\mu g\,L^{-1}$ Rh internal standard solution in 2% HNO_3 and was subsequently nebulized by a MicroMist nebulizer during PVG. Isotopes of ^{59}Co and ^{103}Rh were monitored. Measurements were performed in time resolved analysis mode and in He collision mode ($4.1\,mL\,min^{-1}$). All tubing used was made from PTFE with the exception of tygon tubing in the peristaltic pump (Reglo ICC, Ismatec, Switzerland). The high-efficiency flow-through photoreactor was a 19 W low-pressure mercury discharge lamp (Beijing Titan Instruments Co., Beijing, China) with a quartz central channel (≈ 720 µL internal volume). Sample solutions were introduced into a stream of reaction medium using an injection valve (V-451, IDEX Health and Science, USA; sample loop volume 0.5 ml). Effluent from the photoreactor was mixed with a flow of argon and carried to the chilled gas-liquid separator (internal volume 15 mL), where the volatile species were separated from the liquid waste
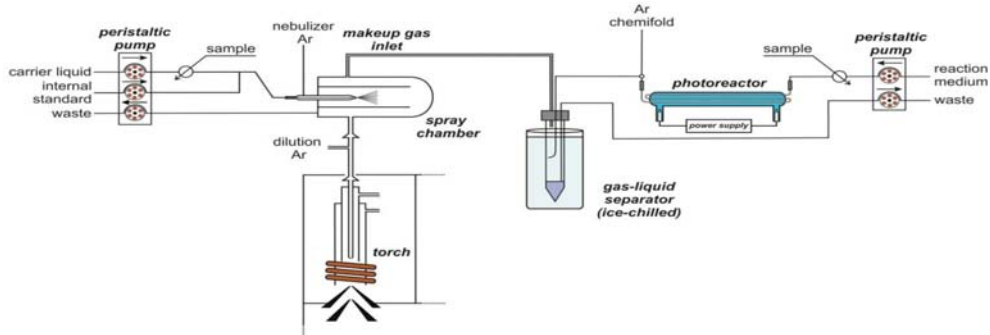
and carried to the inlet of a Scott-type spray chamber (originally the inlet for makeup argon) of the ICP-MS.

3. Results and discussion

The starting conditions were adopted from our earlier work [14] which used atomic absorption spectrometer as a detector and miniature diffusion flame as an atomizer. The first parameter optimized was the composition of reaction medium (Fig. 2). The addition of ammonium formate (created in-situ by the addition of a calculated amount of ammonium hydroxide to formic acid) was found crucial to effectively generate volatile species of cobalt, 10% (*v/v*) formic acid and 4 mol L^{-1} ammonium formate was chosen as the optimum and was used for all further experiments. Although higher concentrations of both components led to even higher signals, these conditions were not used further because of the laborious process of preparation (mixing of concentrated acid with concentrated base) and to limit the consumption of chemicals.

The influence of irradiation time was also examined, and the highest peak area was obtained for 4 mL min^{-1}, corresponding to an irradiation time of approxi‐ mately 13 s.

To enhance the generation efficiency, addition of various metals to the reaction medium was tested to "sensitize" the photochemical reaction. The metals were chosen with respect to their significant enhancement effect described recently for photochemical vapor generation of other analytes [1, 5, 8]. The only metal ion that led to an enhancement of the signal was Cu^{2+} (Fig. 3a), but even in this case the effect was rather negligible reaching only 1.2-fold enhancement in the range 0.01 to 0.1 mg L^{-1} Cu^{2+}. Further addition of more Cu^{2+} led to a decrease in the signal. The addition of Zn^{2+} did not exhibit any positive or negative effect across the tested range (0.1 to 1500 mg L^{-1}, not shown in figure), and the addition of higher concentrations (tens to hundredths of mg L^{-1}) of Cd^{2+}, Fe^{2+} and W^{6+} (Fig. 3b) caused severe interferences.
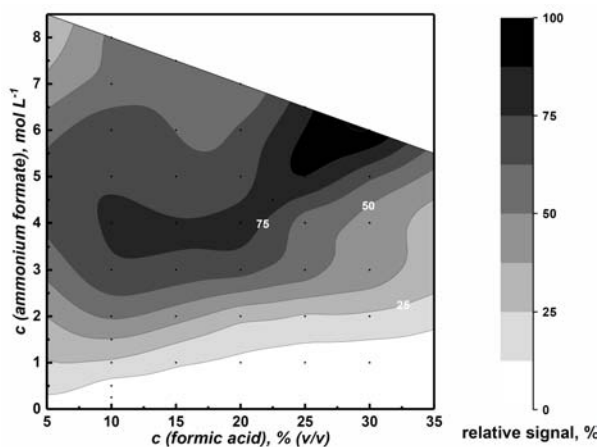
Fig. 2 Effect of the composition of reaction medium on peak area experimental conditions: 2 µg L^{-1} Co, reaction medium flow rate 4 mL min^{-1} (black dots correspond to measured points).
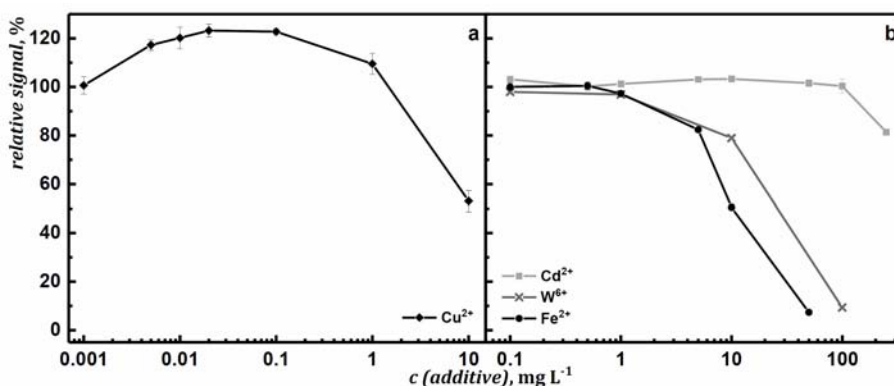

Fig. 3 Effect of various metal ions on the peak area: (a) metal ions with a positive effect; (b) metal ions without a positive effect. Experimental conditions: 2 µg L^{-1} Co, reaction medium 10% (v/v) formic acid and 4 mol L^{-1} ammonium formate, flow rate 4 mL min^{-1}.

Interferences caused by common inorganic anions (NO_3^-, Cl^-, SO_4^{2-}, added as their respective acids) were also investigated. Out of these, NO_3^- was found to cause the most severe interferences even at concentrations of single mmol L^{-1}. The methodology was more robust towards the interferences from Cl^- and SO_4^{2-}, but they still caused significant drop in sensitivity at higher concentrations. Considering the wide use of these acids in analytical chemistry for sample preparation, this poses a big challenge in the application of this method to real samples.

Using optimal conditions (10% (v/v) formic acid, 4 mol L^{-1} ammonium formate and irradiation time of 13 s), a calibration curve was measured and evaluated. The limit of detection was determined as 3 times the standard deviation of 10 blank measurements and was calculated as 1.3 ng L^{-1}. The repeatability of 10 consecutive measurements of 250 ng L^{-1} was 4.1%.

4. Conclusions

The conditions of the photochemical vapor generation of cobalt were optimized and are in good agreement with previous works [11, 13]. Copper ions were identified as a potential sensitizer, increasing the signal by about 1.2-fold but their potential use is severely limited by the narrow range of concentrations in which the positive effect is exhibited. Severe interferences from inorganic anions were observed which is in line with other works dealing with photochemical generation [1, 3, 5, 8]. Further experiments will follow, namely: (i) further investigations in new potential sensitizers to enhance generation efficiency and thus decrease the limit of detection to sub ng L^{-1} levels, (ii) determination of the generation efficiency (from comparison with nebulization and/or using a radioactive isotope ^{58}Co), (iii) verification of the accuracy and practical feasibility of this methodology by analysis of certified reference materials.

Acknowledgments

References

[1] Sturgeon R.E.. Photochemical vapor generation: a radical approach to analyte introduction for atomic spectrometry. *J. Anal. Atom. Spectrom.* **32** (2017), 2319–2340.

[2] Xu T., Hu J., Chen H.J.: Transition metal ion Co(II)-assisted photochemical vapor generation of thallium for its sensitive determination by inductively coupled plasma mass spectrometry, *Microchem. J.* **149** (2019), 103972.

[3] Šoukal J., Sturgeon R.E., Musil S.: Efficient photochemical vapor generation of molybdenum for ICPMS detection. *Anal. Chem.* **90** (2018), 11688–11695.

[4] de Oliveira R.M., Borges D.L.G.: UV photochemical vapor generation of noble metals (Au, Ir, Pd, Pt and Rh): A feasibility study using inductively coupled plasma mass spectrometry and seawater as a test matrix. *J. Anal. Atom. Spectrom.* **33** (2018), 1700–1706.

[5] Vyhnanovský J., Sturgeon R.E., Musil S.: Cadmium assisted photochemical vapor generation of tungsten for detection by inductively coupled plasma mass spectrometry. *Anal. Chem.* **91** (2019), 13306–13312.

[6] Guo X., Sturgeon R.E., Mester Z., Gardner G.J.: Vapor generation by UV irradiation for sample introduction with atomic spectrometry. *Anal. Chem.* **76** (2004), 2401–2405.

[7] Hu J., Sturgeon R.E., Nadeau K., Hou X., Zheng C., Yang L.: Copper ion assisted photochemical vapor generation of chlorine for its sensitive determination by sector field inductively coupled plasma mass spectrometry. *Anal. Chem.* **90** (2018), 4112–4118.

[8] Leonori D., Sturgeon R.E.: A unified approach to mechanistic aspects of photochemical vapor generation. *J. Anal. Atom. Spectrom.* **34** (2019), 636–654.

[9] Sturgeon R.E., Pagliano E.: Evidence for photochemical synthesis of fluoromethane. *J. Anal. Atom. Spectrom.* (2020), https://doi.org/10.1039/D0JA00108B.

[10] Grinberg P., Mester Z., Sturgeon R.E., Ferretti A.: Generation of volatile cobalt species by UV photoreduction and their tentative identification. *J. Anal. Atom. Spectrom.* **23** (2008), 583–587.

[11] Deng H., Zheng C.B. , Liu L.W., Wu L., Hou X.D., Lv Y.: Photochemical vapor generation of carbonyl for ultrasensitive atomic fluorescence spectrometric determination of cobalt. *Microchem. J.* **96** (2010), 277–282.

[12] de Quadros D.P., Borges D.L.: Direct analysis of alcoholic beverages for the determination of cobalt, nickel and tellurium by inductively coupled plasma mass spectrometry following photochemical vapor generation. *Microchem. J.* **116** (2014), 244–248.

[13] de Jesus H.C., Grinberg P., Sturgeon R.E.: System optimization for determination of cobalt in biological samples by ICP-OES using photochemical vapor generation. *J. Anal. Atom. Spectrom.* **31** (2016), 1590–1604.

[14] Vyhnanovský J.: Fotochemické generování těkavých specií kobaltu pro analytickou atomovou spektrometrii. *Master thesis.* Faculty of Science, Charles University, Prague, 2018.

Optimization of condition for cold plasma deposition of thin layers for surface modification of working electrodes

Justyna Lipińska[a, *], Maria Madej[b], Bogusław Baś[a], Jacek Tyczkowski[c]

[a] *Department of Analytical Chemistry, Faculty of Materials Science and Ceramics, AGH University of Science and Technology, Adama Mickiewicza 30, 30-059 Kraków, Poland*
✉ *justyna.lipinska@agh.edu.pl*
[b] *Department of Analytical Chemistry, Faculty of Chemistry, Jagiellonian University in Kraków, Gronostajowa 2, 30-387 Kraków, Poland*
[c] *Department of Molecular Engineering Faculty of Process and Environmental Engineering, Lodz University of Technology, Wolczanska 213, 90-924, Łódź, Poland*

Keywords
cold plasma deposition
electrochemical
    applications
surface modification
thin layers

Abstract
Currently, research is focused on the search for new, physically and chemically stable materials as well as volume or surface modification. One of the methods used for surface modification is the application of thin layers from inorganic and organic compounds. The plasma enhanced chemical vapor deposition is a method that allows material modification and also deposition of thin layers. This work concerns optimization of cold plasma deposition parameters and to achieve the best electrical conductivity while maintaining the high mechanical strength of the formed layers. Preliminary tests were focused on optimizing the layering parameters such as the deposition time, discharge power, pressure of monomer and the flow of argon. The obtained samples were subjected to thermal treatment after which they were covered with a layer of aluminum. The thickness of the obtained layers was determined on the basis of interference microscopy measurements. As a result of the experiments, layers with a thickness of 20 nm to 600 nm were obtained. The conductivity of the deposited layers was also determined and values from 0.03 to 150 S m^{-1} were obtained.

1. Introduction

One of the methods that allow obtaining materials with new properties is the plasma enhanced chemical vapor deposition method. In this method, compounds, called precursors, are supplied to the plasma reactor as a gas phase. Thanks to plasma enhanced chemical vapor deposition, it is possible to obtain materials with unique properties. This is due to the fact that the plasma affects the surface in four different ways: etching, cleaning, chemical modification and crosslinking.

This method is used to produce catalytic structures or to modify the properties of materials, e.g. improve hydrophobicity. The growing popularity of surface modification methods using cold plasma is associated with the fact that it is an environmentally friendly and versatile method [1, 2].

Working electrodes used in voltammetry are a subgroup of chemical sensors, which are small devices that convert real-time chemical information into a measurable and analytically useful measurement signal. Chemical information, ranging from the concentration of a specific component of the tested sample, to the overall composition of the matrix, can come from both the initiated chemical reaction and be the result of physico-chemical transformations taking place in the tested object. Chemical sensors are equipped with two basic elements, i.e. receptor and transducer. The receptor is responsible for the conversion of chemical information from the tested object into a specific form of energy, in the converter this energy is transformed into a useful analytical signal.

Parameters characterizing the electrochemical sensor include: accuracy, precision, selectivity, accuracy, presentation, selectivity, sensitivity, dynamic range, limit of quantification, limit of detection, lifetime, response time and reliability. The most numerous and the oldest group of chemical sensors are electrochemical sensors. Commonly observed interest in this group of sensors results from the fact that with relatively low production and operating costs, they offer the best metrological and operational parameters [3–5]. One of the main trends of modern analytics is the search for new electrode materials and various geometries of working electrodes. One way to improve the performance of working electrodes is to modify their surface, for example, by applying thin layers. In this work were considered plasma enhanced chemical vapor deposition method as the method of surface modification designed to perform working electrode for voltammetric determinations. As part of the initial research, plasma processing parameters such as discharge power, time of treatment and composition of gas mixture in which plasma was generated were optimized. The layers obtained in different conditions have been tested for suitability for electrochemical applications (layer thickness measurement and the measurement of conductivity).

2. Experimental

2.1 Reagents and chemicals

The precursor solutions, such as acrylonitrile, dietoxydimethylsilane, trietoxymethylsilane, and tetramethyldisiloxane which are supplied by ABCR were used. Other reagents of analytical purity, such as *n*-hexane (Sigma Aldrich) and argon were used.
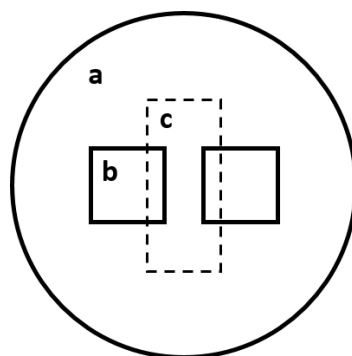
Fig. 1 Scheme of sample distribution in plasma reactor: (a) reactor electrode, (b) corning glass samples, (c) microscope coverslip.

2.2 Instrumentation

The thin layers were deposited in a parallel-plate plasma reactor (frequency 13.56 MHz). The samples obtained were calcined in a tunnel furnace under an argon atmosphere. The thickness of the deposited layers was measured after the aluminum was sputtered; using a Nikon microscope, type: ECLIPSE LV150N. Electrometer/high resistance system (KEITHLEY) was used to measure conductivity.

3. Results and discussion

Each of the monomers was deposited on prepared 1×1 corning glass samples. Samples, prepared with *n*-hexane, were placed in a plasma reactor, and additionally partially covered with a microscope coverslip. Schematic layout of samples in the reactor shown in Fig. 1. The first step was to etch the system using argon plasma. This stage allowed for the elimination of impurities that were not removed by the help of n-hexane and the preparation of the surface of the samples for the deposition of the proper layer. The proper stage is the application of a thin layer with the plasma induced by the selected precursor: acrylonitrile, dietoxydimethylsilane, trietoxymethylsilane, and tetramethyldisiloxane. The thickness and properties of the obtained layers depend on the deposition parameters such as: discharge power, time of treatment and composition of gas mixture in which plasma was generated.

Table 1 shows all combinations of parameters tested for all four precursors. Four different discharge powers for acrylonitrile and two different discharge powers for organosilicon monomers were tested, with two different treatment times. Each time and power combination was performed in plasma induced by pure monomer and monomer with argon. After applying the layers, the samples were placed in a quartz boat and calcined in a tunnel furnace. All samples were calcined at 500 °C for 2 hours under argon flow. Samples after calcination were covered with a layer of aluminum.

Table 1
Conditions for layers deposition- parameter which were tested.

Monomer	Discharge power / W	Time of treatment / min
Acrylonitrile	10, 20, 40, 80	2, 4
Dietoxydimethylsilane	20, 40	2.5, 5
Trietoxymethylsilane	20, 40	2.5, 5
Tetramethyldisiloxane	20, 40	2.5, 5

The thickness of the obtained layers was measured using an interference microscope. Measurements were carried out at a magnification 10×, recording the image in monochrome light. The image was set so that the interference fringes were perpendicular to the arc on the sample. In order to calculate the layer thickness D [nm], the following formula was used:

$$D = \frac{d}{L} \cdot \frac{546}{2} \qquad (1)$$

where d and L were determined on the basis of the registered image (d is fringe shift due to refraction of light on the slope, L is distance between the fringes).

The last stage of the study was to determine the current-voltage characteristics to determine the conductivity of the obtained layers. The sample was placed in a measuring cell and attached with silver paste to the electrometer wires. The change in current was recorded with the application of alternating voltage in time. Based on the results obtained, the graphs of dependence U–I were obtained, from which the value of resistance (R) was determined. An example of current-voltage characteristics is shown in Fig. 2.
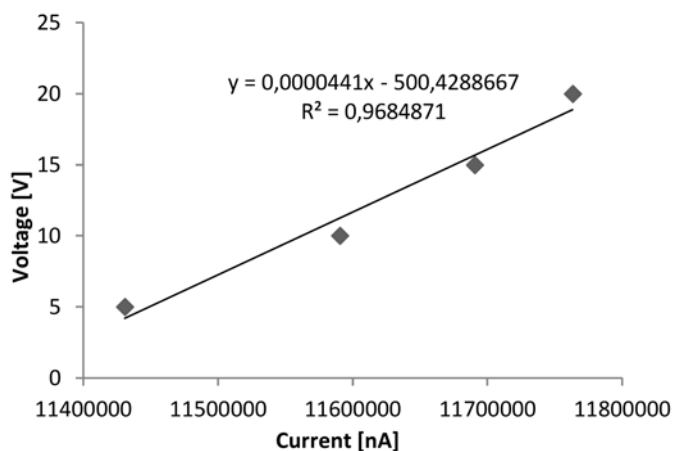
Fig. 2 Current-voltage characteristics determined for the acrylonitrile layer (deposition parameters: W = 10 W, t = 2.5 min, gas mixture: only acrylonitrile).

Knowing the value of the resistance and the geometry of the system, the specific resistance was determined, followed by the specific conductivity of the sample, the following equation was used:

$$\varrho = R\,\frac{b\,D}{l} \tag{2}$$

where ρ is specific resistance [Ω m], R is resistance [Ω], b is sample length [m], D is deposited layer thickness [m], and l distance between electrodes (wires) [m].

The results of thickness measurements and specific conductivity are presented in the Tables 2–5. For electrochemical applications it is important that the obtained layer has the highest specific conductivity. Analyzing the data presented in Tables 2–5 shows that the thinnest layers have the greatest application potential as the electrode material.

Table 2
The results of thickness measurements and conductivity specific to the acrylonitrile layers.

Discharge power / W	40	40	80	80	10	10	20	20
Time of treatment / min	2	4	2	4	2	4	2	4
Thickness / nm	158.45	311.67	250	464.4	24.7	67	75.31	122.36
Specific conductivity / S m^{-1}	0.002	15.6	19.1	0.003	151.2	45.4	31.1	18.5

Table 3
The results of thickness measurements and conductivity specific to the dietoxydimethylsilane layers.

Discharge power / W	20	20	40	40
Time of treatment / min	2.5	5	2.5	5
Argon flow / sccm	1.0	1.0	1.0	1.0
Thickness / nm	139.98	375.19	284.31	495.56
Specific conductivity / S m^{-1}	16.40	5.5	10.5	4.0

Table 4
The results of thickness measurements and conductivity specific to the trietoxymethylsilane layers.

Discharge power / W	20	20	40
Time of treatment / min	2.5	5	5
Argon flow / sccm	1.0	1.0	1.0
Thickness / nm	146.86	242.82	353.11
Specific conductivity / S m^{-1}	16.5	9.3	6.7

Table 5

The results of thickness measurements and conductivity specific to the tetramethyldisiloxane layers.

Discharge power / W	20	40	40
Time of treatment / min	2.5	2.5	5
Argon flow / sccm	1.0	1.0	1.0
Thickness / nm	167.59	315.9	616.52
Specific conductivity / S m^{-1}	21.3	9.5	3.1

4. Conclusions

In this work, plasma enhanced chemical vapor deposition method was used for applying layers of four different materials: acrylonitrile, dietoxydimethylsilane, trietoxymethylsilane and tetramethyldisiloxane. By changing parameters such as: discharge power, time of treatment and composition of gas mixture, a number of samples were obtained with layers of different thickness and what is associated with other electrical properties.

Tests performed as part of this work were used to perform innovative working electrodes for voltammetric determinations. The surface was modified using the cold plasma of three substrates: graphite, glassy carbon and gold.

References

[1]   Kapica R., Tyczkowski J., Balcerzak J., Makowski M., Sielski J., Worwa E.: Enhancing adhesive joints between commercial rubber (SBS) and polyurethane by low-pressure plasma surface modification. *Int. J. Adhes. Adhes.* **95** (2019), 102415.
[2]   Tyczkowski J., Kapica R., Łojewska J.: Thin cobalt oxide films for catalysis deposited by plasma-enhanced metal–organic chemical vapor deposition. *Thin Solid Films* **515** (2007), 6590–6595.
[3]   Hulanicki A., Głab S., Ingman F.: Chemical sensors: Definitions and classification. *Pure Appl. Chem.* **63** (1991), 1247–1250.
[4]   Brzózka Z., Wróblewski W.: *Sensory chemiczne.* Warszawa, Oficyna Wydawnicza Politechniki Warszawskiej 1999. (In Polish).
[5]   Skoog D.A., West D.W., Holler F.J., Crouch S.R.: *Fundamentals of Analytical Chemistry.* 9th Ed. Boston, Cengage Learning 2013.

Advanced GC-MS method for quality and safety control of alcoholic beverages

Anton Korban[a, b,]*

[a]　*Department of Analytical Chemistry, Faculty of Science, Charles University, Hlavova 2030/8, 128 40 Prague 2, Czech Republic ✉ karbonat7@gmail.com*
[b]　*Department of Analytical Chemistry,Chemistry Faculty, Belarusian State University, Leningradskaya 14, 220050, Minsk, Belarus*

Keywords
alcoholic beverages
gas chromatography-
　　mass spectrometry
　　(GC-MS)
internal standard method
volatile compounds
　　quantification

Abstract
Recently developed and validated simple and reliable quantitative method employing ethanol as an internal standard for GC-MS quantification of volatile compounds in alcoholic products was applied to 36 samples including commercially available world-famous brand spirits from 18 countries and homemade distillates. The GC-MS analyses were performed simultaneously by the suggested approach and official internal standard method that is prescribed in the legislation of EU and USA. The independent samples *t*-test was employed to evaluate the statistical difference of results of these two methods. The test revealed no difference in the results and their repeatability. The main benefits of the suggested method are the elimination of the necessity of manual internal standard addition and samples density measurement thus making it more economical and productive.

1. Introduction

Concentration and composition of volatile compounds, or congeners, is one of the most important parameters responsible for quality of produced alcoholic drinks, and hence for their sensory characteristics and consumer acceptance. Today, gas chromatography (GC) is conventionally used to determine qualitative and quantitative compositions of volatile compounds with various external and/or internal standard calibration procedures.

Method employing ethanol as an internal standard (IS) for GC quantitative determination of volatile compounds in alcoholic beverages has been suggested quite long ago [1], and since that time great research work has been carried out. Recently, an interlaboratory study of the method involving 9 testing laboratories from 4 countries was carried out [2]. The results demonstrated great perspectives of "Ethanol as IS" method and proved its reference character and ease of routine implementation.

All previous studies were utilizing flame ionization detectors since GC-FID is prescribed in the legislation [3], where mass-spectrometry detectors are not yet officially referred. However, GC-MS instruments are employed in practice to qualify and/or quantify volatiles in commercial spirits, in traditional homemade alcoholic drinks, in newly developed beverages, in spirit wastes and in distillates obtained with different manufacturing processes.

Our recent research was directed towards development of an algorithm of "Ethanol as IS" method application on GC-MS instruments [4]. We have showed that to prevent MS detector from saturation ethanol should be registered in the corresponding SIM time window, at characteristic *m/z* of low abundance, for instance, by *m/z* of 47 ions. This ion corresponds to non-fragmented ethanol molecules containing 1 heavy isotope (mainly ^{13}C). Finally, the results of measured standard solutions showed that the suggested approach is valid and "Ethanol as IS" method may be successfully used on GC-MS instruments too.

The objective of this study was to test and further approve the suggested approach on a larger set of 36 real samples of alcoholic drinks either commercial or homemade. The samples were simultaneously analysed by two GC-MS methods – a classical IS method prescribed in the legislation and the suggested "Ethanol as IS" method.

2. Experimental

2.1 Reagents and chemicals

The following volatile compounds were determined in tested samples of alcoholic beverages: 1,1-diethoxyethane (acetal), acetaldehyde, methyl acetate, ethyl acetate, methanol, 2 propanol, 1-propanol, 2 methylpropan-1-ol (isobutanol), 1-butanol, 2-butanol, and 3 methylbutan-1-ol (isoamyl alcohol). 1-pentanol was employed as a traditional IS compound.

2.2 Instrumentation

Shimadzu GCMS-QP2010 Ultra equipped with a quadrupole mass spectrometry detector was employed for GC-MS measurements. Rxi-1301Sil MS capillary column (60 m length, 0.25 mm i.d., 0.25 µm film thickness; Restek) was used for the separation of compounds. Injections were performed in a split mode (ratio 1:75). Helium (99.999% purity) was used as a carrier gas; injector temperature was 170 °C. The oven temperature was held at 30 °C for 5 min, then raised to 210 °C at a rate of 30 °C min^{-1} and held isothermally for 4 min. Measurements were performed in a SIM mode. For the analysed compounds and 1-pentanol 2–3 most abundant ions in the corresponding MS spectrum were selected; ethanol SIM time window contained only 47 *m/z* ions. All GC-MS measurements were carried out in triplicate under repeatability conditions.

Analysis of each alcoholic sample was performed in a following way. Aliquot of 0.9 mL of a tested sample was pipetted into a standard 2 mL glass vial and weighed. After that, 0.1 ml of the IS solution (2355 mg kg^{-1} of 1-pentanol in WES) was added to the tested sample and the mass was recorded. The obtained mixture was mixed thoroughly and 0.5 µl of it was injected into the GC system.

The origin of tested alcoholic beverages was either commercial or homemade. 33 world-famous spirits manufactured at different parts of the world were purchased from commercially available sources. The list of types of purchased and analysed spirits included bourbon, calvados, cognac, gin, grappa, liquor, metaxa, port wine, rum, sake, tequila, vodka, whiskey and various fruit distillates. The purchased drinks were produced at the territory of the following countries: Belarus, Bermuda, Cuba, Czech Republic, Denmark, France, Germany, Greece, Guatemala, Jamaica, Japan, Mexico, Moldova, Portugal, Slovakia, Trinidad and Tobago, UK (England and Scotland), USA. Three homemade fruit distillates produced by fermentation of pulpy fruits or their musts were obtained from local spirit makers. The declared ABV values of all tested samples varied from 15 to 81%.

3. Results and discussion

To fulfil the main goal of this work, i.e. to evaluate the statistical difference of results yielded by the compared methods, we have employed Students *t*-test for independent samples to verify statistical differences on the significance level of $p = 0.05$. The obtained empirical values for all pairs of congeners' concentrations were lower than critical one in all cases, demonstrating that concentrations obtained by the two methods have no statistical difference and lead to the same results.

In addition, repeatability of the two methods was compared; therefore, all RSD values obtained from triplicate measurements were split in two groups with respect to the corresponding concentrations (lower than 50 mg L^{-1} AA and higher than 50 mg L^{-1} AA). The obtained results are presented in the form of box plot in Fig. 1. Analysis of the chart in Fig. 1 showed that both the tested methods have yielded statistically similar repeatability.

All of the tested alcoholic drinks satisfied the requirements of EU Regulation (EC) no. 110/2008 [5]. The concentrations of undesirable compounds, such as methanol, did not exceed the levels specified in the same regulation for corresponding beverages. In Table 1 the description of the used SIM method and summary of the experimental results are presented.

To compare the trueness of the methods one of the spirit samples was spiked with standard solutions (ABV 40%) containing all analysed volatile compounds at concentrations of 50, 500, and 5000 mg L^{-1} AA. The original sample was used as a reference. Each of the spiked solutions was measured in triplicate. Selected spirit (cherry distillate) initially contained all 11 volatile compounds in various
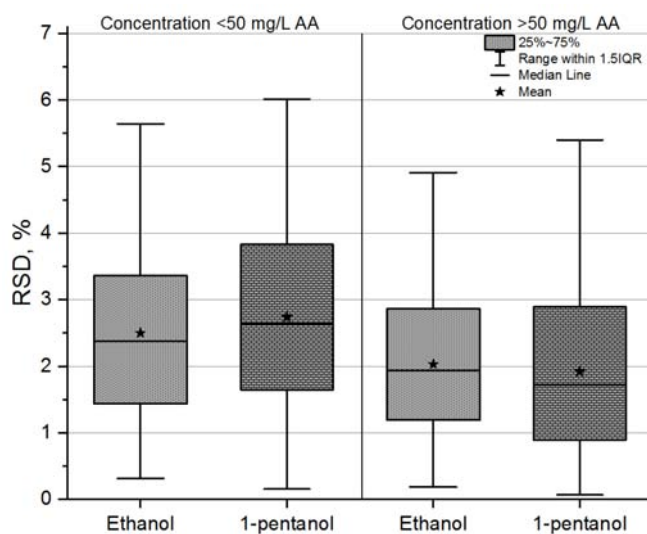
Fig. 1 Box charts of RSDs of used IS methods at 2 concentration ranges. Mean is equal to arithmetic mean or average, Interquartile Range (IQR) means is the distance between the upper (the median of the upper half of the dataset) and lower (the median of the lower half of the dataset) quartile.

Table 1
Description of the used SIM method and some statistics concerning all measured 36 spirit samples, both purchased and homemade.

Compound	Time/min	Registered m/z	Number of results	Concentration / mg L^{-1} AA	
				Minimal	Maximal
Acetaldehyde	0–4.2	31, 43, 44	36	2.4	715
Methanol			36	1.3	13600
Ethanol (IS)	4.2–4.8	47	—	—	—
2-Propanol	4.8–7.0	29, 31, 43, 45,	14	2.7	19.9
Methyl acetate		59, 61, 74	10	3.4	320
1-Propanol			26	36.1	12070
Ethyl acetate			27	16.6	10700
2-Butanol			11	1.8	2080
Isobutanol	7.0–20.0	31, 41–43, 45,	28	1.9	2000
1-Butanol		55, 56	13	2.8	155
Acetal			26	4.5	270
Isoamylol			31	3.9	2650
1-Pentanol (IS)			—	—	—
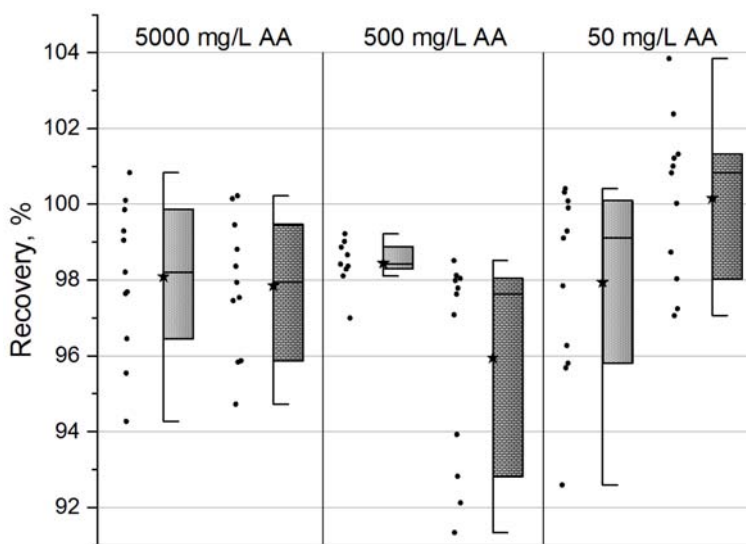
Fig. 2 Box charts of recoveries of the suggested (dotted pattern) and traditional (brick pattern) IS methods at different spike concentrations. Symbols definitions are the same as in Figure 1.

concentrations. The obtained recoveries box charts are shown in Fig. 2. Comparison of the recoveries obtained with two methods indicates that they have no significant difference in terms of trueness. Average obtained recovery was 98.1% when using suggested method and 98.0% when using traditional IS method.

4. Conclusions

In this work the results of testing the advantageous "Ethanol as IS" method for the GC-MS quality control analysis of alcoholic beverages were presented. 33 purchased samples of world-famous alcoholic beverages originating from 18 countries and 3 homemade fruit distillates were analysed to make a thorough and comprehensive study of the developed method. The concentrations of volatile compounds in analysed samples varied from 1 to 13500 mg L^{-1} AA, the ABV value of analysed samples varied from 15 to 81%. The suggested method was compared with the traditional IS method that is currently stated in legislation. The independent samples t-test revealed that with a probability of 0.95 results obtained with two methods do not differ significantly. The results of within-run precision (repeatability) showed relative standard deviations within 3 measurements to be less that 6%, indicating that the technique is reproducible. The trueness of the method was evaluated by recovery calculation. According to the obtained results recovery of the suggested method (98.1±3.3%) was slightly better than that of the traditional one (98.0±5.8%).

These facts prove that developed "Ethanol as IS" method is true, precise and reliable when employed on GC-MS instruments. At the same time to obtain

concentrations of volatile compounds in the officially required units of measure ($mg\,L^{-1}$ AA, $g\,L^{-1}$ AA etc.), suggested method requires no densitometry measurements of the tested sample and no addition of IS compound or any other sample pre-treatment. This method provides an invaluable analytical tool for the quality control of alcoholic products and should be used in routine analysis.

Acknowledgments

References

[1]   Cherepitsa S.V., Bychkov S.M., Kovalenko A.N. Mazanik A.L., Selemina N.M., Seredinskaya O. B.: The use of the major component (solvent) as an internal standard in the gas-chromatographic determination of impurities. *J. Anal. Chem.* **58** (2003), 368–371.

[2]   Charapitsa S., Sytova S., Korban A., Sobolenko L., Egorov V., Leschev S., Zakharov M., Čabala R., Busarova R., Shestakovich I., Tolstouhova A., Ondroušek S., Vávra J., Yilmaztekin M., Cabaroglu T.: Interlaboratory study of ethanol usage as an internal standard in direct determination of volatile compounds in alcoholic products. *BIO Web Conf.* **15** (2019), 02030. https://doi.org/10.1051/bioconf/20191502030

[3]   Commission Regulation (EC) No 2870/2000 laying down Community reference methods for the analysis of spirits drinks. http://data.europa.eu/eli/reg/2000/2870/oj

[4]   Korban A., Charapitsa S., Cabala R., Sobolenko L., Sytova S.: The perspectives of ethanol usage as an internal standard for the quantification of volatile compounds in alcoholic products by GC-MS. *J. Mass Spectr.* **55** (2020):e4493.

[5]   European Union (2008) Regulation (EC) No 110/2008 of the European Parliament and of the Council of 15 January 2008 on the Definition, Description, Presentation, Labelling and the Protection of Geographical Indications of Spirit Drinks and Repealing Council Regulation. http://data.europa.eu/eli/reg/2008/110(1)/oj

Utilization of a carbon felt as a material for working electrodes

Martin Baroch*, Hana Dejmková, Šárka Sládková

*Department of Analytical Chemistry, Faculty of Science, Charles University,
Hlavova 8/2030, 128 43 Prague 2, Czech Republic* ✉ *martin.baroch@natur.cuni.cz*

Keywords
amperometry
carbon felt
FIA
HPLC

Abstract
Working electrode made of carbon felt was used in combination with HPLC for verification of practical applicability of the electrode. All developed methods confirm advantageous physical and chemical properties of carbon felt. For electrochemical utilization it is possible to operate at higher positive potentials and even in low concentrations of electrolyte in mobile phase. Obtained limits of detection were mostly in submicromolar range and standard deviations of measurement repeatability were under 5%.

1. Introduction

Carbon or graphite felts are used as electrode material since the 1990s and their utilization still grows, in analytical electrochemistry as well as in other areas. This is due to their suitable properties, from which we can name high porosity, high specific surface area, good electric conductivity and high physical and chemical stability. The first two parameters are given by structure of felt, which consists of orderless carbon fibres with about ten to twenty micrometers in diameter [1], the others by the advantageous electrical properties of carbon fibre. On the other hand, porous flow-through electrodes including carbon felt electrode have disadvantage in a potential drop in the electrode volume, which causes difficult controlling of the exact potential applied on the electrode and therefore results in different current efficiencies on the opposite sides of the electrode [2].

Carbon felt electrode can be utilized for detection of structurally different compounds at various conditions. For example operating at reduction potential of −0.8 V [3], oxidation at relatively high potential +1.5 V [4] or measuring at low concentrations of electrolyte [5] can be named. Developed techniques also shows that carbon felt can be used for determination at submicromolar concentrations. This is mainly due to its ability to operate as a high-efficiency amperometric detector.

The main aim of this paper is to overview and compare parameters of several determination methods of different analytes using carbon felt detector in

combination with HPLC (for example their detection potentials, limits of detection or linear range).

2. Experimental

2.1 Reagents and chemicals

Stock solutions of propyl gallate, butylhroxyanisole, *tert*-butylhydroquinone, butylhydroxytoluene, chlortoluron, 2-amino-4-nitrophenol, and 4-amino-2-nitrophenol (all Sigma–Aldrich) with concentration of $1{\times}10^{-3}\,mol\,L^{-1}$ were prepared by dissolving the appropriate amount of the respective substance in methanol (HPLC grade, Lach-Ner, Czech Republic). Stock solutions of indole-3-acetic acid and indole-3-butyric acid were prepared in the same manner but in deionized water. Mobile phase consisted of methanol and phosphate-acetate buffer prepared from phosphoric and acetic acid (both Lach-Ner, Czech Republic) and sodium hydroxide (Fluka).

2.2 Instrumentation

The electrochemical cell consisted of carbon felt (Karbotechnik, Czech Republic) flow-through electrode, which was placed in cap with platinum wire electrical contact and drilled outlet hole on one side and with flat ferrula with capillary on the other side. Schematic picture of the assembly is shown in ref. [5]. Other electrodes were auxiliary platinum wire electrode and reference silver chloride (3M KCl) electrode (both Monokrystaly Turnov, Czech Republic). Potentiostat used in combination with this cell was Amperometric Detector ADLC 2 (Laboratoní přístroje Praha, Czech Republic).

HPLC apparatus consisted of Beta 10 gradient pump (ECOM, Czech Republic), degasser DG 4014 (ECOM, Czech Republic), six-way valve with 20 μl loop (Rheodyne, USA). HPLC column used for separation of propyl gallate, butylhydroxytoluene, *tert*-butylhydroquinone and butylhroxyanisole from their mixture and for indole-3-acetic acid and indole-3-butyric acid from their mixture was Lichrospher® RP-18 (125×4 mm, 5 μm, Merck, Germany), For separation of chlortoluron, column Purospher® RP-18 (125×4 mm, 5 μm, Merck, Germany) was used. In case of mixture 2-amino-4-nitrophenol and 4-amino-2-nitrophenol, column Gemini® C18 110 Å (150×4.6 mm,5 μm, Phenomenex, USA) was used for separation.

Measurements of pH were carried out at Conductivity and pH-meter 3510 using combined glass electrode (Jenway, UK).

Table 1

Parameters of detection potentials and limits of detection for different compounds using carbon felt detector.

Compound	E_{det} / V	LOD / μmol L^{-1}	Ref.
Propyl gallate	0.80	0.88	[5]
	1.40	1.86	[5]
Butylhroxyanisole	0.80	1.44	[5]
	1.40	3.48	[5]
tert-Butylhydroquinone	0.80	1.21	[5]
	1.40	2.66	[5]
Butylhydroxytoluene	0.80	31.28	[5]
	1.40	4.63	[5]
Chlortoluron	1.40	0.13	
Indole-3-acetic acid	1.50	0.33	[4]
Indole-3-butyric acid	1.50	0.54	[4]
4-Amino-2-nitrophenol	0.80	0.16	[3]
2-Amino-4-nitrophenol	0.80	0.21	[3]
4-Amino-2-nitrophenol	−0.80	3.5	[3]
2-Amino-4-nitrophenol	−0.80	3.7	[3]

3. Results and discussion

Performance of carbon felt was tested on several types of analytes which needed different separation conditions, namely amount of organic solvent in mobile phase and buffer pH. The lowest amount of methanol (30%) was used for separation of 2-amino-4-nitrophenol and 4-amino-2-nitrophenol [3]. Higher concentrations of methanol in mobile phase was used for determination of chlortoluron and for separation of indole-3-acetic acid and indole-3-butyric acid [4], namely 40% and 60%, respectively. The highest concentrations of methanol and therefore electrolyte with lowest conductivity was used in separation of antioxidants, namely propyl gallate, butylhroxyanisole, butylhydroxytoluene and *tert*-butylhydroquinone, where amount of methanol was ramping from 55% to 95% [5]. Detection potentials of mentioned analytes and their limits of detections are shown in Table 1.

HPLC separation of antioxidants was the first method chosen for testing of carbon felt electrode performance with this technique. Due to differences in their structure, when butylhydroxytoluene has a different oxidation mechanism, detection with two applied potentials was necessary. According to the hydrodynamic voltammograms potentials 1.4 V and 0.8 V were chosen for determination of butylhydroxytoluene and for the other three analytes, respectively [5]. As shown in Table 1, when the higher potential was applied limits of detection for propyl gallate, butylhroxyanisole, and *tert*-butylhydroquinone had increased. Contrary, determination of butylhydroxytoluene had approximately six times lower detection limit at higher potential.

Detection of auxins (indole-3-acetic acid and indole-3-butyric acid) was carried out at potential 1.5 V. Measurements at this potential gives repeatability with standard deviation 3.1% for indole-3-acetic acid and 2.5% for indole-3-butyric acid even with exchanging of the working electrode material. Calibration curves for both analytes were observed from 0.4 to 100 µmol L^{-1} with linearity in whole concentration range. Limits of detection for both analytes reached submicromolar concentrations, even with relatively high potential [4].

In case of determination of 2-amino-4-nitrophenol and 4-amino-2-nitrophenol, carbon felt electrode was used in both oxidation and reduction mode. Hydrodynamic voltammograms showed that optimal detection potential in reduction mode was –0.8 V. This low potential is close to the end of the potential window and therefore, interferences with remnants of dissolved oxygen in mobile phase were observed. These interferences resulted in approximately 20 times higher limit of detection for 2-amino-4-nitrophenol or 4-amino-2-nitrophenol obtained in reduction than in oxidation mode. On the other hand, maximum values of linear range were the same for both analytes in both detection modes [3].

For HPLC of chlortoluron, the optimal detection potential of 1.4 V was found. Its calibration dependence, although observed from 0.25 to 100.0 µmol L^{-1}; was linear only in the range from 0.25 to 5.0 µmol L^{-1}. Limit of detection based on standard solutions was 0.13 µmol L^{-1} and reproducibility of measurement, given by twenty consecutive measurements, gave relative standard deviation of 0.5%.

For all the determination methods, attention was paid to the applicability of the carbon felt in detection of analytes in complex matrices. In case of antioxidants edible oils were chosen as real samples [5], nitrophenol derivates were determined in urine samples [3] and auxins in rooting preparation [4]. Chlortoluron determination was performed in soil and surface water. The found values show a negligible matrix influence on detection.

4. Conclusions

Carbon felt working electrode was successfully used in combination with HPLC for determination of different types of electroactive compounds, e.g. antioxidants, auxins, or pesticides. All mentioned applications show great performance of the carbon felt as a flow-through electrode material in electroanalytical chemistry for oxidation and reduction way of analytes determination. Limits of detection for analytes are mostly in submicromolar concentrations, the exceptions are oxidation of analytes at higher potentials and their reduction, where limits of detections are in micromolar concentrations. Applicability of the electrode on real matrices was proven on analysis of edible oil samples, groundwater, soil, and rooting preparation.

Acknowledgments

References

[1]   Gonzalez-Garcia J., Bonete P., Expósito E., Montiel V., Aldaz A.,Torregrosa-Maciá R.: Characterization of a carbon felt electrode: Structural and physical properties. *J. Mater. Chem.* **9** (1999), 419–426.

[2]   Nava J.L., Recéndiz A., González L.G., Carreño G.,Martínez F.: Mass Transport and potential studies in a flow-through porous electrode reactor. *Portugal. Electrochim. Acta* **27** (2009), 381–396.

[3]   Dejmková H., Knaf M.: Application of carbon felt detector for the determination of dinitrophenol metabolites. In: *XXXIX. Modern Electrochemical Methods.* Fojta M., Schwarzova K., Navrátil T. (Eds.), Ústí nad Labem, Best Servis 2019, p. 41–43.

[4]   Dejmkova H., de Araújo Daniel M.: Electrochemical determination of indole-3-acetic acid and indole-3-butyric acid using hplc with carbon felt detector. *Monatsh. Chem.* **150** (2019), 439–442.

[5]   Dejmková H., Baroch M., Krejčová M., Barek J.,Zima J.: Coulometric detector based on carbon felt. *Appl. Mater. Today* **9** (2017), 482–486.

Electroanalytical methods for determination of 7-dehydrocholesterol in artificial serum

Lenka Benešová*, Adéla Zárybnická, Jan Klouda, Karolina Schwarzová-Pecková

UNESCO Laboratory of Environmental Electrochemistry, Department of Analytical Chemistry, Faculty of Science, Charles University, Hlavova 8/2030, 128 43 Prague 2, Czech Republic
✉ benesole@natur.cuni.cz

Keywords

amperometric detection
boron doped diamond
    electrode
7-dehydrocholesterol
differential pulse
    voltammetry
flow injection analysis
Smith-Lemli-Opitz
    syndrome

Abstract

7-Dehydrocholesterol is a biomarker of Smith-Lemli-Opitz syndrome, an autosomal recessive genetic disorder, caused by the inborn deficiency of 7-dehydrocholesterol reductase. In this study, procedures for its determination in artificial serum using flow injection analysis with electrochemical detection and voltammetric detection on boron doped diamond electrode were optimized. The proteins were precipitated by acetonitrile and after centrifugation the supernatant used for analysis. For quantitation of 7-DHC by differential pulse voltammetry the optimal ratio acetonitrile-artificial serum 9:1 (*v/v*) was applied. In FIA-ED, the ratio 3:1 (*v/v*), run electrolyte consisting of water-acetonitrile containing $0.01 \, \mathrm{mol \, L^{-1}}$ $NaClO_4$ in the same ratio and detection potential of +1.3 V *vs.* Ag/AgCl ($3 \, \mathrm{mol \, L^{-1}}$ KCl) were used. Quantitation of 7-DHC was possible using calibration dependence with limit detection of $20 \, \mathrm{\mu mol \, L^{-1}}$ in artificial serum. Nevertheless, the method has low recovery and for sensitive determination in real matrices of human serum and amniotic fluid a liquid-liquid extraction needs to be applied to prevent presence of 7-dehydrocholesterol in the phase with precipitated proteins.

1. Introduction

Smith-Lemli-Opitz syndrome (SLOS) is an autosomal recessive genetic disorder, firstly described in 1964 [1]. It is caused by the inborn deficiency of 7-dehydrocholesterol reductase. This enzyme transforms 7-dehydrocholesterol (7-DHC; Fig. 1) to cholesterol during the final step of biosynthesis of cholesterol in cells.

The clinical symptoms of SLOS are decreased blood level of cholesterol and
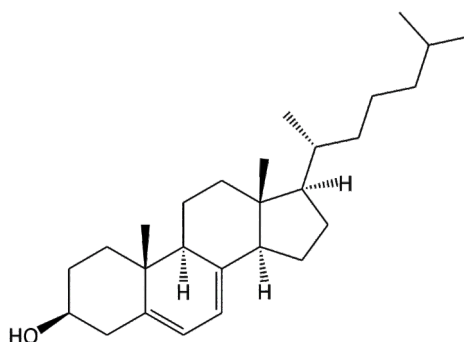
Fig. 1 Structure of 7-dehydrocholesterol.

Table 1
Concentration of 7-dehydrocholesterol in clinical matrices for healthy persons and for Smith-Lemli-Opitz syndrome (SLOS) patients detected by GC-FID.

Author(s), ref.	Matrix	Concentration / μmol L^{-1}	
		Healthy	SLOS
Kelley [4]	Plasma	0.3±0.01	385±309
	Amniotic fluid	< 0.2±0.01	16±9
Rossiter et al. [5]	Plasma	< 5	179–335
	Amniotic fluid	< 0.3	12–15

increased concentration of 7-DHC in blood and nervous system [2]. SLOS is a complex of multiple anomalies including mental retardation. It is manifested by holoprosencephaly (anomalies in brain development with imprecise division into the right and left hemispheres), mild dysmorphisms, cardiac, renal and gastro-intestinal malformations.

The characteristic facial anomalies of SLOS [2] are microcephaly, bitemporal narrowing, ptosis, short nasal root, short nose with anteverted nares and micrognathia, epicanthal folds and capillary hemangioma over the nasal root extending onto the glabella, the ear appear low-set and are posteriorly rotated. Oral finding includes a high-arched and narrow hard plate, broad and ridge alveoral ridges and redundancy of sublinqual tissues. CNS anomalies are agenesis or hypoplasia. Bilateral and unilateral postaxial polydactyly can be presented in the hands or feet or both.

Concentration of 7-DHC in blood is crucial for clinical diagnostic of SLOS in patients. Concentration levels in amniotic fluid are used for fetal diagnostics. Table 1 summarizes concentration of 7-DHC in plasma and amniotic fluid of healthy person and SLOS patients. Analytical methods used for determination of concentration of 7-DHC in these matrices include combination of GC or HPLC with MS [3] or GC with flame ionization detection (FID) or UV detection [4, 5].

The possibilities of electrochemical methods for detection of 7-DHC are limited as generally, the steroid core is rather redox-inactive (detail in review [6]) under variety of conditions. Nevertheless, 7-DHC possesses conjugated double bonds on steroid core and its oxidation was reported in several studies [7–9]. Its voltam-metric signal +0.95 V *vs.* SCE on glassy carbon electrode was firstly observed in non-aqueous media of methanol-benzene 75:25 (*v/v*) using 0.05 mol L^{-1} LiClO$_4$ as supporting electrolyte in a study dealing with electrochemical behaviour of vitamin A and D, and their provitamins D (7-DHC is precursor of vitamin D3) [7]. Determination of 7-DHC in human skin is possible by HPLC with UV (λ = 286nm) and amperometric detection (E_{det} +1.7 V *vs.* Ag/AgCl) on glassy carbon electrode using methanol-tetrahydrofuran17.5 mmol L^{-1} KH$_2$PO$_4$ (95:1:4, *v/v/v*) as mobile phase. 7-DHC was detected in the range from 12 to 81 μg g^{-1} dry weight, with detection limit of 3.9 pmol L^{-1} [8]. Another study [9] is devoted to determination of

7-DHC and vitamin D3 in fish using HPLC with electrochemical detection. The analytical cell was a serial combination of two-flow-through porous graphite working electrodes. The first standard coulometric electrode was used to eliminate potentially interfering compounds, using the second linear dynamic range from 0.013 to 0.312 μmol L^{-1} for 7-DHC was achieved.

Herein, we studied possibilities to detect 7-DHC based on its oxidation on boron doped diamond (BDD) electrode using differential pulse voltammetry and electrochemical detection in flow injection analysis (FIA-ED) in artificial serum, and peripherally in human serum and amniotic fluid.

2. Experimental

2.1 Reagents and chemicals

7-dehydrocholesterol (purity 95%) was obtained Sigma Aldrich (USA) and its standard solution was prepared in acetonitrile (Honeywell, Germany). The artificial serum was prepared from KCl (Penta, Czech Republic), $CaCl_2.2H_2O$ (Penta, Czech Republic), NaCl (Penta, Prague, Czech Republic), urine, D-glucose and 0.1% albumin from Sigma-Aldrich (USA). NaClO4 (Penta, Czech Republic) was used as supporting electrolyte.

2.2 Instrumentation

Voltammetric measurement were governed by the potentiostat PalmSens using working BDD electrode (Windsor Scientific, UK, d = 3.1 mm), $Ag/AgNO_3$ (0.1 mol L^{-1} $AgNO_3$, 1 mol L^{-1} $NaClO_4$ in acetonitrile) non-aqueous reference electrode and platinum wire counter electrode. BDD surface was polished before each scan using suspension of Al_2O_3 (Elektrochemické detektory, Turnov, Czech Republic). HPLC system (Hitachi, Merck) consisting of control unit D-7000, gradient pump L-7100, autosampler L-7200 and UV detector L-7400 was used for FIA-ED detection of 7-DHC. Run electrolyte was composed of 0.01 mol L^{-1} $NaClO_4$ in acetonitrile and deionised water in ratio 3:1 (*v/v*). Flow rate of mobile phase was 3.0 ml min^{-1}, injection volume was 40 μL, and λ = 280 nm was used for UV detection. Wall-jet detection cell was employed with working BDD electrode, Ag/AgCl (3 mol L^{-1} KCl) reference electrode, and platinum wire auxiliary electrode. Optimal detection potential of +1.3 V was controlled using ADLC2 potentiostat (Laboratorní přístroje, Prague, Czech republic).

3. Results and discussion

In this study electroanalytical methods were developed for determination of 7-DHC in artificial serum, namely FIA-ED and DPV. Both methods are based on direct oxidation of 7-DHC on boron doped diamond electrode, resulting in anodic

peak at ca +0.8 V (*vs.* Ag/AgNO$_3$ in acetonitrile) in non-aqueous medium of acetonitrile, or mixed medium acetonitrile-water using NaClO$_4$ as supporting electrolyte. The oxidation is presumably initiated by one electron removal from the conjugated double bonds on the steroid core of 7-DHC.

For determination of 7-DHC in real matrices, it is necessary to remove present proteins. Artificial serum containing albumin was used as model matrix to study the possibilities. Firstly, albumin was removed simply by precipitation with acetonitrile (serum-water 1:3 (*v/v*)) and the supernatant was analysed.

Different ratios water:acetonitrile were tested in run electrolyte (5:95, 10:90, 20:80, 25:75, 30:70, 40:60, and 50:50 (*v/v*)) to evaluate the influence of its composition on the FIA-ED signal of the blank and 7-DHC. The same ratio 1:3 as used for precipitation of albumin was chosen as optimal because of minimal and stable signal of the blank injected in FIA-ED system. Further, detection potential E_{det} in the range from +1.0 V to +1.5 V was optimized by evaluation of the hydrodynamic voltammograms, resulting in E_{det} of +1.3 V set as optimal value.

Concentration dependence of 7-DHC is linear in the range from 25 µmol L^{-1} to 300 µmol L^{-1} (concentration in artificial serum) with detection limit of 20 µmol L^{-1} and this concentration dependence can be used for quantitation of 7-DHC in artificial serum. Nevertheless, determination of 7-DHC in human serum and amniotic serum failed, as they represent more complicated matrices and 7-DHC is presumably partially adsorbed in the present proteins and cannot be quantified in the supernatant.

Further, differential pulse voltammetry with optimized parameters was used for determination of 7-DHC. In the presence of proteins in artificial serum (human serum albumin) an unacceptably high detection limit of 178 µmol L^{-1} was achieved. When the proteins were precipitated using acetonitrile (aceto-nitrile:artificial serum ratio 9:1 (*v/v*)) the limit of detection of 7-DHC was lowered to 1.5 µmol L^{-1} in artificial serum. Nevertheless, the recovery of the method was only 43 to 70% depending on the concentration of 7-DHC, again reflecting the loss of 7-DHC due to protein precipitation.

Therefore, a second approach of sample pretreatment based on liquid-liquid extraction of all lipids described in [10] was tested (Bligh-Dyer extraction). The procedure has two parts. Firstly, methanol, chloroform and the sample of artificial serum is mixed and shaken to form a monophasic system. After addition of chloroform and water a biphasic system is formed, where chloroform phase contains all of lipid compounds and methanol-water phase contains all non-lipids compounds. Chloroform phase is then dried under N2 atmosphere at 50 °C and dried extract dissolved in acetonitrile. Preliminary experiments using DPV resulted in recovery of 97% for Bligh-Dyer extraction of 7-DHC from in artificial serum.

4. Conclusions

FIA-ED and DPV were optimized for determination of 7-DHC in artificial serum. Using precipitation of proteins by acetonitrile, limit of detection of 7-DHC in artificial serum using FIA-ED was 20 µmol L^{-1} and this method can be used for their quantification using calibration dependence. Nevertheless, determination using DPV is unreliable due to low recovery of the procedure. Development of a method including liquid-liquid extraction step is in progress so that 7-DHC could be determined in real matrices as human serum and amniotic fluid.

References

[1] Smith D.W., Lemli L., Opitz J.M.: A newly recognized syndrome of multiple congenital anomalies. *J. Pediatr.* **64** (1964), 210–217.
[2] Nowaczyk M., Waye J.: The Smith–Lemli–Opitz syndrome: a novel metabolic way of understanding developmental biology, embryogenesis, and dysmorphology. *Clin. Genet.* **59** (2001), 375–386.
[3] Becker S., Röhnike S., Empting S., Haas D., Mohnike K., Beblo S., Mütze U., Husain R.A., Thiery J., Ceglarek U.: LC-MS/MS-based quantification of cholesterol and related metabolites in dried blood for the screening of inborn errors of sterol metabolism. *Anal. Bioanal. Chem.* **407** (2015), 5227–5233.
[4] Kelley R.I.: Diagnosis of Smith-Lemli-Opitz syndrome by gas-chromatography mass-spectrometry of 7-dehydrocholesterol in plasma, amniotic-fluid and cultured skin fibroblasts. *Clin. Chim. Acta.* **236** (1995), 45–58.
[5] Rossiter J.P., Hofman K.J., Kelley R.I.: Smith-Lemli-Opitz Syndrome: Prenatal-diagnosis by quantification of cholesterol precursors in amniotic-fluid. *Am. J. Med. Genet.* **56** (1995), 272–275.
[6] Klouda J., Barek J., Nesměrák K., Schwarzová-Pecková K.: Non-enzymatic electrochemistry in characterization and analysis of steroid compounds. *Crit. Rev. Anal. Chem.* **47** (2017), 384–404.
[7] Atuma S.S., Lundström K., Lindquist J.: The electrochemical determination of vitamin A. Part II. Further voltammetric determination of vitamin A and initial work on the determination of vitamin D in the presence of vitamin A. *Analyst* **100** (1975), 827–834.
[8] Moody J.P., Humphries C.A., Allan S.M., Paterson C.R.: Determination of 7-dehydrocholesterol in human skin by high-performance liquid-chromatography. *J. Chromatogr. B* **530** (1990), 19–27.
[9] Ostermeyer U., Schmidt T.: Vitamin D and provitamin D in fish. *Eur. Food Res. Technol.* **222** (2005), 403–413.
[10] Bligh E.G., Dyer W.J.: A rapid method of total lipid extraction and purification. *Can. J Biochem. Physiol.* **37** (1959), 911–917.

Author Index

Keyword Index